

**TWO-PHOTON IMAGING OF GLUTATHIONE LEVELS IN INTACT
BRAIN INDICATES SITES OF ENHANCED REDOX BUFFERING**

by
XIAOJIAN SUN

B.Sc., Tsinghua University, Beijing, P. R. China, 2003

THESIS SUBMITTED IN PARTIAL FULFILLMENT OF
THE REQUIREMENTS FOR THE DEGREE OF

Master of Science

In

The Faculty of Graduate Studies

Neuroscience

THE UNIVERSITY OF BRITISH COLUMBIA

February, 2006

© Xiaojian Sun 2006

Abstract

Oxidative stress, the metabolic imbalance between oxidant creation and destruction is proposed as a final common pathway for neurodegenerative disease and injury. To map sites of antioxidant homeostasis in brain, I used two-photon imaging of monochlorobimane (MCB) fluorescence, a selective enzyme-mediated marker, for reduced glutathione (GSH) in both brain slices and *in vivo* preparations. I found that cells at the CSF or blood brain interface such as lateral ventricle ependymal cells, meningeal cells, and astroglia contain both high levels of MCB conjugation activity (glutathione S-transferase dependent) and GSH content. In comparison, cortical neurons in Layer II contained approximately 20% of the GSH content of their astrocyte counterparts. Regional mapping of GSH indicated that the highest levels were present in cells lining the lateral ventricles, specifically ependymal cells and the subventricular zone. The enrichment of GSH content along the lateral ventricle suggested a possible function in oxidant homeostasis for developing neuronal progenitors. Consistent with this, I observed that developing neurons found in the subgranular zone of dentate gyrus, contained 3-fold more GSH than older neurons found in the neighbouring granular layer.

Besides imaging GSH distribution with MCB, I also developed an assay to measure different kinetic parameters of GSH metabolism. With this assay, I found that meninges are more active than cortical cells in GSH metabolism.

In conclusion, I have developed a powerful approach to map sites of antioxidant homeostasis in brain directly, demonstrating a unique role for GSH in developing neurons and cells at the CSF and blood-brain interface.

TABLE OF CONTENTS

ABSTRACT.....	ii
TABLE OF CONTENTS.....	iv
LIST OF TABLES.....	ix
LIST OF FIGURES.....	x
LIST OF ABBREVIATIONS.....	xii
ACKNOWLEDGEMENTS.....	xvi
1 CHAPTER 1 Introduction.....	1
1.1 Overview of GSH metabolism in brain.....	1
1.1.1 Functions of GSH.....	1
1.1.2 Basic metabolism of GSH.....	2
1.1.3 GSH metabolism in brain.....	5
1.1.3.1 Synthesis and Consumption of GSH in brain.....	5
1.1.3.2 Release of GSH from astrocytes.....	6
1.1.3.3 Functions and fate of extracellular GSH in brain.....	7
1.1.3.4 Export of GSSG from astrocytes during oxidative stress.....	11
1.1.4 GSH deficiency and neurological diseases.....	12
1.1.4.1 GSH in Parkinson's disease (PD).....	13
1.1.4.2 GSH and stroke.....	14
1.1.4.3 Therapeutic approaches for neurodegenerative diseases.....	15
1.2 Imaging and measurement of GSH in brain.....	16
1.2.1 Different dyes to image GSH.....	17

1.2.2	Two photon imaging of GSH with MCB.....	18
1.3	Structure and function of meninges.....	19
1.3.1	Function of meninges.....	20
1.3.2	Meninges express high level of xCT, cystine/glutamate antiporter.....	21
1.4	Rationale of research.....	21
2	CHAPTER 2. Materials and methods.....	23
2.1	Chemicals.....	23
2.2	Astrocytes and meninges culture.....	23
2.3	Plate reader GSH assay.....	24
2.4	Calibration of the GSH-MCB fluorescence.....	25
2.5	Rat brain slices preparation.....	25
2.6	Animal preparation for in vivo imaging.....	26
2.7	Two-photon microscopy.....	27
2.8	Immunostaining.....	28
2.9	Glutathione S-transferase (GST) assay.....	29
2.10	Total intracellular GSH assay.....	30
2.11	Data and image analysis.....	30
3	CHAPTER 3. Results.....	32
3.1	Specificity of MCB labelling.....	32
3.1.1	MCB labelling of GSH is dependent on GST.....	32
3.1.2	MCB could be used to label intracellular GSH with the plateau level of fluorescence intensity indicating the cellular GSH level.....	35

3.2	GSH metabolism assay.....	39
3.2.1	Plate reader assay is a powerful system to measure intracellular GSH level in cultures.....	39
3.2.2	Plate reader assay can measure rate of GSH precursor uptake and synthesis.....	40
3.2.3	Plate reader assay can measure efflux of GSH-MCB conjugate.....	42
3.2.4	Plate reader assay can detect changes in GSH metabolism under oxidative stress.....	45
3.2.5	Conclusion.....	50
3.3	Feasibility of two-photon laser scanning microscopy (TPLSM) measurement of cellular glutathione level.....	50
3.3.1	Assumption 1: Efflux of GSH-MCB at room temperature is negligible.....	52
3.3.2	Assumption 2: MCB labelled all GSH content in cells	55
3.3.3	Conclusion.....	57
3.4	MCB labelling of different brain regions in slices.....	57
3.4.1	Meningeal and astrocytes in neocortex are labelled strongly by MCB in rat brain slices.....	59
3.4.2	MCB labelling of neurons in slices is much weaker than labelling of astrocytes.....	62
3.4.3	Lateral ventricle ependymal cells have the highest GSH content in brain slices	66

3.4.4	A subpopulation of developing neurons in dentate gyrus are labelled by MCB.....	73
3.4.5	Measurement of GSH concentration in different brain regions in acute brain slices.....	80
3.4.6	Conclusion.....	84
3.5	MCB labels a subpopulation of meningeal and neocortical cells in vivo.....	84
3.6	Meningeal cells have a more active GSH system than astrocytes in neocortex.....	89
3.6.1	Meninges contain higher level GSH and GST activity than cortical cells.....	89
3.6.2	Meninges cells are more efficient in taking up GSH precursors and synthesizing GSH.....	90
3.6.3	Immunostaining of cortical cell cultures.....	94
4	CHAPTER 4. Discussion.....	96
4.1	MCB labelling with two-photon microscopy resolves cellular GSH in situ..	96
4.2	Cellular GSH distribution in brain slices.....	98
4.2.1	GSH is highly expressed in cells at CSF interface.....	98
4.2.2	GSH in neurons.....	99
4.2.3	Summary of types of cells labelled by MCB in slices.....	103
4.3	Manipulation of GSH metabolism.....	106
4.4	Measurement of GSH within the cortex of live animals.....	109

4.5	Meninges may be an ideal position for protecting brain against oxidative load.....	110
4.6	Conclusion.....	111
	REFERENCES.....	113

4.5	Meninges may be an ideal position for protecting brain against oxidative load.....	110
4.6	Conclusion.....	112
	REFERENCE.....	113

LIST OF TABLES

Table 3-1. Comparison of all kinetics parameters of GSH metabolism between tBHQ treatment and control (DMSO) groups.....	49
Table 3-2. Comparison of kinetic parameters of GSH metabolism between meninges and cortical cell cultures.....	92
Table 4-1. Types of cells labelled by MCB.....	105

LIST OF FIGURES

Figure 1-1. Metabolism of GSH.....	4
Figure 1-2. Metabolic interaction between astrocytes and neurons in the GSH metabolism of the brain.....	9
Figure 3-1. MCB can specifically label GSH.....	34
Figure 3-2. Monitoring GSH metabolism in astrocytes cultures with plate reader.	37
Figure 3-3. Fluorescence images (10X) of GSH-MCB in untreated (A) and MK571-treated (B) astrocytes cultures.....	44
Figure 3-4. Changes in GSH metabolism induced by activation of ARE-mediated gene expression.....	48
Figure 3-5. Standard curve for the relationship between fluorescence intensity and GSH-MCB concentration.....	51
Figure 3-6. Efflux of GSH-MCB in slices at room temperature can be neglected.	53
Figure 3-7. GSH-MCB efflux can be neglected in room temperature.....	54
Figure 3-8. Time course curve of MCB labelling in different brain regions.....	56
Figure 3-9. MCB and PI labelling of slices.....	58
Figure 3-10. MCB labels the meninges and astrocytes robustly.....	61
Figure 3-11. MCB labelling of mature cortical neurons.....	64
Figure 3-12. MCB labelling of GSH-containing ependymal cells lining the lateral ventricle.....	67

Figure 3-13. Many cells labelled by MCB in subventricular zone (SVZ) are labelled by doublecortin (DCX).....	69
Figure 3-14. Some cells labeled by MCB along lateral ventricle and in SVZ are also labeled by S100 β	70
Figure 3-15. Cells labeled by MCB along lateral ventricle and in SVZ are not labeled by GFAP.....	71
Figure 3-16. Mature neurons in SVZ are not labelled by MCB.....	72
Figure 3-17. MCB labelling of GSH-containing cells in dentate gyrus.....	74
Figure 3-18. Many cells in subgranular zone are colabelled by MCB and S100 β	76
Figure 3-19. MCB labelled cells in dentate gyrus are GFAP-positive.....	77
Figure 3-20. Many cells in subgranular zone are colabelled by MCB and DCX.	78
Figure 3-21. Mature neurons labelled by NeuN are not labelled by MCB.....	79
Figure 3-22. Quantification of GSH concentration in different brain regions.....	83
Figure 3-23. <i>In vivo</i> two-photon fluorescence image of the somatosensory cortex of a live anesthetized mouse after application of MCB and SR 101.....	87
Figure 3-24. GSH metabolism is more active in meninges than in cortical cells.....	93
Figure 3-25. MCB labelled cells in cortical cells culture are s100 β positive.....	95
Figure 4-1. Comparison of MCB labelling in young and mature rat slices.....	101
Figure 4-2. DEM depletion of intracellular GSH content.....	108

LIST OF ABBREVIATIONS

°C	Degrees centigrade
γGT	γ-glutamyl transpeptidase
μm	micrometer
μM	micromolar
ABC	ATP-binding cassette
ACSF	artificial cerebral spinal fluid
ANOVA	analysis of variance between groups
ApN	aminopeptidase N
ATP	adenosine triphosphate
BSO	DL-buthionine-(S,R)-sulfoximine
CDNB	1-chloro-2,4-dinitrobenzene
Cktl	cocktail
CMAC	t-butoxycarbonyl-Leu-Met-7-amino-4-chloromethylcoumarin
CMAC-blue	7-amino-4-chloromethylcoumarin
CMFDA	5-chloromethylfluorescein diacetate
CSF	cerebral spinal fluid
DCX	doublecortin
DEM	diethyl maleate

DG	dentate gyrus
DTNB	5,5'-dithio-bis-2-nitrobenzoic acid
FITC	fluoresceine isothiocyanate
GFAP	glial fibrillary acidic protein
GPx	glutathione peroxidase
GR	glutathione reductase
GSH	glutathione
GSSG	glutathione disulfide
GST	glutathione S-transferase
h	hour
HBSS	Hank's Balanced Salt Solution
HPLC	high performance liquid chromatography
LV	lateral ventricle
MapII	microtubule associated protein 2
MBB	monobromobimane
MCB	monochlorobimane
min	minute
mM	millimolar
MRP	multidrug resistance protein

NADPH	nicotinamide adenine dinucleotide phosphate (reduced form)
NDA	2,3-naphthalenedicarboxaldehyde
NMDA	N-methyl-D-aspartate
NSE	neuronal specific enolase
Nrf2	NF-E2-related factor 2
OPD	o-phthaldehyde
PBS	phosphate buffered saline
PFA	para formaldehyde
PI	propidium iodide
PMT	photomultiplier tube
QBB	monobromotrimethylammoniumbimane
ROS	reactive oxygen species
RT-PCR	real-time polymerase chain reaction
sec	second
SEM	standard error of the mean
SGZ	subgranular zone
SOD	superoxide dismutase
SR101	sulforhodamine 101
SVZ	subventricular zone

tBHQ

tert-Butylhydroquinone

TPLSM

two-photon laser scanning microscopy

Acknowledgements

First, I would like to thank my husband for his unconditioned support all the time.

I would also like to thank my parents for their kindly support during my study.

I would also like to thank Dr. Timothy H. Murphy for his guidance, inspiration, supportiveness and encouragement during the course of my Master study. I would also like to thank Dr. Lynn Raymond, who gave me lots of advices in our lab meeting.

I would like to thank all the members of the Murphy lab and Raymond, especially Andy Y. Shih, Shengxiang Zhang and Zhi Liu, for advice and friendship; and Ping Li, Heidi Erb, Lei Jiang, for help on my experiments, as well as other members, all of whom are wonderful colleagues and friends to work with.

I would also like to thank my supervisory committee, including Dr. Brian MacVicar, Dr Yutian Wang, and Dr Lynn Raymond for helpul suggestions on my projects.

Chapter 1 Introduction

The cells of the human brain utilize 20% of the oxygen consumed by the body but constitute only 2% of the body weight (Clarke and Sokoloff, 1999). This indicates the potential generation of a high quantity of reactive oxygen species (ROS) during oxidative phosphorylation in the brain. ROS generation has to be counter-balanced by an appropriate antioxidative defense to enable a long human life. Glutathione (GSH), as an essential cellular antioxidant, plays a key role in the defense of brain cells against oxidative stress (Cooper, 1997; Cooper and Kristal, 1997; Dringen, 2000). Insufficient antioxidative defense or increased generation of ROS can cause oxidative stress. For the brain, oxidative stress has been connected with the loss of neurons during the progression of neurological diseases, e.g., Parkinson's disease (PD), Alzheimer's disease (AD), Huntington's disease (HD) and stroke (Bains and Shaw, 1997; Cooper, 1997; Dringen, 2000; Schulz et al., 2000; Bharath et al., 2002).

1.1 Overview of GSH metabolism in brain

1.1.1 Functions of GSH

The tripeptide GSH is the major cellular thiol in mammalian cells (Cooper, 1997). It has important functions as antioxidant, is a reaction partner for the detoxification of xenobiotica, is a cofactor in isomerization reactions, and is a storage and transport form of cysteine (Meister and Anderson, 1983; Cooper, 1997). In addition, GSH is essential

for cell proliferation (Poot et al., 1995) and maintains the thiol redox potential in cells, keeping sulfhydryl groups of proteins in the reduced form (Cotgreave and Gerdes, 1998). Besides, GSH also plays a role in the regulation of apoptosis (van den Dobbelen et al., 1996; Ghibelli et al., 1998; Hall, 1999).

The GSH system is very important for the cellular defense against ROS. A high intracellular concentration of GSH protects against a variety of different ROS. GSH reacts directly with radicals in nonenzymatic reactions (Saez et al., 1990; Winterbourn and Metodiewa, 1994) and is also an electron donor in the reduction of peroxides catalyzed by glutathione peroxidases (GPx) (Chance et al., 1979). It should be noted that the GSH system is only part of the cellular defense system against ROS. Other enzymes, such as superoxide dismutase (SOD) and catalase, as well as antioxidants, such as ascorbate and α -tocopherol, are also involved in ROS detoxification (Meister, 1994; Wolf et al., 1998; Gate et al., 1999).

1.1.2 Basic metabolism of GSH

GSH is synthesized *in vivo* by the consecutive action of two enzymes (Meister, 1974; Figure 1-1). γ GluCys synthetase uses glutamate and cysteine as substrates forming the dipeptide γ GluCys, which can be combined with glycine in a reaction catalyzed by glutathione synthetase to generate GSH. Adenosine triphosphate (ATP) is a cosubstrate for both enzymes. The intracellular level of GSH is regulated by a feedback inhibition of γ GluCys synthetase by the endproduct GSH (Richman and Meister, 1975; Misra and Griffith, 1998). Therefore, cellular synthesis and consumption of GSH are balanced.

During detoxification of ROS, GSH is involved in two types of reactions: (i) GSH reacts nonenzymatically with radicals such as the superoxide anion, nitric oxide or the hydroxyl radical (Saez et al., 1990; Clancy et al., 1994; Winterbourn and Metodiewa, 1994; Singh et al., 1996) and (ii) GSH is the electron donor for the reduction of peroxides in the GSH peroxidases (GPx) reaction (Chance et al., 1979). The final product of the oxidation of GSH is glutathione disulfide (GSSG). Within cells GSH is regenerated from GSSG by the reaction catalyzed by glutathione reductase (GR). This enzyme transfers electrons from nicotinamide adenine dinucleotide phosphate (reduced form) (NADPH) to GSSG, thereby regenerating GSH. During the reaction catalyzed by GPx and GR, GSH is not consumed but recycled (Figure 1-1).

In contrast, during the generation of glutathione-S-conjugates by glutathione-S-transferases (GST) (Commandeur et al., 1995; Salinas and Wong, 1999) or by release of GSH from cells (Akerboom and Sies, 1990; Kaplowitz et al., 1996), the level of total intracellular GSH is lowered. Therefore, the GSH used for these processes has to be replaced by resynthesis from the constituent amino acids. Extracellular GSH and GSH conjugates are substrates for the ectoenzyme γ -glutamyl transpeptidase (γ GT). This enzyme catalyzed the transfer of the γ -glutamyl moiety from GSH or a GSH conjugate onto an acceptor molecule, thereby generating the dipeptide CysGly or the CysGly conjugate, respectively (Meister et al., 1981; Commandeur et al., 1995). CysGly can be hydrolyzed by ectopeptidases (Tate, 1985) to cysteine and glycine, which are subsequently taken up by cells and can serve again as substrates for cellular glutathione synthesis (Figure 1-1).

Figure 1-1

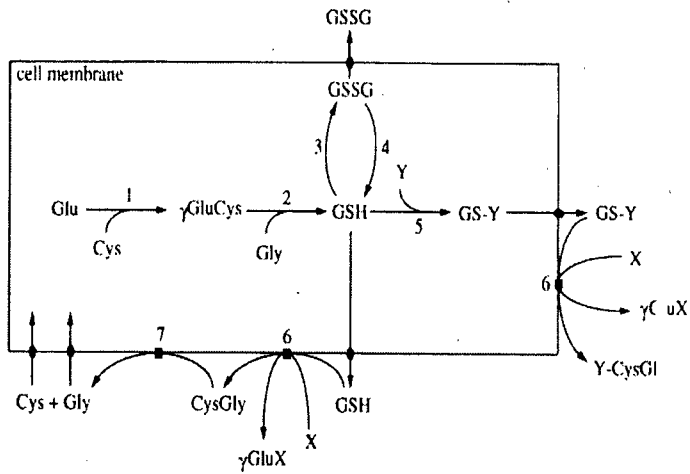


Figure 1-1. Metabolism of GSH (modified from Dringen 2000). 'X' represents an acceptor of the γ -glutamyl moiety transferred by γ GT from GSH. 'Y', a substrate of GST. 1, γ -glutamylcysteine synthetase; 2, GSH synthetase; 3, GSH peroxidase; 4, GSH reductase; 5, GST; 6, γ -glutamyl transpeptidase; 7, ectopeptidase.

1.1.3 GSH metabolism in brain

1.1.3.1 Synthesis and Consumption of GSH in brain

GSH synthesis depends on the intracellular availability of the substrates, glutamate, cysteine and glycine. In the brain, these amino acids are not present extracellularly in high concentrations, since glutamate and glycine are neurotransmitters (Moss and Smart, 2001; Nedergaard et al., 2002) and cysteine in higher concentration is neurotoxic (Janaky et al., 2000b). Therefore GSH synthesis in certain type of brain cells will depend on its ability to use available extracellular GSH precursors. Neurons rely on the presence of extracellular cysteine for GSH synthesis and cannot use the cysteine-oxidation product cystine as GSH precursor (Sagara et al., 1993; Kranich et al., 1996). For neurons the best extracellular precursor for the glutamate moiety of GSH is glutamine (Kranich et al., 1996). In contrast to neurons, astrocytes prefer glutamate and cystine as extracellular GSH precursors (Kranich et al., 1996, 1998; Dringen and Hamprecht, 1998). This difference preference for extracellular GSH precursors prevents competition between neurons and astrocytes. However, since neurons cannot use extracellular cystine, these brain cells depend for their GSH synthesis on the supply of cysteine or a cysteine-precursor from neighboring astrocytes (Dringen et al., 2000).

Responsible for the cellular export of GSH, GSSG and GSH-S-conjugates are members of the family of multidrug resistance proteins (MRPs for human transporters; Mrps for the transporters of other species) (Borst et al., 1999; Konig et al., 1999; Leslie et al., 2001). These transporters belong to the subgroup ABCC of the ATP-binding cassette

transporters and are ATP-driven export pumps of organic anion (Borst and Oude Elferink, 2002). For the human genome, nine paralogs have been reported (MRP1 to MRP9) (Borst et al., 1999; König et al., 1999). MRP1/Mrp1 and MRP2 have been reported to mediate export of GSH and GSSG (Borst et al., 1999; König et al., 1999; Leslie et al., 2001). Of these two transporters, MRP1/Mrp1 is expressed in parenchymal brain cells *in vitro* (Decleves et al., 2000; Hirrlinger et al., 2001) and *in vivo* (Sisodiya et al., 2002). Therefore MRP1/Mrp1 is responsible for cellular export of GSH in brain.

1.1.3.2 Release of GSH from astrocytes

Release of GSH from brain cells has been reported so far only for astrocytes (Yudkoff et al., 1990; Sagara et al., 1996; Hirrlinger et al., 2002). These cells release under unstressed conditions GSH and not GSSG (Sagara et al., 1996; Stone et al., 1999) and even protect the GSH exported against oxidation by a factor released into the medium (Stone et al., 1999; Stewart et al., 2002). In contrast to astrocytes, only marginal amounts of GSH are released from cultures of neurons, microglial cells and oligodendrocytes (Hirrlinger et al., 2002c).

The release of GSH from astrocytes was initially underestimated due to the consumption of extracellular GSH by the ectoenzyme γ GT. When this enzyme is inhibited, the extracellular amount of GSH increases as a constant rate of about 3 nmol/(h \times mg protein) (Dringen et al., 1997; Hirrlinger et al., 2002c). Astroglial cultures export within 1h about 10% of their intracellular GSH (Dringen et al., 1997), which has continuously to be resynthesized from its precursors in order to maintain a constant cellular concentration. These data and the reported half life of about 5h for astroglial

GSH (Devesa et al., 1993) indicate that the export of GSH is quantitatively the most important process consuming astroglial GSH.

MRP1 and MRP2 have been reported to mediate cellular export of GSH and GSSG (Borst et al., 1999; König et al., 1999; Leslie et al., 2001). Of these two transporters only Mrp1 is expressed in cultured rat astrocytes (Decleves et al., 2000; Hirrlinger et al., 2001). In the presence of the competitive Mrp-inhibitor MK571, at a concentration of 50 μ M, the rate of GSH release from astrocytes was strongly reduced, indicating that Mrp1 is predominately responsible for the observed GSH export from astrocytes (Hirrlinger et al., 2001).

Mrp1-mediated GSH export was only observed for cultured astrocytes, although substantial amount of mRNA of this transporter have also been found in cultured neurons, oligodendrocytes and microglial cells (Hirrlinger et al., 2002a). Currently it is unclear whether these brain cell types do not express functional Mrp1 protein or whether the expressed protein is not functional as GSH exporter in these cells. An astrocyte-specific cosubstrate necessary for Mrp1-mediated GSH export has been discussed to lower the high K_m value of this transporter for GSH (Loe et al., 2000; Leslie et al., 2001). However, such a cosubstrate in astrocytes remains to be identified. Alternatively, Mrp1-mediated GSH export might depend on cell type-specific modifications of the transporter or on the presence of an additional regulatory protein that is expressed only in astrocytes.

1.1.3.3 Functions and fate of extracellular GSH in brain

Besides the intracellular functions of GSH (Cooper, 1997; Cooper and Kristal, 1997; Dringen, 2000) this tripeptide has special extracellular functions in the brain.

Extracellular GSH is a key requirement for the metabolic interaction between astrocytes and neurons in GSH metabolism. The availability of cysteine determines the level of neuronal GSH (Dringen et al., 1999). Since the presence of astrocytes maintains (Sagara et al., 1993; Keelan et al., 2001) or even increases GSH in cultured neurons (Bolanos et al., 1996; Dringen et al., 1999), cysteine is provided to neurons in the presence of astrocytes. The mechanism of the supply of cysteine from astrocytes to neurons has been resolved (Figure 1-2). First step is the export of GSH from astrocytes. Using extracellular GSH as substrate the astroglial ectoenzyme γ GT produces the dipeptide CysGly in equimolar concentrations to the GSH consumed (Dringen et al., 1997). Inhibition of γ GT completely prevented the astroglia-induced effect on the GSH content in neurons, indicating the key role of astroglial γ GT in the supply of cysteine for neuronal GSH synthesis (Dringen et al., 1999). On the other hand, inhibition of the neuronal aminopeptidase N (ApN) prevented the use of extracellular CysGly for GSH synthesis, demonstrating that intact CysGly is not taken up into neurons by a peptide transporter, but is hydrolyzed by ApN (Dringen et al., 2001). Consequently, cysteine availability for neuronal GSH synthesis depends on astroglial GSH export and extracellular processing of GSH by γ GT and ApN. With the release of the glutamate precursor glutamine by astrocytes (Hertz et al., 1999) and the extracellular generation of CysGly from GSH, all three constituent amino acids of GSH are provided from astrocytes to neurons (Dringen et al., 2000).

Figure 1-2

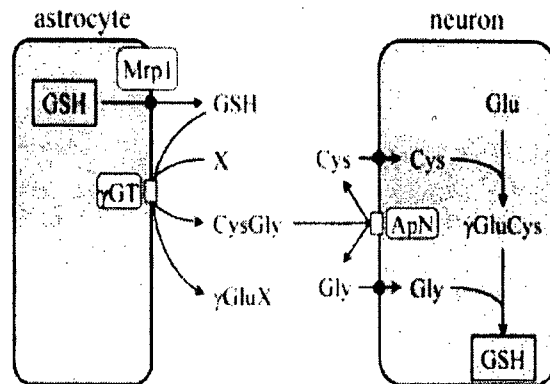


Figure 1-2. Metabolic interaction between astrocytes and neurons in the GSH metabolism of the brain (modified from Dringen and Hirrlinger, 2003). The GSH released from astroglial cells via Mrp1 is a substrate for the astroglial ectoenzyme γ GT. The CysGly generated serves as extracellular precursor of neuronal GSH. After hydrolysis of the dipeptide by aminopeptidase N (ApN), the amino acids cysteine and glycine are taken up into neurons. 'X' represents an acceptor of the γ -glutamyl moiety transferred by γ GT from GSH.

GSH reacts non-enzymatically with a variety of different radicals. Therefore, extracellular GSH might function as a first line of defense against ROS generated in the extracellular space. Extracellular GSH could also serve as substrate for extracellular GPx (Brigelius-Flohe, 1999). However, the expression of this enzyme in brain cells and its function in the brain remains to be elucidated. In addition, the GSH released from astrocytes may, at least in part, contribute to the maintenance of the GSH level in cerebrospinal fluid (Anderson et al., 1989). Interestingly, a reduced concentration of GSH in the cerebrospinal fluid of schizophrenic patients can be correlated with a lowered amount of GSH in the prefrontal cortex of the brain (Do et al., 2000).

The cellular GSH consumed by export or by reactions of GSTs has to be replaced by synthesis of GSH from the constituent amino acids to maintain a constant intracellular steady state level. Alternatively, cellular uptake of intact GSH could replenish intracellular GSH levels. However, since extracellular concentrations of GSH in brain are at best 2 μM (Yang et al., 1994; Lada and Kennedy, 1997; Han et al., 1999), such an uptake would require high amounts of energy to accumulate GSH in cells against the steep concentration gradient established by the millimolar intracellular concentration of GSH. Elevation of cellular GSH content after incubation of cultured neurons (Sagara et al., 1996) or astrocytes (Dringen, 2000) with extracellular GSH has not been observed. Therefore, such uptake processes can most likely not substantially contribute to the replenishment of cellular GSH.

1.1.3.4 Export of GSSG from astrocytes during oxidative stress

For several tissues and cell types, a release of GSSG during oxidative stress has been reported and proposed as a mechanism of cellular self-defense (Sies et al., 1972; Akerboom et al., 1982; Sies and Akerboom, 1984; Ishikawa and Sies, 1989). The transporters responsible for the cellular export of GSSG have been identified as the MRP-family members MRP1 (Leslie et al., 1996) and MRP2 (Fernandez-Checa et al., 1992; Paulusma et al., 1999). Of these two transporters rat astrocytes express only Mrp1 (Hirrlinger et al., 2001, 2002a). GSSG is effectively transported by MRP1 with a K_m value of 93 μ M (Leier et al., 1996). Under non-stressed conditions astrocytes do not export GSSG, since cellular GSSG is hardly present in the cells due to the function of GR (Hirrlinger et al., 2001). However, after application of peroxide, GSSG is transiently detectable in astrocytes (Dringen and Hamprecht, 1997; Dringen et al., 1998; Kussmaul et al., 1999) and a loss of cellular GSH was observed (O'Connor et al., 1995; Peuchen et al., 1996; Dringen and Hamprecht, 1997; Dringen et al., 1998; Kussmaul et al., 1999). In contrast to a bolus application of peroxides, application of a chronic hydrogen peroxide-induced oxidative stress by a peroxide generating system caused in cultured astrocytes a rapid and prolonged increase in intracellular GSSG (Hirrlinger et al., 2001). This export of GSSG from astrocytes was strongly inhibited in the presence of MK571 (Hirrlinger et al., 2001), demonstrating that Mrp1 mediates the export of GSSG from cultured astrocytes during oxidative stress. Consequently, besides its involvement in astroglial GSH export under unstressed conditions, Mrp1 mediates also GSSG export during oxidative stress.

Accumulation of extracellular GSSG can be a consequence of the oxidation of GSH released from astrocytes or of intracellular accumulation of GSSG during oxidative stress and subsequent export from cells. Consequently, extracellular GSSG can be considered as an indicator for oxidative stress. Nevertheless, GSSG may also have important extracellular functions in the brain. GSSG has been discussed as agonist and modulator of glutamate receptors in brain (Sucher and Lipton, 1991; Varga et al., 1994, 1997; Ogita et al., 1995; Janaky et al., 1999). Such functions may be especially important to protect neurons against glutamate excitotoxicity, since extracellular GSSG downregulates the response to stimulation of the NMDA type of glutamate receptors on neurons (Sucher and Lipton, 1991). Whether such an antioxidative function of GSSG is important for the brain remains to be elucidated.

1.1.4 GSH deficiency and neurological diseases

Oxidative stress was reported to connect with physiological processes such as aging (Finkel and Holbrook, 2000) and with pathological processes in neurological disorders (Bains and Shaw, 1997; Jenner and Olanow, 1998; Schulz et al., 2000; Vila et al., 2001; Bharath et al., 2002). A reduction in GSH content of given areas of the human brain has been reported for PD (Sofic et al., 1992; Sian et al., 1994), schizophrenia (Do et al., 2000), Alzheimer's disease (Gu et al., 1998) and epilepsy (Mueller et al., 2001) as well as in rat models for Huntington's disease (Cruz-Aguado et al., 2000a, b). Presently it is not known whether the decline in the GSH concentration in pathological brains is due to insufficient synthesis of GSH, or to elevated consumption of GSH, which is not

compensated by increased GSH synthesis. Disturbance of GSH metabolism as well as GSSG export from brain cells during oxidative stress could contribute to the reduced GSH levels of diseased brain.

1.1.4.1 GSH in Parkinson's disease (PD)

Best evidence for a disturbed GSH metabolism in brain as an important factor contributing to the pathogenesis of a disease has been reported for PD (Schulz et al., 2000; Bharath et al., 2002). This disease is characterized by a progressive degeneration of dopaminergic neurons in the substantia nigra pars compacta. The etiology of the disease is unknown, but biochemical analysis of post mortem tissues provides evidence for oxidative stress in the substantia nigra during this disease (Jenner and Olanow, 1998; Schulz et al., 2000). The GSH content in this brain region is decreased by 40-50% compared with controls (Sofic et al., 1992; Sian et al., 1994). On the cellular level a significant loss of GSH in the surviving nigral neurons has been reported (Pearce et al., 1997). The importance of the decline of GSH levels during the progression is underscored by the lowered GSH level in the substantia nigra found for incidental Lewy body disease, a presymptomatic form of PD (Dexter et al., 1994). A loss of GSH alone appears not to be responsible for the nigrostriatal damage in PD, since reduction of brain GSH levels by chronic infusion of buthionine sulfoximine, an inhibitor of γ GluCys synthetase, did not reduce the number of dopaminergic neurons (Toffa et al., 1997). The GSH depletion may rather enhance the susceptibility of brain cells against other harmful events, such as the reduction of mitochondrial energy production. A synergistic effect of

a lowered intracellular GSH concentration and a reduced ATP production in increasing the susceptibility of dopaminergic neurons has been described for the *in vitro* and *in vivo* situation (Zeevalk et al., 1997, 1998).

1.1.4.2 GSH and stroke

Stroke is one of the main causes of adult disability and death. This disorder most commonly results from the occlusion of a major blood vessel in the brain (Ameriso and Sahai, 1997), resulting in localized reductions in blood flow. The affected tissue typically contains a severely ischemic core or focus surrounded by more moderately ischemic perifocal or penumbral regions (Jacewicz et al., 1992; Memezawa et al., 1992a). Reactive oxygen species (ROS) have been implicated in many studies as one important contributor to ischemic cell death (see for example Liu et al., 1989; Kinouchi et al., 1991; Cao and Phillis, 1994; Yu et al., 1998). GSH is a central component in the antioxidant defences of cells, acting both to directly detoxify ROS and as a substrate for several peroxidases (Dringen, 2000). Thus, alterations in the availability of this metabolite during ischemia or early reperfusion are likely to influence tissue damage. Consistent with this possibility, a treatment that depletes GSH by inhibiting synthesis has been found to increase infarct volume resulting from focal ischemia in rat brain (Mizui et al., 1992). Anderson et al. (2002) have found that total GSH was substantially decreased in mitochondria prepared from severely ischemic focal tissue in both cerebral cortex and striatum. Injecting GSH monoethyl ester, which can be converted to GSH in cells, to third ventricle prevented the

GSH loss in mitochondria and significantly decreased infarct size after stroke (Anderson et al., 2004a, 2004b).

1.1.4.3 Therapeutic approaches for neurodegenerative diseases

If alterations in glutathione metabolism play an important role in the pathogenesis of the neurodegenerative diseases, treatments that lead to enhanced synthesis of GSH or that inhibits its degradation may result in a slowing of disease progression. Because GSH itself penetrates the blood-brain barrier only poorly and cannot be taken up by neurons directly, treatments with GSH monoethyl ester, GSH precursors or other GSH analogs have been used in patients or animal models.

The GSH analog YM737 provides protection against cerebral ischemia in rats by inhibiting lipid peroxidation (Yamamoto et al., 1993). Since GSH synthesis in neurons is limited by the availability of cysteine (Dringen et al., 2000), compounds that can be metabolized to cysteine could be used as pro-drugs to increase neuronal GSH concentrations. In mice, treatment with the GSH precursor N-acetyl-L-cysteine resulted in a significant reduction of motor neuron loss and elevated GSH peroxidase levels with the cervical spinal cord (Henderson et al., 1996). Treatment with L-2-oxothiazolidine-4-carboxylate, a cysteine precursor, stimulates growth and normalizes tissue GSH concentrations in rats fed a sulphur amino acid deficient diet (Jain et al., 1995). Unfortunately, the therapeutic window for treatment with substances that increase brain cysteine may be narrow, because cysteine is potentially toxic for neurons (Olney et al., 1990). Alternatively, GSH in brain can be increased by intracerebroventricular

administration of the dipeptide γ -glutamylcysteine (Pileblad et al., 1992). Neurons can utilize either glutamylcysteine or cysteinylglycine for the synthesis of GSH (Dringen et al., 1999).

Although a disturbance of GSH homeostasis has been implicated in the pathogenesis of several neurodegenerative diseases it remains open to debate whether: (1) at least in some illnesses, this is a primary defect or only a consequence of ROS generation; (2) brain GSH can be increased safely using different treatment strategies; and (3) an increase of brain GSH will result in clinical benefit and neuroprotection in animal models or in human diseases.

1.2 Imaging and measurement of GSH in brain

Quantitative measurements of GSH usually involve extraction of the tissues followed by derivatization to give a chromogenic or fluorogenic compound that can be analysed by spectrophotometry or high performance liquid chromatography (HPLC) (Newton et al., 1981), or by absorption measurement after oxidation by 5,5'-dithio-bis-2-nitrobenzoic acid) (DTNB) (Anderson, 1985) or following conjugation to 1-chloro-2,4-dinitrobenzene (CDNB) in the presence of glutathione S-transferase (GST) (Hermsen et al., 1997).

Although specific and sensitive, these methods require extraction of the tissue and only provide an average estimate for all cells in the tissue.

1.2.1 Different dyes to image GSH

In principle, imaging GSH with GSH-sensitive fluorescent dyes would permit monitoring of the relative cellular distribution of GSH. Choice of an optimum dye for use is dependent on several factors. Adducts are formed between the dye and the sulfhydryl group of GSH, resulting in a dramatic increase in fluorescence intensity and/or altered excitation/emission spectral properties of the dye. A primary concern is that dyes may react with intracellular thiol other than GSH, particularly protein sulfydryls, resulting in high levels of background fluorescence. Adduct formation between GSH and the dyes containing a chloromethyl group is catalyzed by GST, conferring a high degree of specificity of these dyes to GSH, thereby allowing staining at concentrations that impart very low background labelling of proteins (Meister et al., 2001). However, GSTs consist of several isoenzymes and, due to differing specificities for fluorophores, differ in their ability to catalyze adduct formation (Lowndes et al., 1994). Furthermore, the isoenzyme classes differ markedly with regard to cellular distribution and expression levels during development in the brain (Johnson et al., 1993; Lowndes et al., 1994; Beiswanger et al., 1995; Philbert et al., 1995). GST-independent dyes isolate the GSH-dependent component of cellular fluorescence, but may not possess the higher selectivity for GSH over other thiols. Other factors affecting the utility of GSH-sensitive dyes include feedback inhibition by the conjugate on GST activity, new synthesis of GSH, transport of the fluorescent adduct out of the cell and decomposition to other fluorescent products (van der Ven et al., 1994; Barhoumi et al., 1995; Poot et al., 1996).

There are six fluorophores that can be used to evaluate GSH. Four of the dyes require GST to form a fluorescent conjugate. These include: t-butoxycarbonyl-Leu-Met-7-amino-4-chloromethylcoumarin (CMAC), 7-amino-4-chloromethylcoumarin (CMAC-blue), monochlorobimane (MCB), and 5-chloromethylfluorescein diacetate (CMFDA). The other two dyes don't require GST for adduct formation with GSH. These include: 2, 3-naphthalenedicarboxaldehyde (NDA) and o-phthaldehyde (OPD) (Tauskela et al., 2000). In Tauskela et al. (2000) paper, they tested the specificity of these dyes for GSH in neurons and astrocytes cultures. They found that three of the four GST-sensitive dyes- CMAC, CMAC-blue, and MCB-displayed substantial sensitivity to GSH, as staining was lost when immature cultures were depleted of GSH by pretreatment with DEM (diethyl maleate) or BSO (DL-buthionine-(S,R)-sulfoximine). Of these three dyes, CMAC and MCB seem most appropriate for use in immature cultures, although the basis for why these dyes produce different intracellular staining patterns is unknown. CMAC-blue did not stain all cells in immature cultures. CMFDA was not sensitive to GSH, indicating that generation of the fluorescent 5-chloromethylfluorescein by esterase hydrolysis within the cells preceded the reaction with thiol-containing species. Of the two GST-independent dyes, OPD was partially specific to GSH, while NDA was insensitive to GSH (Tauskela et al., 2000).

1.2.2 Two-photon imaging of GSH with MCB

In our study, we used MCB as a specific probe for GSH. MCB can be conjugated with GSH, catalyzed by GST. The fluorescent adduct can be excited at 390 nm, and emits at

450~575nm. It can also be excited with two-photon at 780nm (Meister et al, 2000). The ability to measure GSH at the cellular level by two-photon laser scanning microscopy (TPLSM) overcomes some of the limitations inherent with conventional biochemical techniques, which require extraction of the tissue and therefore give average levels in whole tissues.

Several features of TPLSM combine to allow imaging deeper into highly scattering biological tissues and generate images with enhanced contrast (Meister et al, 2000). Near infrared light typically penetrates biological material significantly better than blue or UV light with less scattering and refraction (Duck, 1990). In our study, we were able to use TPLSM to image as deep as -250 μm in live animal brain, providing direct evidence on the GSH distribution in neocortex.

1.3 Structure and function of meninges

Meninges include the three membranous layers of connective tissue that envelop the brain and spinal cord. The outermost layer, or dura mater, is extremely tough and is fused with the membranous lining of the skull. In the brain it forms a vertical sheet that separates the cerebral hemispheres and a horizontal sheet that lies between the cerebrum and the cerebellum. The thin arachnoid membrane lies below and in close contact with the dura mater. The innermost layer, or pia mater, is in direct contact with the brain and spinal cord and contains the blood vessels that supply them. The pia mater and arachnoid membrane are separated by the subarachnoid space containing the cerebrospinal fluid, which carries nutrients, absorbs the impact of shocks, and acts as a barrier to disease

organisms. Thus, the meninges provide a fluid-filled jacket for the protection of neural tissues and allow for the flexing and twisting of the vertebral column about the spinal cord (Zigmond et al., 1999).

1.3.1 Function of meninges

Little attention has been paid to the meninges except for the physical role at the CSF-blood barrier (Nilsson et al., 1992; Smith and Shine, 1992; Tanno et al., 1993). So far, there are a few physiological findings suggesting their participation in the trophic support of neurons. For example, fetal brain neurons transplanted into the subarachnoid or meningeal space can survive, grow over the brain surface, and exhibit facilitated neuritic elongation (Ueda et al., 1989; Kyoshima et al., 1992; Risling et al., 1992). When fetal meningeal tissues are transplanted onto the median eminence of adult rats, regenerating fibers of vasopressin neurons innervate the grafts heavily following hypophysectomy (Ishikawa et al., 1995). Furthermore, the medium conditioned with cultured meningeal cells promotes the survival of various brain neurons *in vitro*. These findings may raise the possibility that the meninges secrete some biologically active substances that play an important role in the maintenance or regulation of brain function. Consistent with this, Ohe et al. (1996) examined the profile of the proteins secreted from cultured meningeal cells with sodium dodecyl sulphate-polyacryl-amide gel electrophoresis, and found that meningeal cells can secrete cerebrospinal fluid proteins that play important roles in certain biological events in the brain (Ohe et al., 1996).

1.3.2 Meninges express high level of xCT, cystine/glutamate antiporter

Recently, Sato et al. (2002) used *in situ* hybridization to show that meninges express a high level of xCT. xCT is a subunit of system x_c⁻, which transports an anionic form of cystine in exchange for glutamate (Bannai, 1986). xCT has 12 putative transmembrane domains, whereas the other subunit, 4F2hc, is predicted to have a single transmembrane domain (Sato et al., 1999). The xCT subunit is responsible for the specificity of this antiporter, and is expressed in the area postrema, subfornical organ, habenular nucleus, hypothalamic area, ependymal cells of the lateral wall of the third ventricle, and meninges (Sato et al., 2002). Since meninges faces CSF, which has plenty supply of cystine, it is possible that meninges can take up cystine efficiently from xCT. With this high level of cystine, meninges may have high level of GSH. In our study, we looked into the GSH metabolism in meninges, and found meningeal cells are very active in GSH metabolism.

1.4 Rationale of research

There have been several biochemical assays to measure GSH level in tissue. However, these methods can only give an average value of GSH concentration in tissue homogenate. In my project, I used TPLSM to image GSH distribution in brain with MCB, which can give a detailed map of GSH distribution and measure GSH concentration in single cells. First I established that MCB is a specific probe for GSH. The fluorescence of the conjugate can be imaged with TPLSM, and the intensity can reflect intracellular

GSH level. After that, I set out to measure GSH distribution in different brain regions in rat brain slices with TPLSM. By converting the fluorescence intensity to GSH concentration, I can get a detailed map of GSH distribution in brain. With TPLSM, I was also able to measure GSH distribution *in vivo* with live animals. This is closer to biological reality since there is no blood supply in slices. With this approach, I found that *in vivo*, GSH is highly expressed in meninges and astrocytes.

Since there is some preliminary data in our lab that meninges may be efficient in protecting neurons, I examined the GSH metabolism in meninges in more detail. I developed an assay, with MCB and plate reader, to measure different kinetic parameters of GSH metabolism in cultures. With this assay, I found that meninges are more active in GSH metabolism than cortical cells, which may be able to explain the neuroprotection function of meninges.

Chapter 2 Materials and Methods

2.1 Chemicals

All reagents were purchased from Sigma-Aldrich Canada (Ontario, Canada) unless mentioned. Monochlorobimane was purchased from either Fluka or Molecular Probes and made as a 100 mM stock solution in dimethyl sulfoxide (DMSO) and stored at -20°C. Sulforhodamine 101 (SR 101) was prepared as a 10 mM stock solution in DMSO and also stored at -20°C. MK-571 was purchased from Alexis Biochemicals. Propidium iodide (PI) was purchased from Molecular Probes and made as a 10 mM solution in PBS, and stored at 4 °C. Primary antibodies used in this study included anti-laminin (rabbit), anti-S-100 β (mouse), anti-NeuN (mouse, Chemicon), anti-doublecortin (goat, Santa Cruz). Secondary antibodies included FITC-anti rabbit, FITC anti-mouse, Alexa 594-anti mouse (Molecular Probes), and Alexa 488-anti goat (Molecular Probes).

2.2 Astrocytes and meninges culture

Astrocyte cultures were prepared from 0 to 2 day old Wistar rats. The animals were anesthetized with cold, sacrificed by decapitation, the skulls opened and the brains removed in sterile PBS. The meninges were carefully removed from the brains. The remaining cortices were digested in papain at 37°C for 10min. The meningeal and cortical cells were plated separately in MEM (Invitrogen Cat# 51200-038) amended to 15.6mM glucose, 2mM glutamine, 10% fetal bovine serum, and 100U/mL penicillin/

streptomycin (Invitrogen Cat# 15140). Cells were passaged by trypsinization at 1 week at a concentration to yield 75 to 90% confluence on the day of the MCB assay. Cells were plated into 24 well plates from either Corning or Falcon. To inhibit the GSH synthesis, the cultures were incubated with 10 μ M L-Buthionine-sulfoximine (BSO) overnight. To induce the phase II pathway, the cultures were incubated with 20 μ M *tert*-Butylhydroquinone (tBHQ) overnight.

2.3 Plate reader GSH assay

Fluorometric assays were performed using a plate reader (Fluoroskan Ascent FL); $\lambda_{\text{ex}} = 355 \pm 19\text{nm}$, $\lambda_{\text{em}} = 527 \pm 5\text{nm}$. Although these excitation/emission filters are sub-optimal for MCB detection, they prevented saturation of the detector within the plate reader permitting linearity between the concentration of MCB-GSH and detected fluorescence over the range associated with the fluorescence values in our measurements. Purified 200 μ M GSH and 10 μ M MCB were added together, with varying concentrations of purified GST enzyme (0, 0.01, 0.02, 0.04 units). Fluorescence was measured using a plate reader over a 4 h reaction period. All cell reactions were carried out in Hank's Balanced Salt Solution (HBSS) (138mM NaCl, 5mM KCl, 0.34mM Na_2HPO_4 , 10mM Na^+ HEPES, 1mM NaHCO_3 , 20mM Glucose, 2.5mM CaCl_2 , and 1mM MgSO_4). During the assay cells were bathed in either HBSS as control, or HBSS with the following: 100 μ M GSH, 100 μ M cystine, or a 100 μ M cocktail of GSH precursors (glutamate, cystine, glycine). Efflux was estimated by measuring the change in cell fluorescence after changing the media. To inhibit the efflux, 25 μ M MK571 was added to

the cultures. To test temperature effect on GSH-MCB efflux, room temperature (20°C) and 37°C were present respectively during plate reader assay. Plates were not agitated between the measurements, so that cells sedimented and formed a thin layer at the bottom of the wells.

2.4 Calibration of the GSH-MCB fluorescence

A 5 mM stock solution of GSH-MCB was made from 20 mM GSH and 3 mM MCB in the presence of a GST. Excess GSH and GST were used to ensure that all MCB was conjugated. A dilution series of 5 mM, 1.5 mM, 0.5 mM, 0.15 mM was made from this stock. The standard solutions were contained within in vitro cells (glass microcuvettes, ID = 50 μ m VitroCom), and imaged with two-photon microscopy. This method of GSH-MCB calibration was routinely used in our studies in brain slices.

2.5 Rat brain slices preparation

Coronal brain slices were prepared from P15-21 or P1-2 Wistar rats (Charles River, Canada). Under halothane anaesthesia, animals were decapitated with a guillotine and the brain was quickly removed from the skull and placed in ice-cold cutting solution containing (in mM): 200 sucrose, 2.5 KCl, 0.5 CaCl₂, 26.2 NaHCO₃, 10 MgSO₄·7H₂O, 1 NaH₂PO₄, 11 glucose (pH maintained at 7.4 by saturation with 95%O₂ and 5%CO₂). Using a scalpel blade (FisherScientific, 08-916-5A, No. 10), the brain was manually sliced into two hemispheres. One of the hemispheres will be sectioned to slices. The total

period from decapitation to cutting brain to two halves is restrained in 5 minutes. Slices (300 μm) were obtained with a vibratome (Leica VT 1000 S) and then transferred to a static bath chamber where they were maintained at room temperature for at least 1 h before imaging. The slices were kept in artificial cerebral-spinal-fluid (ACSF) containing (in mM): 120 NaCl, 26.2 NaHCO₃, 24.2 glucose, 2.5KCl, 1.25 NaH₂PO₄, 1 MgCl₂·6H₂O, 2 CaCl₂, saturated with 95% O₂ and 5% CO₂. For imaging, individual slices were transferred to a recording chamber and perfused with ACSF saturated with 95% O₂ and 5% CO₂. MCB was added to the perfusion system at a final concentration of 60 μM . To identify dead cells, we added 10 μM propidium iodide together with MCB.

2.6 Animal preparation for in vivo imaging

All experiments were approved by the University of British Columbia Animal Care Committee and were conducted in strict accordance with guidelines by the Canadian Council on Animal Care. C57Bl/6 mice were purchased from the Jackson Laboratory (Bar Harbor, ME) and bred at the University of British Columbia animal facilities. Cranial windows for *in vivo* imaging were produced as described previously in (Zhang et al., 2005). In brief, mice aged 3–5 months were deeply anesthetized with an intraperitoneal injection of urethane (0.12% w/w, supplemented with 0.02% w/w as needed) (Kleinfeld et al., 1998) and 20 mM glucose in PBS was supplemented to maintain animal hydration (0.2–0.3 ml, intraperitoneal injection, every 1 h). Body temperature was maintained at 37°C using a feedback regulated heating pad. An air-powered dental drill was used to produce a 2 x 2 mm² cranial window over the

somatosensory cortex at coordinates of 0.8 mm from bregma and 2.0 mm lateral, leaving the dura intact. A stainless-steel chamber that surrounded the craniotomy was glued to the skull with Krazy Glue (Elmer's Products, Columbus, OH). To reduce movement artifacts, the area between the chamber and the skull was filled with dental acrylic (Kleinfeld and Denk, 2000). The exposed cortical surface and chamber were filled with 2% (w/v) agarose (diluted in PBS or a HEPES-buffered ACSF) and sealed with a cover glass. For *in vivo* labeling, MCB and SR 101 stocks were dissolved in PBS to a final concentration of 100 μ M and applied directly to the exposed brain surface. During the entire imaging session, mice were maintained under urethane anesthesia.

2.7 Two-photon microscopy

Two-photon excitation of GSH-MCB conjugates was achieved using a Coherent (Santa Clara, CA) Mira 900 Ti:sapphire laser pumped by a 5 W Verdi laser tuned to 780 nm. Images were acquired using custom software routines (IgorPro; Wavemetrics, Eugene, OR) and by using an Olympus (Tokyo, Japan) IR-LUMPlanFl water-immersion objective (40x; 0.80 numerical aperture). When MCB was used in combination with SR 101, the laser was operated at 800 nm and fluorescence was collected using photo-multiplier tube 1 (PMT1) for the GSH-MCB signal (512-562 nm), and PMT2 for the SR 101 signal (620-645 nm). For immunostaining, FITC, Alexa 488 and Alexa 594 were used as secondary antibody fluorophores. All fluorophores were excited at 800 nm. FITC and Alexa 488 were collected on PMT1 and Alexa 594 was collected on PMT2. All images were taken at 1024 \times 1024 pixels. For imaging in rat brain slices to measure GSH concentration, certain laser intensity was used for entire imaging and a standard curve

was made at this intensity with GSH-MCB 0.1mM, 0.3mM, 1mM, and 3mM. For imaging *in vivo*, to minimize photodamage, the excitation laser intensity was adjusted depending on the depth of the focal plane (lower intensity at shallower depths) and always kept at a minimum for a sufficient signal-to-noise ratio.

2.8 Immunostaining

After MCB labeling and two-photon imaging, slices were fixed with 4% paraformaldehyde in 0.1 M phosphate buffer (pH 7.2) for 1 h. Slices were then rinsed twice with PBS, and then incubated in Triton X-100 (0.5% in PBS) for 0.5 h to make the membrane permeable to antibodies. After that, slices were immunostained with primary antibody against S-100 β (from mouse, 1:1000 in antibody buffer), NeuN (from mouse, 1:100 in antibody buffer), GFAP (from mouse, 1:200 in antibody buffer), laminin (from rabbit, 1:500 in antibody buffer), or doublecortin (from goat, 1:200 in antibody buffer) for 48 h at 4 °C. The antibody buffer contained 0.1% Triton X-100 and 2% goat serum in PBS. After washing twice with PBS, the slices were incubated with secondary antibodies (FITC-anti rabbit, FITC-anti mouse, Alexa 488-anti goat, Alexa 594 anti-mouse; diluted 1:200 in antibody buffer) for 48 h in dark at 4 °C. After secondary antibody labelling, slices were washed with PBS twice, and imaged with two-photon microscopy.

For immunostaining of meninges, astrocytes, or cortical cell cultures after plate reader assay with MCB labelling, we fixed the cells with 0.2% glutaraldehyde (in 4% PFA) for 0.5h. Experiments showed that under these conditions, MCB-GSH conjugate was retained within the cells after treatment with Triton X-100 (0.5% in PBS) for 0.5h.

Cell cultures were then treated with a blocking solution (4% normal goat serum in PBS) and incubated with mouse IgG anti-s100 β , or mouse IgG MapII, 1:1000 diluted in antibody buffer (as we described above). After three washing steps of 10 min each with 0.1M PBS, cell cultures were incubated overnight with a fluorescent secondary antibody 1:200 (goat antimouse IgG, Alexa 594-labeled) following which these cells were washed and embedded with a drop of Immunomount. Fluorescence images were collected at a Axiophot photomicroscope (Zeiss) equipped with a CCD camera.

2.9 Glutathione S-transferase (GST) assay

Mouse brain and live tissue were dissected in ice-cold PBS and homogenized with 10 strokes of a dounce homogenizer in tissue buffer containing 25 mM Tris, pH 7.4 and 250 mM sucrose. Crude homogenate supernatants were collected and promptly assayed for enzyme activity. The GST assay consisted of 1mM 1-chloro-2, 4-dinitrobenzene (CDNB), 1mM GSH, and 100 μ g/ml protein at 37°C in 100 mM potassium phosphate buffer, pH 6.5 (final concentration in 150 μ l reaction volume). The GST reaction was monitored at 340 nm, and the spontaneous nonenzymatic slope was subtracted from the total observed slope. The extinction coefficient for CDNB was 9600 M/cm. Protein concentration was measured using the bicinchronic acid method according to the protocol of the manufacturer (Pierce, Rockford, IL).

2.10 Total intracellular GSH assay

Total GSH was quantified by the method of Tietze (1969). Briefly, the acid-soluble fraction was obtained by adding perchloric acid to a final concentration of 3%, followed by centrifugation at 14,000×g for 10 min. The acid-soluble fraction was neutralized to pH 7 with 0.5M KOH/50mM Tris. After the removal of precipitate (potassium perchlorate) by a second centrifugation, 50 µl aliquots of sample were combined with 100 µl of reaction mixture consisting of 2.5 ml of 1mM 5, 5', dithiobis-(2-nitrobenzoic acid) (DTNB), 2.5 ml of 5mM NADPH, and 2.65 ml of phosphate buffer (100 mM NaPO₄, pH 7.5, 1mM EDTA), glutathione reductase (5U/ml final). The increase in A₄₁₂ from GSH-mediated reduction of DTNB was measured at 30 sec intervals over 30 min. GSH content among treatment groups was normalized to protein.

2.11 Data and image analysis

All plate reader experiments were done at least five different times unless otherwise stated. Results are presented as the mean±SE. Statistical analysis of raw data was performed with Excile XP and Origin 6.0. Experimental groups were compared by Student's t-test. A statistical probability of p<0.05 was considered significant, p<0.01 was considered very significant.

Image analysis was performed using NIH ImageJ software (<http://rsb.info.nih.gov/ij/>). To reduce photon and PMT noise, a median filter (radius = 1) was applied. The

fluorescence intensity was converted to GSH-MCB concentration according to a standard curve. The time course curves of MCB labeling of rat brain slices were fitted with Origin 6.0. For statistical analyses, two-tail paired *t*-test or repeated measures one-way ANOVA was used with GraphPad Prism (version 2.01). Data were expressed as mean \pm SEM.

Chapter 3 Results^{1,2}

3.1 Specificity of MCB labelling

Currently, monochlorobimane (MCB) is the probe of choice for measuring GSH levels in intact cells. MCB is essentially non-fluorescent in the absence of GSH. In a reaction catalyzed by GSH-S-transferase (GST), GSH is added to MCB to make a product with blue-green fluorescence (Figure 3-1A, Cook et al., 1991, Ublacker et al., 1991). MCB has advantages over other bimane derivative dyes for measuring GSH level, such as monobromobimane (MBB) and monobromotrimethylammoniumbimane (QBB), since it shows very low affinity for other low molecular weight or protein thiols (Meyer et al., 2001).

3.1.1 MCB labelling of GSH is dependent on GST

We further tested the specificity of MCB in *in vitro* experiments using purified GST, the reduced form GSH, and MCB to produce a fluorescent GSH-MCB adduct quantified by plate reader. In the absence of GST, addition of 200 μ M GSH to 10 μ M MCB resulted in a modest linear increase in fluorescent product over time. Addition of purified GST resulted in a robust single exponential phase increase in the fluorescence intensity,

¹ A version of part of this chapter has been published: Sun X, Erb H, Murphy TH (2005) Coordinate regulation of glutathione metabolism in astrocytes by Nrf2. *Biochemical and Biophysical Research Communication*. 326: 371-377.

² A version of part of this chapter has been submitted to *Journal of Neuroscience*: Sun X, Shih AY, Johannssen HC, Erb H, Li P, Murphy TH (2005): Two photon imaging of glutathione levels in intact brain indicates sites of enhanced redox buffering.

indicating that this is an enzyme-catalyzed reaction following first order kinetics (Figure 3-1B). The curve can be fitted with an equation:

$$F = F_0 + F_{\max} (1 - \exp(-(t-t_0)/\tau)) \quad \text{..... (Equation 1)}$$

F is the fluorescence intensity, F_{\max} is the maximum level of fluorescence intensity, and τ is the time constant of the reaction. The plateau level of the reaction was only related to the amount of GSH and MCB added, regardless of GST amount, while the initial conjugation rate was proportional to the GST amount (Copeland, 2000). The time constants of the exponential phase were 1437, 691, 344 sec, respectively for 0.01, 0.02, 0.04 units of GST. The dependence on GST confers the specificity of MCB for labelling GSH.

Figure 3-1

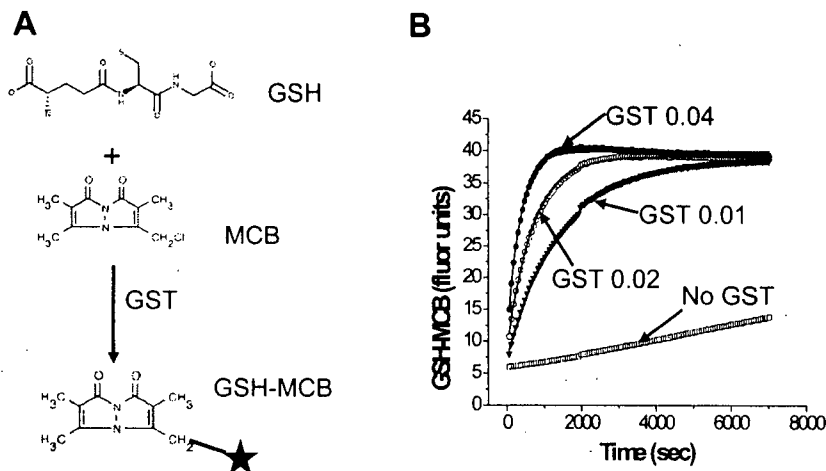


Figure 3-1. MCB can specifically label GSH. (A). Reaction between GSH and MCB, catalyzed by GST. The product has blue-green fluorescence. (B). *In vitro* experiments with the reduced form of GSH (200 mM), MCB (10 mM) and the indicated amounts of purified GST (0, 0.01, 0.02, 0.04 units). The reaction was carried out at 37°C. The fluorescence intensity was measured with a plate reader ($\lambda_{ex} = 355 \pm 38$ nm, $\lambda_{em} = 527 \pm 5$ nm).

3.1.2 MCB could be used to label intracellular GSH with the plateau level of fluorescence intensity indicating the cellular GSH level

The formation of a highly fluorescent GSH-MCB conjugate is catalyzed by glutathione-S-transferase (GST), which has three isoforms, alpha (α), mu (μ), and pi (π), with the μ form being the most efficient. The μ GST isoform is present in neurons and glia and in most brain regions (Beiswanger et al., 1995). Since MCB is a membrane permeable dye (Chatterjee et al., 1999) and GST is widely expressed in brain cells, we assumed that the GSH in brain cells should be able to be labelled by MCB and the fluorescence intensity of GSH-MCB will be related to the cellular GSH level. We confirmed this by showing that MCB labelling of astrocyte cultures which had been pretreated with glutathione synthesis inhibitor buthionine sulfoximine (BSO) have a significantly reduced MCB fluorescence (Sun et al., 2005a). We applied 10 μ M MCB to the astrocyte culture to label intracellular GSH and monitored the time course of the reaction by measuring the fluorescence intensity of GSH-MCB conjugates with a plate reader, with $\lambda_{ex}=355\pm 19\text{nm}$, $\lambda_{em}=527\pm 5\text{nm}$. After about 15min, the reaction reached a plateau amount of fluorescence reflecting the GSH content of the cells (Figure 3-2). After the plateau had been reached exogenous GSH was added and the fluorescence intensity showed a further linear increase indicating that MCB is in large excess over GSH and that the fluorescence values observed were not saturating (data not shown). In order to confirm that the plateau level represented intracellular GSH content, we depleted the cells of GSH by addition of BSO, which is a specific inhibitor of γ -glutamylcysteine synthetase, the rate-limiting enzyme for glutathione synthesis (Anderson, 1998).

Pretreatment with BSO is known to deplete the level of nonprotein thiols such as GSH while having a minimal effect on other cellular sulphhydryls (Hedley and Chow, 1994; Thomas et al., 1995). For astrocytes BSO is reported to decrease the level of glutathione with a half-life of approximately 5 h (Devesa et al., 1993). MCB labelling of astrocytes cultures which have been pretreated with 10 μ M BSO for 24h showed a significant decrease in the fluorescence intensity, supporting our hypothesis that the GSH-MCB fluorescence reflects the amount of GSH within cells (Figure 3-2 A). The reduced fluorescence was not due to a direct effect of the BSO itself since addition of exogenous glutathione produced GSH-MCB fluorescence within these cells (Sun et al, 2005a). Consistent with the proposal that the initial rate of GSH conjugation with MCB reflects GST activity and not necessarily glutathione levels, we observed that treatment with BSO to lower GSH did not affect the initial GSH-MCB conjugation rate (data not shown). From the results described above we confirmed that MCB could be used to label intracellular GSH. The plateau level of fluorescence intensity indicates the GSH level, while the initial conjugation rate reflects the GST activity.

Figure 3-2

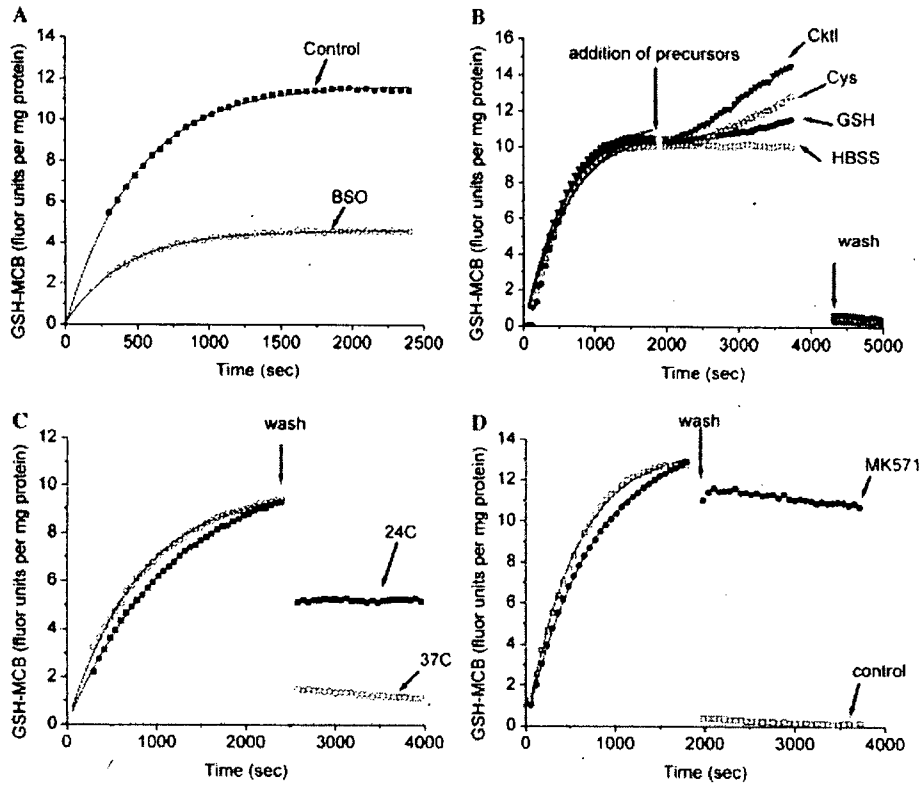


Figure 3-2. Monitoring GSH metabolism in astrocytes cultures with plate reader.

(A). Addition of 10 mM BSO inhibits GSH synthesis, reduces the GSH content of the culture and lowers the plateau level of MCB fluorescence (in this experiment 30 mM MCB was used) (B). The exponential phase reflects MCB labelling of a limited amount of intracellular GSH. The four curves all fit well to exponential equations: $F=12.5(1-\exp(-t/521.6))$, $R^2=0.9985$ (HBSS); $F=13.5(1-\exp(-t/507.4))$, $R^2=0.9935$ (GSH); $F=12.1(1-\exp(-t/505.1))$, $R^2=0.9982$ (Cys); $F=12.9(1-\exp(-t/490.6))$, $R^2=0.9981$ (Cocktail). Linear phase is in response to the addition of 100mM GSH, or cystine, or a cocktail of GSH precursors (Glu, Gly, Cys, all at 100 mM). In efflux stage, we washed cells to determine how much of the fluorescence was associated with the cells versus the media. (C, D). GSH-MCB can be exported out of cells through Mrp, which is temperature-dependent and MK571 sensitive. (C). Reaction at 37°C and 24°C. (D). Reaction with or without MK571, an inhibitor of MRP-1 mediated efflux (25mM).

3.2 GSH metabolism assay

We developed an assay to monitor the metabolism of GSH in astrocytes, using a fluorescence plate reader and monitoring the kinetics of the GST catalyzed reaction between GSH and the substrate MCB (Sun et al., 2005a).

3.2.1 Plate reader assay is a powerful system to measure intracellular GSH level in cultures

We applied 10 μ M MCB to the astrocyte culture to label intracellular GSH and monitored the time course of the reaction by measuring the fluorescence intensity of GSH-MCB conjugates with a plate reader. Since MCB is in large excess over intracellular GSH (based on the volume of cells versus the media), the reaction between GSH and MCB can be regarded as a pseudo-first order reaction. The time course of GSH-MCB production fit well to Equation 1 (Figure 3-2 B):

$$F = F_0 + F_{\max} (1 - \exp(-(t-t_0)/\tau))$$

F is the fluorescence intensity normalized to protein amount. F_{\max} is the maximum level of fluorescence intensity per mg protein, and τ is the time constant of the reaction. After subtracting the background from the measured value, the curve usually starts from the origin, and F_0 and t_0 are usually zero. F_{\max} represents the plateau level of fluorescence, while the initial slope of the curve can represent the initial formation rate of GSH-MCB conjugate and is related to the GST activity. Together, this data suggest that our plate reader time course assay is a powerful system to study the astrocytic intracellular GSH

levels. Its advantage over other techniques lies in that it can not only measure the intracellular GSH level, but also provide a measurement of kinetics parameters for GST-catalysed conjugation reactions *in situ*.

3.2.2 Plate reader assay can measure rate of GSH precursor uptake and synthesis

Astrocytes actively synthesize GSH through the consecutive reactions of two enzymes, γ -glutamylcysteine synthetase and GSH synthetase (Dringen and Hirrlinger, 2003). Our assay can also be used to monitor the GSH synthesis in astrocytes. After the MCB labelling of endogenous GSH in astrocytes has reached a plateau level, we added 100 μ M cystine, the rate-limiting precursor for GSH synthesis, or a cocktail of precursors, glutamate, glycine and cystine (100 μ M for each component), to the cultured cells. We found a significant linear increase in the fluorescence intensity, indicating that the astrocytes are active in taking up the precursors and synthesizing GSH (Figure 3-2 B). The slopes are 0.111 ± 0.0075 and 0.126 ± 0.0079 (fluorescence unit per mg protein/min), respectively for cystine and cocktail, averaged from 5 different experiments. When exogenous GSH (100 μ M) was added, the fluorescence also showed a linear increase, with a slope of 0.067 ± 0.0095 (fluorescence units per mg protein/min), significantly smaller than cystine ($p=0.013 < 0.05$) and the cystine, glutamate, glycine cocktail ($p=0.0059 < 0.05$), indicating that astrocytes are more efficient at taking up the precursors for GSH synthesis and then synthesizing GSH rather than taking up GSH directly.

However, when we add HBSS, a cerebrospinal fluid (CSF)-like solution, to the culture, the fluorescence level does not change (Figure 3-2), indicating that astrocytes could not synthesize detectable levels of GSH. This suggests that even in the condition of complete depletion of the GSH pool, astrocytes cannot synthesize GSH unless exogenous precursors are available. Since HBSS is widely used in most *in vitro* electrophysiology experiments, our data suggest that oxidative stress may be apparent in these conditions.

Our assay can also be used to explore astrocytes' preference for different precursors. When we replace the glutamate in cocktail to glutamine, the fluorescence intensity also shows a linear increase, with a slope of 0.118 ± 0.0065 (fluorescence unit per mg protein/min). The slopes are similar between cocktail with glutamate or glutamine ($p=0.278 > 0.05$), indicating that astrocytes do not show significant preference for glutamate or glutamine. This is inconsistent with other groups' data that astrocytes prefer glutamate rather than glutamine for GSH synthesis (Kranich et al, 1996, 1999; Dringen and Hamprecht 1998). One possible explanation is that in their study, they examined GSH synthesis in astrocytes after a starvation in a minimal medium lacking glucose and amino acids. While in our assay, we used normal medium, which consists enough substrates for energy metabolism. Maybe the difference in energy metabolism condition will affect astrocytes' preference for different precursors.

3.2.3. Plate reader assay can measure efflux of GSH-MCB conjugate

After labelling with MCB, the glutathione S-conjugates can be effluxed from astrocytes through Mrp1, a member of a family of multi-drug resistance proteins (Mrps) (Borst et al., 1999; Leslie et al., 2001). Mrp transporters constitute a subgroup of the ATP-binding cassette transporters and are ATP-driven export pumps of organic anions (Borst and Oude Elferink, 2002). We can also use our assay to examine the efflux of GSH-MCB conjugates through the Mrp1 transporter. Since the fluorescence plate reader reads both intracellular fluorescence and fluorescence from medium with almost equal efficacy, we were not able to determine what proportion of the GSH was effluxed to medium versus cell associated during the exponential phase of the MCB labelling. However, if we washed the wells with HBSS after the reaction, the fluorescence conjugate within the medium would be washed out, and the fluorescence signal left in the well represents the conjugate associated with cells (Figure 3-2 B). Comparing the fluorescence intensity before and after washing the cells, we can determine the amount of conjugate effluxed from cells. We found that the efflux process was highly temperature dependent (Figure 3-2 C). At 37°C, greater than 75% of the fluorescence product was associated with the medium, while at room temperature (24 °C), the efflux percentage was less than 50%, which is consistent with previous results that the ABC pump is highly temperature dependent (Borst and Oude Elferink, 2002). Treatment with MK571 (25µM), a competitive inhibitor of Mrp1 (Hirrlinger et al., 2002), resulted in a nearly complete retention of GSH-MCB fluorescence within cells (Figure 3-2 D), which further confirmed that the Mrp1 is predominately responsible for the GSH conjugate efflux from astrocytes.

Fluorescent microscope images showed that the MK571 treated cells contain more GSH-MCB fluorescence, confirming that more of the conjugates were kept within the cells in the presence of MK571 (Figure 3-3).

Figure 3-3

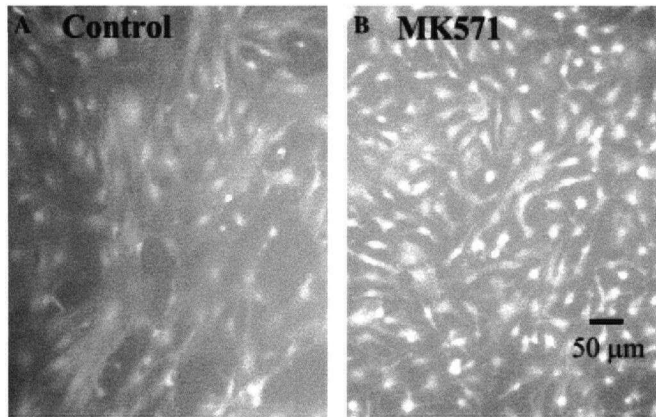


Figure 3-3. Fluorescence images (10X) of GSH-MCB in untreated (A) and MK571-treated (B) astrocytes cultures. Cultures were either maintained in normal HBSS, or HBSS with 25 mM MK571 added for 80 min at 37 °C. Addition of MK571 blocks the efflux of MCB-GSH and increases its content within cells.

3.2.4 Plate reader assay can detect changes in GSH metabolism under oxidative stress

It has been well established that GSH is an important intracellular antioxidant that protects against a variety of different reactive oxygen species (ROS) (for review, see Schulz et al., 2000; Dringen et al., 2000; Anderson et al., 2003). We are particularly interested in how the metabolism of GSH will be affected under oxidative stress. Data from our lab and others have found that astrocytes can induce a family of phase II detoxification enzymes that control ROS accumulation (Murphy et al., 2001; Johnson et al., 2002; Eftekharpour et al., 2000). The activation of the phase II pathway is dependent on the translocation of NF-E2-related factor 2 (Nrf2), an important transcription factor responsible for upregulating antioxidant response element (ARE)-mediated gene expression from the cytoplasm into the nucleus (Alam et al., 1999; Itoh et al., 1999). We activated the phase II response by incubating the astrocyte culture with 20 μ M *tert*-butylhydroquinone (tBHQ), a well-characterized Nrf2 activity inducer (Ishii et al., 2000; Lee et al., 2001; Shih et al., 2003, Eftekharpour et al., 2000), for 24h. Labelling these astrocytes with MCB and monitoring the time course of the reaction showed that the GSH level (F_{\max}) in tBHQ treated cells was 1.5 times of that of control groups (tBHQ: 14.9 \pm 0.75 fluor unit per mg protein; DMSO: 10.1 \pm 0.14 fluor unit per mg protein, $p=0.0057<0.05$), while the initial conjugation rates were similar between the two groups, indicating the bulk GST activity was not rate limiting or affected by tBHQ significantly (tBHQ: 0.043 \pm 0.004 fluor unit per mg protein/sec, DMSO: 0.045 \pm 0.003 fluor unit per

mg protein/sec, $p=0.92>0.05$)(Figure 3-4 A). We then added the cocktail of GSH precursors to the cells after plateau level had been reached and observed that tBHQ treated cells showed a larger slope indicating an increased synthesis/precursor uptake rate (tBHQ: 0.163 ± 0.018 fluor unit per mg protein/min; DMSO: 0.095 ± 0.015 fluor unit per mg protein/min, $p=0.0049<0.05$) (Figure 3-4 A). This difference was not due to more efficient GSH conjugation since no significant difference in fluorescence slope was observed after addition of exogenous GSH (tBHQ: 0.073 ± 0.016 fluor unit per mg protein/min; DMSO: 0.069 ± 0.01 fluor unit per mg protein/min, $p=0.845>0.05$) When we washed the wells to assess efflux, and did not find much difference in the percentage of MCB efflux between tBHQ and DMSO groups (tBHQ: $84.5\pm 3.9\%$, DMSO: $87.7\pm 1.5\%$, $p=0.25$) However, we only monitored efflux at a single time and not the full time course thus these conclusions should be taken with some caution. If we add cocktail of GSH precursors again to the culture after washing, we can also see a much faster linear increase in fluorescence intensity than the increase before washing, with tBHQ group having much larger slope than DMSO group (tBHQ: 0.266 ± 0.021 fluor unit per mg protein/min; DMSO: 0.153 ± 0.015 fluor unit per mg protein/min. $p=0.00047<0.05$) (Figure 3-4 A). This is consistent with our hypothesis that tBHQ can activate the antioxidant system and make cells more efficient in taking up precursors and synthesizing GSH. We conclude that the tBHQ treatment increases the synthesis of GSH in astrocytes, while apparently GST and Mrp activity were relatively unaffected (Table 3-1). This is consistent with our previous finding that γ -glutamylcysteine synthetase, the rate-limiting enzyme for GSH synthesis, and xCT, the cystine-glutamate transporter responsible for precursor uptake, are two important enzymes for GSH synthesis that are

upregulated by Nrf2 (Shih et al., 2003). Although GST and Mrp mRNAs are induced by the Nrf2 pathway in astrocytes (Shih et al., 2003), they did not appear to be greatly affected by tBHQ in the MCB assay. It is possible that this is due to the preference of specific isozymes for MCB-conjugation or some other factor being rate-limiting over the time scales.

Figure 3-4

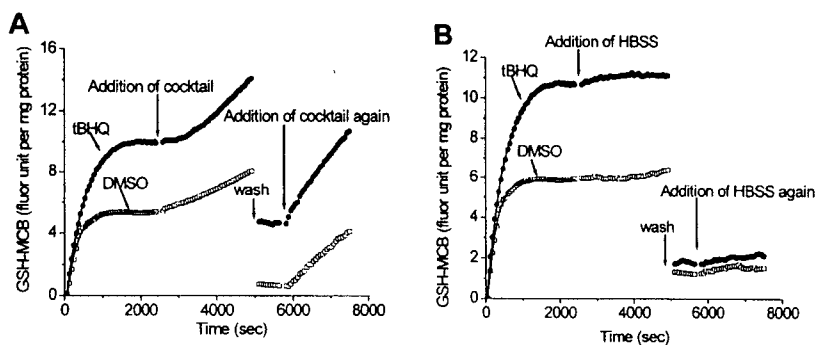


Figure 3-4. Changes in GSH metabolism induced by activation of ARE-mediated gene expression. Astrocyte cultures were treated with tBHQ (20 mM) for 24 hrs before assessing GSH metabolism at 37°C using 10 mM MCB. DMSO (0.01%) was used as the vehicle for tBHQ and was added to control cultures. The MCB labeling phase was fitted with a single exponential equation. (A). After a plateau level of fluorescence was reached, a 100 μ M cocktail of GSH precursors was added to the cultures to measure GSH synthesis. After washing the wells to measure efflux, the cocktail was added again. (B). HBSS was used as a control.

Table 3-1. Comparison of all kinetics parameters of GSH metabolism between tBHQ treatment and control (DMSO) groups.

Treatment	tBHQ	DMSO
Fmax (fluor unit per mg protein)	14.9±0.75	10.1±0.14
Time constant (sec)	346.5±47.2	224.4±20.6
Initial slope (fluor unit per mg protein/sec)	0.043±0.004	0.045±0.003
Slope after 1 st time addition of Cctl (fluor unit per mg protein/min)	0.163±0.018	0.095±0.015
Slope after 1 st time addition of GSH (fluor unit per mg protein/min)	0.073±0.016	0.069±0.010
Efflux percentage (%)	84.5±3.9	87.7±1.5
Slope after 2 nd time addition of Cctl (fluor unit per mg protein/min)	0.266±0.021	0.153±0.015

Data represent the mean±SEM of five independent experiments. Fluor is an abbreviation for fluorescence.

3.2.5. Conclusion

In conclusion, we have established a reliable and powerful assay to monitor glutathione metabolism in astrocyte culture, enabling us to measure the various kinetics parameters of glutathione metabolism, such as the rates of precursor uptake, synthesis, conjugation with xenobiotics, and efflux. The assay is sensitive to detect the changes in GSH metabolism under different conditions, for example, phase II inducers. Since there are still many unaddressed issues about glutathione's mechanism of neuroprotection (Dringen, 2000), we feel our glutathione metabolism assay will provide new insight into this interesting area.

3.3 Feasibility of two-photon laser scanning microscopy (TPLSM) measurement of cellular glutathione level

GSH-MCB conjugate can be excited by TPLSM at 780 nm and emits significant fluorescence at 450-575nm (Meyer et al., 2000). The *in vitro* production of GSH-MCB using purified enzymes allowed us to produce known amounts of GSH-MCB for a standard curve in two-photon imaging experiments. The standard curve indicated that two-photon microscopy was a viable technique to measure up to 5 mM concentrations of GSH (Figure 3-5). The GSH level measurement from TPLSM imaging is based on two assumptions:

Figure 3-5

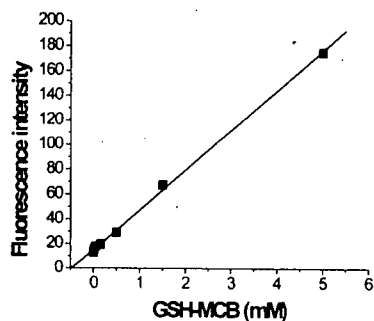


Figure3-5. Standard curve for the relationship between fluorescence intensity and GSH-MCB concentration. GSH-MCB solutions of known concentration were made from a GST catalyzed reaction between the reduced form of GSH and MCB. The standard solution was then filled into Vitrocells (micro-cuvettes) and imaged with two-photon microscopy. Over a range of 0 - 5 mM, a linear relationship was observed between GSH-MCB concentration and fluorescence ($R^2 = 0.9937$).

3.3.1 Assumption 1: Efflux of GSH-MCB at room temperature is negligible

All of experiments with rat brain slices were carried on at room temperature. As mentioned above, cells can efflux the GSH-MCB conjugates through Mrps, a family of multi-drug resistance proteins (Mrps) (Leslie et al., 2001; Borst et al., 1999). We have examined the efflux of GSH-MCB through Mrps in astrocyte cultures (Sun et al., 2005). We found that in culture, Mrps will export around 75% of GSH-MCB conjugate at 37 °C within 10's of min. In comparison to 37 °C, at room temperature efflux was reduced considerably (Sun et al., 2005a). We further tested whether Mrp1 will play a significant role in slices by adding 50µM MK571, a competitive inhibitor of Mrp1 (Hirrlinger et al., 2002), to rat brain slices and compared the fluorescence intensity after MCB labelling with control slices (Figure 3-6). We compared the fluorescence intensity of MCB-labelled cells in lateral ventricle ependymal cells (Figure 3-6 A, B) and in meninges (Figure 3-6 C, D). We found no significant difference with or without MK-571 ($p > 0.05$ for all regions, from 4 separate slice experiments) in neither of these regions (Figure 3-7), indicating in brain slices at room temperature the efflux of GSH-MCB by Mrp1 can be neglected.

Figure 3-6.

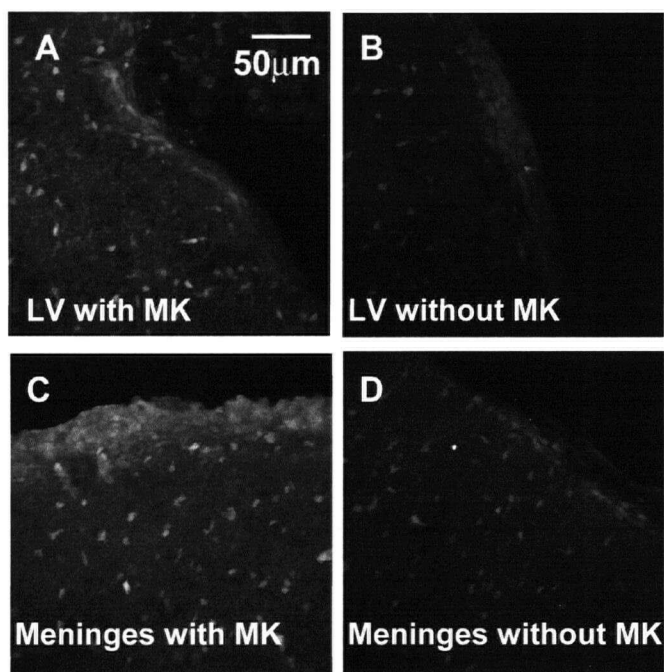


Figure 3-6. Efflux of GSH-MCB in slices at room temperature can be neglected. All slices were imaged at room temperature and after 60 µM MCB labelling for 30 min. In (A) and (C), MK 571 were added to the perfusion system at the same time with MCB, to get to a final concentration of 50µM. In (B) and (D), only MCB was used to label slices.

Figure 3-7

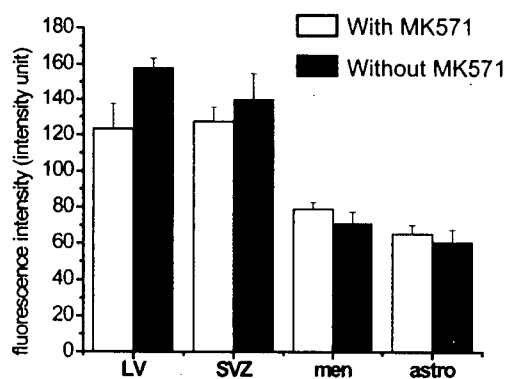


Figure 3-7. GSH-MCB efflux can be neglected in room temperature.

In all these regions, the fluorescence with or without MK 571 did not show significant difference. Data were averaged from 4 experiments. Error bar represents standard error.

LV, SVZ, men and astro are abbreviations for lateral ventricle, subventricular zone, meninges, and astrocytes, respectively.

3.3.2 Assumption 2: MCB labelled all GSH content in cells

In each experiment, by doing a time course we demonstrate that the reaction between MCB and GSH goes to completion; fluorescence intensity usually reaches a maximum level after MCB labelling for 20 min (Figure 3-8). In Figure 3-8, we showed the time course curve of MCB labelling at different regions of brain, including meningeal cells, astrocytes and neurons in cortex (Figure 3-8 A), high and low fluorescent cells in dentate gyrus, and lateral ventricle ependymal cells (Figure 3-8 B). All curves showed an exponential increase over time and the plateau level is usually reached after 20 min. Therefore for all our experiments with slices, we only took two-photon images after MCB labelling for 20 minutes. We assumed that at this time, MCB has labelled all GSH content in cells. We further tested this by adding more MCB to slices after the fluorescence had reached the plateau level and we found no further increase in fluorescence intensity, indicating that MCB is in excess and presumably labels all intracellular GSH (data not shown).

Figure 3-8

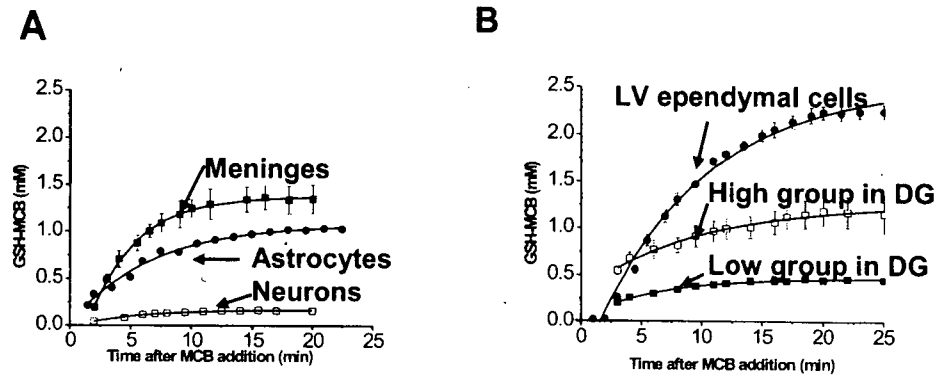


Figure 3-8. Time course curve of MCB labelling in different brain regions. (A).

MCB labelling in meninges, cortical astrocytes, cortical neurons. (B) MCB labelling in

high fluorescence cells of dentate gyrus (subgranular layer, presumed neuronal

progenitors), low fluorescence cells in dentate gyrus (lateral medial granule layer,

presumed neurons), and ependymal cells along lateral ventricle. Data points were

averaged from five cells within a single slice.

3.3.3 Conclusion

Based on the above two assumptions, we expect the GSH-MCB fluorescence intensity measured using the two-photon would be proportional to GSH concentration. To ensure that differences in fluorescence path length do not contribute to the observed differences in GSH levels between cells and tissues, we optically sectioned each cell and made maximal intensity projections over regions of cells that were considerably larger than the axial resolution of the microscope ($<3 \mu\text{m}$), thus being in a regime where fluorescence intensity is proportional to GSH-MCB concentration and not structure path length or volume (Meyer et al., 2000).

3 . 4 MCB labelling of different brain regions in slices

After establishing that MCB can be a relatively specific label for glutathione, we examined the GSH distribution in various brain tissues in acute P15-20 rat slices at room temperature. At surface of the slices there are many unstained cell bodies showing up as black holes which were labelled by the polar membrane impermeable marker PI (St John et al., 1986), indicating that they had ruptured membranes (Figure 3-9 A-C). As we imaged deeper into slices the incidence of unstained cell bodies became lower (Figure 3-9 D-F), indicating that the death of cells at the slice surface was caused by vibratome sectioning.

Figure 3-9

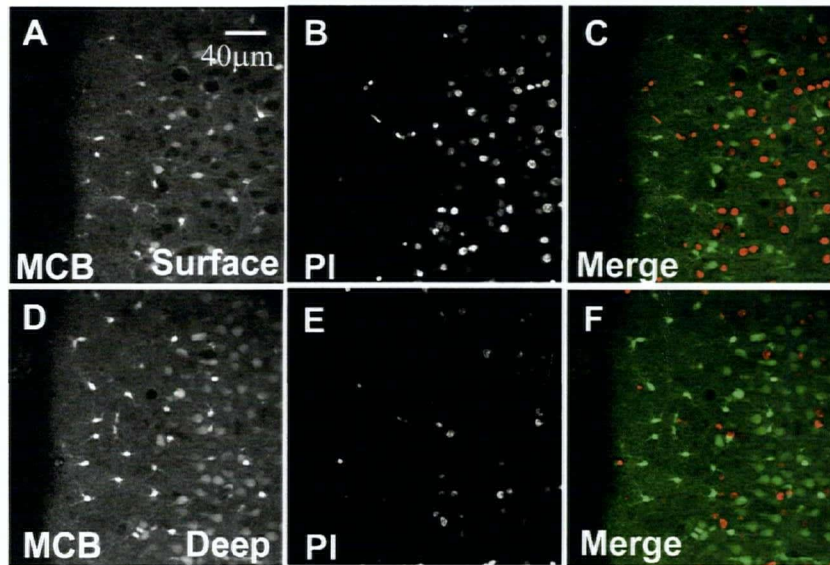


Figure 3-9. MCB and PI labelling of slices. (A). MCB labelling of rat brain slice surface. Many cells are not labelled by MCB, showing as black holes. (B). PI labelling of the same region as (A). (C). Overlay of (A) and (B). Green color represents MCB signal, red color represents PI. The black holes in panel (A) are labelled by PI. (D). MCB labelling in deeper level of slices. (E). PI labelling of same region. (F). Overlay of (D) and (E).

3.4.1 Meningeal and astrocytes in neocortex are labelled strongly by MCB in rat brain slices

Within brain slices MCB robustly labelled the meninges and a subpopulation of cells in neocortex with astroglial morphology, as well as perivascular cells (Figure 3-10 A). In order to verify the cell type of these GSH-positive cells we performed immunostaining with the calcium-binding protein S-100 β , a specific marker of astrocytes (Matthias et al., 2003). We have used S-100 β since well used astrocyte markers such as GFAP fail to label all astrocyte cell populations (Walz and Lang, 1998). Since MCB tends to leak out of cells in paraformaldehyde fixed tissue we also stained the slices with either laminin, which is a major component of basement membranes in blood vessels, or PI as landmarks to locate the same region from which we had imaged GSH-MCB (Figure 3-10 B). As fixation of slices caused some distortion of cell position, we examined co-localization over a relatively small area based on cell morphology and the relative position of cells. Most of the highly fluorescent MCB-labelled neocortical cells were S-100 β positive and thus were presumably astrocytes (75% MCB/S-100 β co-staining, n = 47, from 2 slices of 2 animals, Figure 3-10 C). The perivascular cells were also S-100 β positive astrocytes with their end-feet tightly ensheathing the vessel wall. An increased level of GSH in astrocytes is consistent with their crucial role in the antioxidant defence of the brain (Cooper and Kristal, 1997; Dringen, 2000; Anderson et al., 2003). It has been demonstrated that astrocytes can support other brain cell types by defending them against ROS (Dringen, 2000). For example, astrocytes can protect neurons from oxidative stress

via GSH dependent mechanisms and therefore require an intracellular reservoir of GSH (Iwata-Ichikawa et al., 1999; Chen et al., 2001; Shih et al., 2003; Kraft et al., 2004).

In addition to astrocytes, we also found that meningeal cells (most likely pial and arachnoid cell layers) were intensely labelled by MCB, indicating a very high GSH level. Meningeal cells have received little attention with respect to neuroprotection except for their role in the regulation of blood flow and the blood-cerebrospinal fluid (CSF) barrier (Tanno et al., 1993; Ghersi-Egea et al., 1994). Related structures such as the choroid plexus have been long known to filter and remove exogenous and endogenous toxins from the CSF (McKinnon, 1998). Recently, Sato et al. found that the high affinity cystine-glutamate antiporter system x_c^- (xCT) is expressed at particularly high levels in meninges (Sato et al., 2002). In many cell types, the uptake of cystine is the rate-limiting step for GSH synthesis. Meningeal cells may use xCT-dependent cystine uptake as an efficient means to supply cysteine for maintenance of a large GSH pool. This enhanced GSH production by the meninges may play an important role in buffering brain oxidative stress. Consistent with this proposal, we found meningeal cells to be more potent than cortical astrocytes in protecting neurons from an *in vitro* oxidative stress model (Sun et al., 2004; 2005a and Shih et al. in preparation).

Figure 3-10

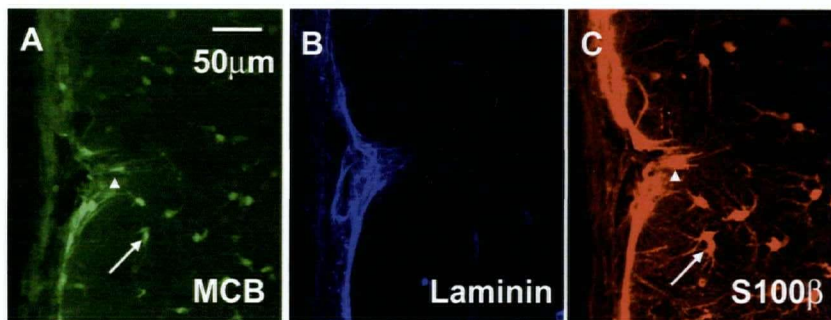


Figure 3-10. MCB labels the meninges and astrocytes robustly. (A). Green fluorescence of rat brain slices labelled with MCB. (B). Laminin labelling pattern of same region, from green detection channel after immunostaining. The MCB signal was lost during paraformaldehyde fixation for immunostaining, therefore it did not interfere with the secondary antibody (FITC anti-rabbit) signal. For presentation a blue color was added. (C). Red fluorescence of cells stained with S-100 β as primary antibody and Alexa 594 anti-mouse as secondary antibody. Panel A and C show that the MCB labelled cells with high fluorescent are astrocytes. Arrow and arrowhead point to an astrocyte and a perivascular cell labelled by both MCB and S-100 β , respectively. Images were taken using two-photon microscopy of a rat brain slice using a 40x objective.

3.4.2 MCB labelling of neurons in slices is much weaker than labelling of astrocytes

When imaging deeper layers of the neocortex in P15-20 rat slices, such as Layer II and III (Figure 3-11 A), we identified another group of cells that were MCB-labelled but with lower fluorescence. These cells had the morphology of neurons with apical dendrites oriented towards the meninges (Figure 3-11 B). Co-labelling the acute live slices with PI showed that these cells had intact membranes, since there was no overlap between the MCB and PI signal, and were thus viable (Figure 3-11 C). After fixation with paraformaldehyde (PFA), the MCB signal was completely lost (data not shown), while the PI signal was preserved within cells that had died during vibratome sectioning and also spread to all fixed cells that were originally labelled by MCB, including those with neuronal morphology (Figure 3-11 E). Immunostaining with NeuN, a neuron-specific nuclear protein (Mullen et al., 1992) confirmed that the cells with a lower level of fluorescence were indeed neurons (Figure 3-11 D, F). As fixation of slices caused some distortion of cell position, we examined co-localization over a relatively small area based on cell morphology and the relative position of cells.

In previous studies using largely developing neurons and glia in cell culture based assays, inferences regarding the cellular distribution of GSH in brain have been inconsistent. Some studies suggest that GSH is substantially lower in cortical neurons than in glia (Slivka et al., 1987; Lowndes et al., 1994; Beiswanger et al., 1995; Tauskela et al., 2000), whereas others do not (Amara et al., 1994; Hjelle et al., 1994; Rice and Russo-Menna, 1998). Our results provide direct evidence that in the cerebral cortex *in*

situ there is heterogeneity in the distribution of GSH between neurons and glia, with neurons in general exhibiting much lower levels of GSH.

Figure 3-11

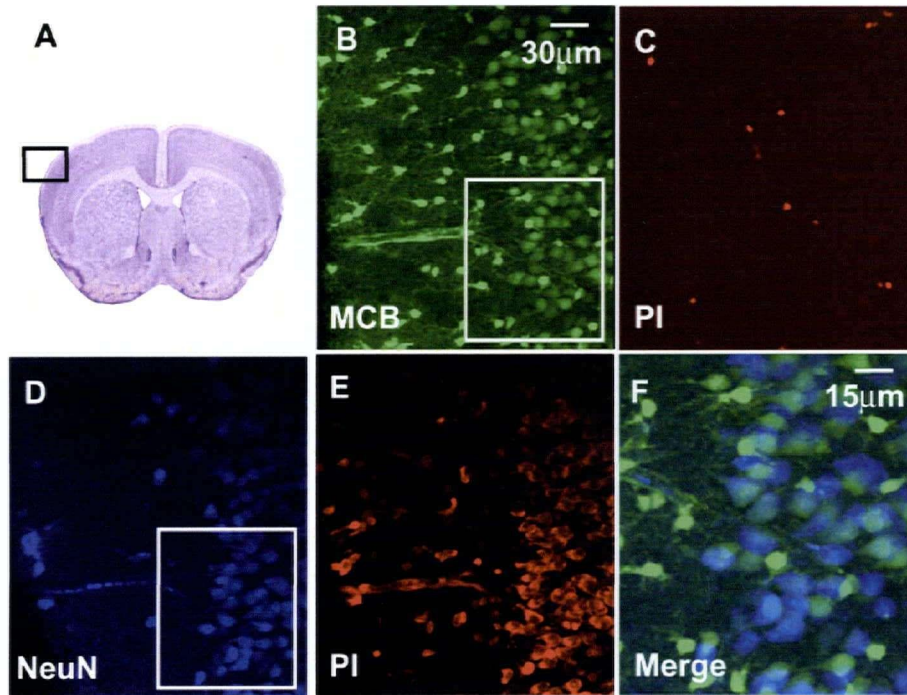


Figure 3-11. MCB labelling of mature cortical neurons. (A). Coronal section of the rat brain showing the location of two-photon imaging, modified from *The Rat Brain in stereotaxic coordinates* (Paxinos and Watson, 1986). (B). MCB labelling of cortical Layers I and II in a rat brain slice. In Layer II, there are many cells with neuronal morphology labelled by MCB, with much lower fluorescence intensity than the MCB-labelled astrocytes in Layer I. (C). PI labelling of the same region as (B) in an acute slice, showing dead cells with ruptured membranes permeable to PI (healthy cells are normally membrane impermeable). (D). Immunostaining of the same region in panel A with NeuN, a neuron specific nuclear protein (primary antibody) and FITC anti-mouse as the secondary antibody, showed that the cells with relatively lower fluorescence in Layer II in panel A are neurons. (E). PI labelling of same region after fixation. (F). Overlay of NeuN and MCB signals (region from inset in panels B and D). Since fixation caused irregular of stretching of slices and MCB staining can be performed on live tissue only, we only overlaid the inset region where cells of interest were best aligned. Images were taken with two-photon microscopy using a 40x objective.

3.4.3 Lateral ventricle ependymal cells have the highest GSH content in brain slices

In addition to meningeal cells and astrocytes, MCB also strongly labelled ependymal cells along the lateral ventricle (Figure 3-12 B). These cells were significantly brighter than any other region of brain slices examined. As with the meninges, ependymal cells also face CSF (Figure 3-12 A) and are known to express a high level of cystine-glutamate transporter xCT, allowing the extraction of cystine for GSH synthesis (Sato et al., 2002). Ependymal cells may also contribute to maintenance of brain redox homeostasis by synthesizing and exporting GSH.

Figure 3-12

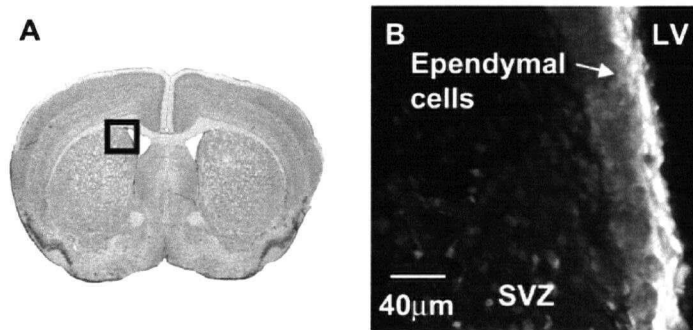


Figure 3-12. MCB labelling of GSH-containing ependymal cells lining the lateral ventricle. (A). Coronal section of rat brain showing the location of two-photon imaging, modified from *The Rat Brain in stereotaxic coordinates* (Paxinos and Watson, 1986). (B). Ependymal cells lining the lateral ventricle show very strong fluorescence after MCB labelling. Although lower in fluorescence than the ependymal layer, cells within the subventricular zone (SVZ) were clearly labelled by MCB. Image was taken with 40x objective.

In close proximity to ependymal cells is the subventricular zone where neurogenesis can occur (even in mature brain) (Doetsch and Alvarez-Buylla, 1996). Cells within the subventricular zone were also strongly labelled by MCB (Figure. 3-13 A). Immunostaining with doublecortin (DCX), a marker of neurogenesis, which is expressed in migrating and differentiating premature neurons (Francis et al., 1999; Brown et al., 2003), indicated that many of these GSH-containing subventricular zone cells were neuronal precursor cells (Figure 3-13). This suggests that a high level of GSH may be required to support the high proliferation rate and consequent increase in metabolic activity of these precursor cells. When cells are dividing, they also express S100 β (Deloulme et al., 2004). Immunostaining with S100 β showed that some MCB labelled SVZ cells are also labelled by S100 β (Figure 3-14). S100 β can also label ependymal cells (Figure 3-14), which are not labelled by DCX (Figure 3-13). However, GFAP can hardly any cells in this region (Figure 3-15). We also immunostained the slices with NeuN, a mature neuron marker, and we found no colocalization between NeuN signal and MCB signal (Figure 3-16). When doing this, we used laminin to label blood vessels, which can help us to find the previous imaged regions after immunostaining. In conclusion, many MCB labelled cells in subventricular zone are DCX positive, some of them are S100 β positive, but almost none of them are GFAP or NeuN positive, indicating these cells are precursor cells.

Figure 3-13

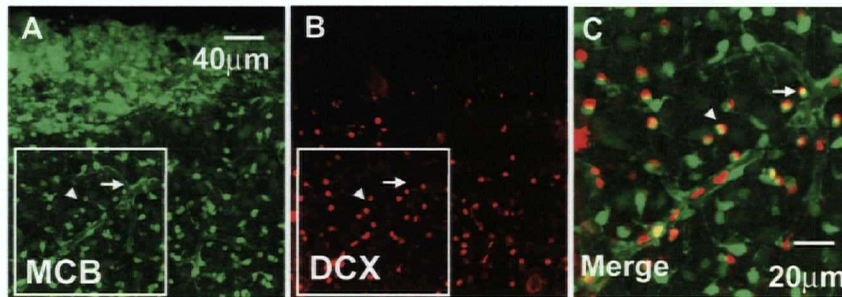


Figure 3-13. Many cells labelled by MCB in subventricular zone (SVZ) are labelled by doublecortin (DCX). (A). MCB labelling of lateral ventricle ependymal cells and cells in SVZ. (B). Immunostaining of the same region in panel A with DCX, a marker of neurogenesis (primary antibody) and Alexa 488 anti-goat as the secondary antibody. (C). Overlay of DCX and MCB signals (region from inset in panels A and B). Since fixation caused irregular of stretching of slices and MCB staining can only be performed on live tissue, we only overlaid the inset region where cells of interest were best aligned. Images were taken with two-photon microscopy using a 40x objective.

Figure 3-14

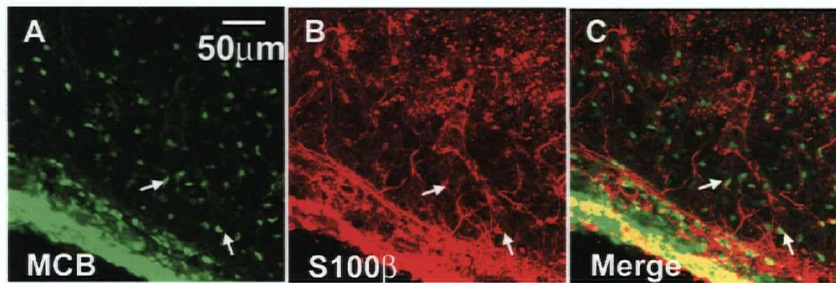


Figure 3-14. Some cells labeled by MCB along lateral ventricle and in SVZ are also labeled by S100β. (A). MCB labelling of lateral ventricle ependymal cells and cells in SVZ. (B). Immunostaining of the same region in panel A with S100β (primary antibody) and FITC-anti-mouse as the secondary antibody. (C). Overlay of S100β and MCB signals. Green and red colors are added artificially to MCB and S100β, respectively.

Figure 3-15

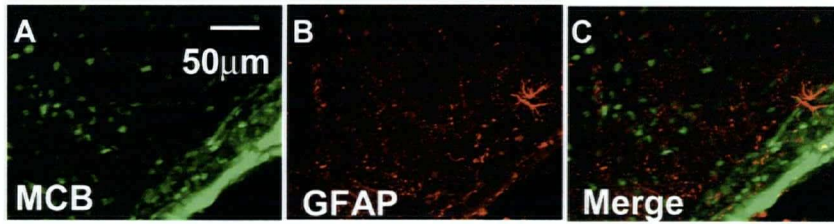


Figure 3-15. Cells labeled by MCB along lateral ventricle and in SVZ are not labeled by GFAP. (A). MCB labelling of lateral ventricle ependymal cells and cells in SVZ. (B). Immunostaining of the same region in panel A with GFAP (primary antibody) and FITC-anti-rabbit as the secondary antibody. (C). Overlay of GFAP and MCB signals. Green and red colors are added artificially to MCB and GFAP, respectively.

Figure 3-16

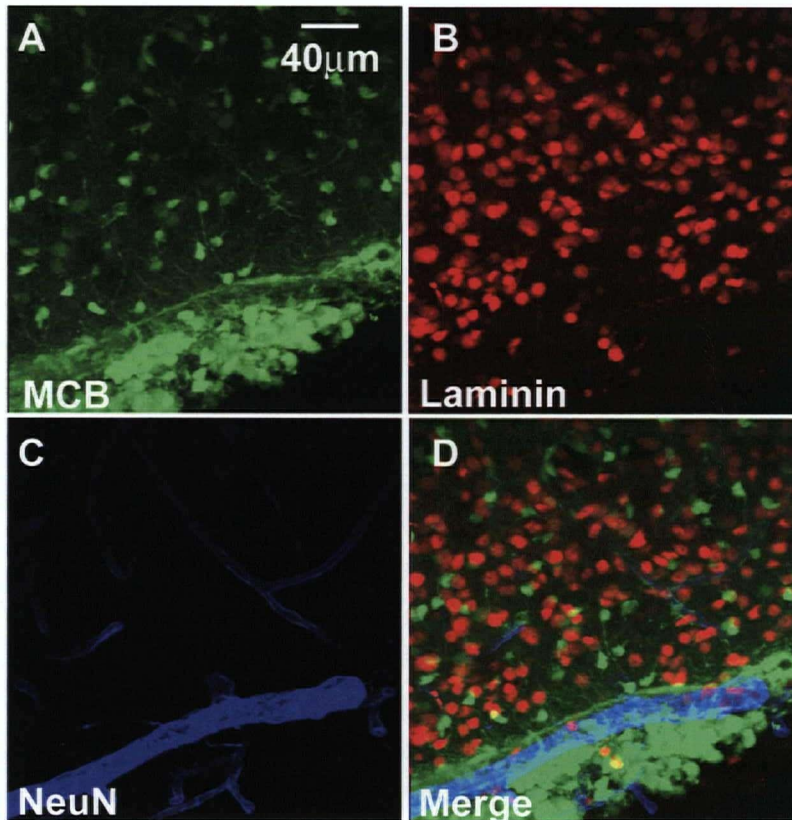


Figure 3-16. Mature neurons in SVZ are not labelled by MCB. (A). Green fluorescence of rat brain slices labelled with MCB. (B). Laminin labelling pattern of same region, from green detection channel after immunostaining. For presentation a blue color table was added. (C). Red fluorescence of cells stained with NeuN as primary antibody and Alexa 594 anti-mouse as secondary antibody. (D). Overlay of panel (A-C), showed that mature neurons are not labelled by MCB. Images were taken with two-photon microscopy of a rat brain slice using a 40x objective.

3.4.4 A subpopulation of developing neurons in dentate gyrus are labelled by MCB.

Given the high levels of GSH in the lateral ventricle ependymal cells and associated subventricular zone and their potential role in neurogenesis, we also examined GSH-MCB labelling in the dentate gyrus. Granule neurons of different developmental stages are found within medial and lateral aspects of the granule cell layers (Kempermann et al., 2003). The most strongly MCB labelled cells were located at the border between the condensed granular cell layer and the hilus (Figure 3-17 A, B, also termed subgranular layer). Cells at this location may be dividing precursor cells that have a unique immunocytochemical profile (Kempermann et al., 2004; Li and Pleasure, 2005) and are expected to be S-100 β and DCX positive, but NeuN and GFAP negative .

Figure 3-17

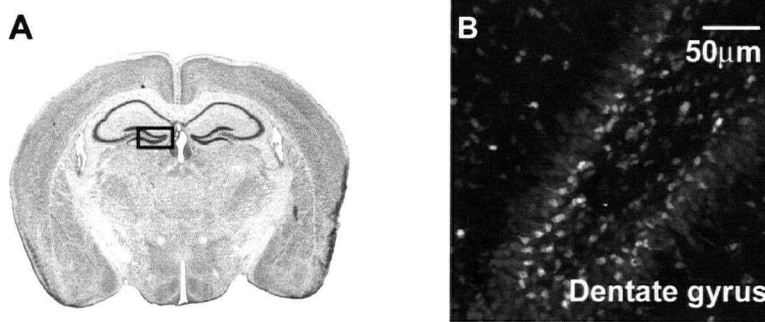


Figure 3-17. MCB labelling of GSH-containing cells in dentate gyrus. (A). Coronal section of the rat brain showing location of two-photon imaging, modified from *The Rat Brain in stereotaxic coordinates* (Paxinos and Watson, 1986). (B). MCB labelled two groups of cells in dentate gyrus. The cells within the most medial portion of granular cell layer and subgranular cell layers (border between condensed granular cell layer and hilus) showed relatively higher fluorescence, while the more laterally positioned cells within the medial granular cell layer showed lower fluorescence. Cells deep within the lateral portion of the granular cell layer were unlabelled by MCB (not significantly above background neuropil) and appeared as black holes.

Approximately 40% of these highly fluorescent cells in dentate gyrus were S-100 β positive (Figure 3-18; n = 226 cells from 2 slices). Immunostaining with GFAP showed no co-localization (0%, 1 GFAP+/MCB+ cell in 402 MCB positive cells from 3 slices) between GFAP-positive cells and GSH-containing cells (Figure 3-19). Since S-100 β is present in dividing cells but not astrocytes until they are mature (Deloulme et al., 2004), the S-100 β and MCB co-labelled cells could represent developing neuronal precursors. Accordingly 55% of MCB labelled cells were also labelled by DCX (Figure 3-20, n = 225 cells in 2 slices). This suggests that a high level of GSH may be required to support the high proliferation rate and consequent increase in metabolic activity of these precursor cells. Lateral to the highly fluorescent group of cells (within the condensed granular cell layer), we found a population of cells labelled weakly by MCB (Figure 3-17B). The most lateral group of cells in the granular cell layer were not labelled by MCB, but strongly labelled by NeuN a marker for mature neurons (Figure 3-21). PI labelling of the live slices showed that the majority of these cells in the granular cell layer had intact membranes and were presumably viable since there was an absence of overlap between MCB and PI signals (Figure 3-21). Thus the reason why the mature neurons do not stain with MCB is not because they are dead. Since newborn granular cells are first present in the inner granular cell layer and migrate to the outer portion as they develop (Kempermann et al., 2003), and the levels of NeuN are correlated with the extent of differentiation (Mullen et al., 1992), we conclude that neurons gradually reduce their GSH content as they mature.

Figure 3-18

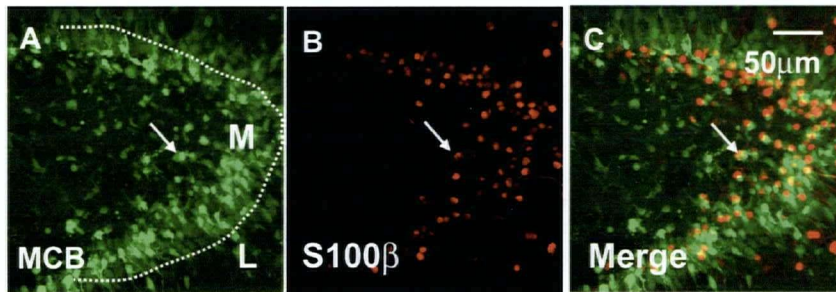


Figure 3-18. Many cells in subgranular zone are colabelled by MCB and S100 β . (A). MCB labelled two groups of cells in dentate gyrus. Approximate border between medial (M) and lateral (L) granular layers is indicated with a dashed line. (B). S-100 β staining of the same region as (A), showing that the highly GSH-MCB fluorescent cells are S-100 β positive. (C). Overlay of MCB and S-100 β signals indicated significant co-localization of MCB and S-100 β positive labelling. The arrow shows a co-localized cell

Figure 3-19

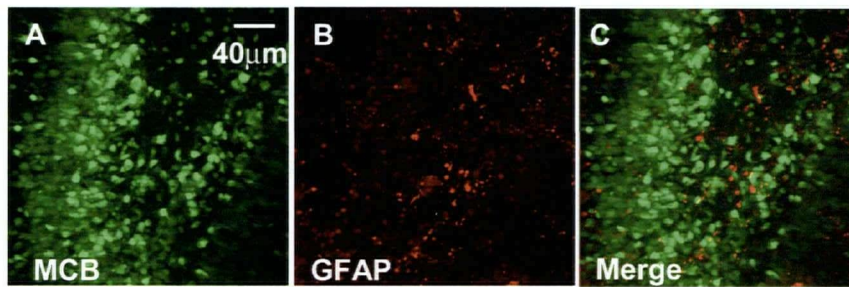


Figure 3-19. MCB labelled cells in dentate gyrus are GFAP-positive. (A) MCB labelling of dentate gyrus. (B) GFAP labelling of the same region as (A). Primary antibody was derived from mouse. FITC-anti mouse was used as secondary antibody. (C) Overlay of panel (A) and (B) showed no colocalization between MCB and GFAP.

Figure 3-20

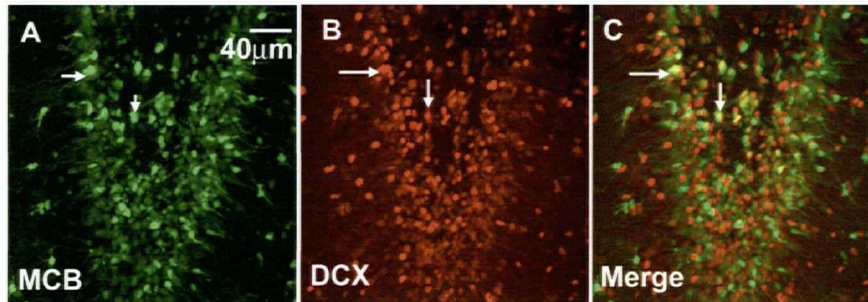


Figure 3-20. Many cells in subgranular zone are colabelled by MCB and DCX. (A). MCB labelled two groups of cells in dentate gyrus. Approximate border between medial (M) and lateral (L) granular layers is indicated with a dashed line. (B). DCX staining of the same region as (A), showing that the highly GSH-MCB fluorescent cells are DCX positive. (C). Overlay of MCB and DCX signals indicated significant co-localization of MCB and DCX positive labelling. The arrows show some co-localized cells.

Figure 3-21

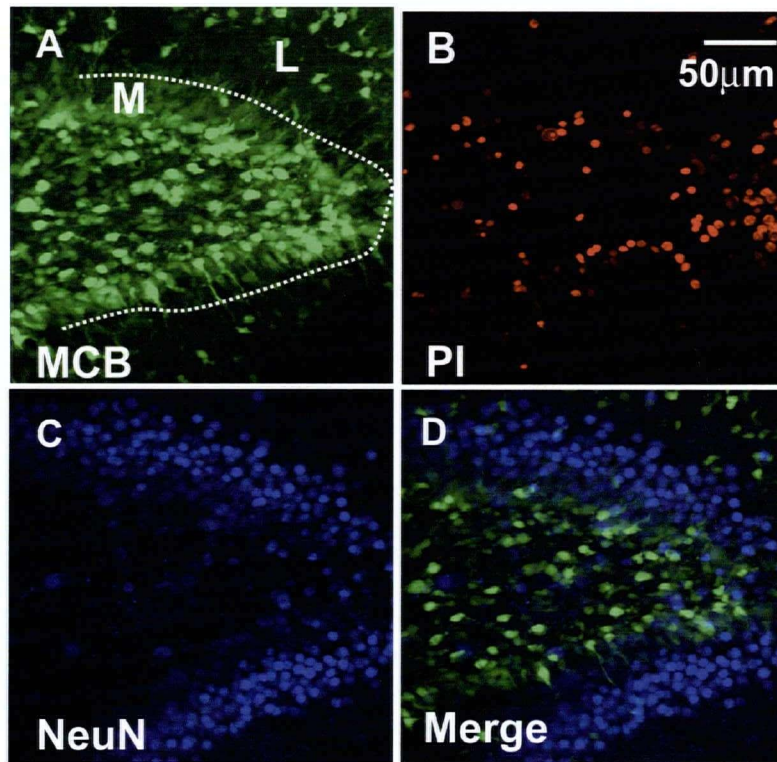


Figure 3-21. Mature neurons labelled by NeuN are not labelled by MCB. (A). MCB labelling of dentate gyrus. (B). Co-labelling the live slice in figure (A) with PI indicated the dead surface neurons in dentate gyrus. There is no overlap between the MCB and PI signals. (C). NeuN staining of the same slice showing that the black holes (no MCB label and no PI label) in outer portion of granular cell layer are viable neurons. (D). Overlay of MCB and NeuN signal showed that the cells in the lateral portion of granular cell layer that were not labelled by MCB could be labelled by NeuN. Images were all taken with 40x objective.

3.4.5 Measurement of GSH concentration in different brain regions in acute brain slices.

Our data indicates that the fluorescence intensity of GSH-MCB is directly proportional to GSH concentration (Figure 3-5). Therefore, when the MCB reaction reaches a plateau we can estimate intracellular GSH concentration in brain slices. We measured the GSH concentration in different brain regions by converting the plateau level of fluorescence to a GSH concentration with the standard curve (Figure 3-22A). In order to standardize for effects of imaging depth on fluorescence intensity (excitation and emission efficiency are reduced at greater depths) (Oheim et al., 2001), we made all of the measurements from the cells at about 50 μm below the surface of the slice. By surveying various brain regions we found that lateral ventricle ependymal cells show the highest level of GSH ($2.73 \pm 0.56 \text{ mM}$, $*p < 0.05$ when compared to all other brain regions measured), which is consistent with their potential role in regulating the redox state of the CSF system. The GSH level in meningeal cells was significantly higher than in cortical astrocytes (meninges, $1.45 \pm 0.09 \text{ mM}$; astrocytes, $0.91 \pm 0.08 \text{ mM}$, $***p < 0.001$). Since astrocytes have been described as a crucial part of antioxidant defence in brain cells (Dringen, 2000; Shih et al., 2003), our finding suggest that meninges which have received little attention in this context so far, may also be an important component of the brain antioxidant system. The GSH level in astrocytes is about 5 times greater than that of cortical Layer II neurons (astrocytes, $0.91 \pm 0.08 \text{ mM}$; neurons, $0.21 \pm 0.02 \text{ mM}$, $***p < 0.001$), suggesting that neighboring astrocytes support neuronal viability by releasing GSH during oxidative stress. In dentate gyrus, presumed neuronal progenitors

(based on cell position and staining with markers) express a relatively high level of GSH (1.75 ± 0.24 mM) and differentiated dentate gyrus neurons contained a significantly lower amount in comparison (0.50 ± 0.08 mM, $^{***}p < 0.01$). Our approach with TPLSM to image GSH provides a more detailed mapping of GSH distribution in brain than the widely used biochemical analyses that are unable to provide information about GSH concentration in at the level of single cells.

As mentioned before, since MCB is in excess and the conjugation between GSH and MCB can be regarded as a first-order reaction, the time course curve should fit a single exponential curve. Figure 3-8 A and B are the time course curves of MCB labelling in meninges, cortical astrocytes, cortical neurons, progenitor cells in dentate gyrus, young neurons in dentate gyrus, and lateral ventricle ependymal cells, respectively. Within the dentate gyrus the putative progenitor cells based on their subgranular position were termed high-fluorescence group, while the medial young neurons of the granule cell layer (weakly NeuN positive) were termed low fluorescence group; lateral granule layer neurons only weakly labelled by MCB and were not plotted. All of these curves exhibited an exponential increase over time and they all reached a plateau level after labelling for 20 min, again indicating that GST activity was not limiting and that MCB staining reflects GSH content. These curves can all be fitted well with Equation 1: $F = F_0 + F_{\max} (1 - \exp(-(t-t_0)/\tau))$. The initial slope of the curve reflects GST activity in these cells (Figure 3-22 B). Comparing GST activity between different cell groups, we found there is a trend but not significant difference between meninges, astrocytes, and neurons. The cells with higher GSH level also exhibit a higher GST activity. This is not surprising since the cells with high GSH level (such as meninges, astrocytes, and lateral ventricle

ependymal cells) are usually more important for antioxidant defence, therefore they need high GST activity to conjugate exogenous and endogenous toxins to GSH and export them out of cells.

Figure 3-22

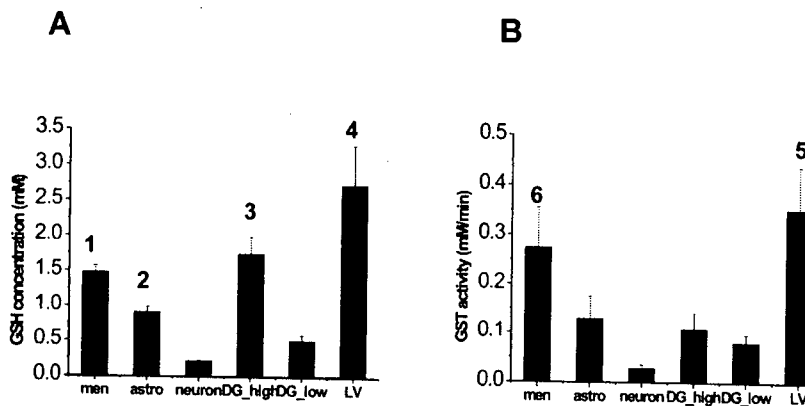


Figure 3-22. Quantification of GSH concentration in different brain regions. (A). GSH concentrations at different regions of P15-P21 rat brain slices. Data for different brain regions were averaged from five experiments respectively. (1): *** $p < 0.001$, significantly higher GSH in meninges when compared to astrocytes and neurons. (2): *** $p < 0.001$, when astrocytes were compared to neurons. (3): ** $p < 0.01$, SVZ cells (high fluorescence) contain significantly higher GSH when compared to the more lateral dentate gyrus cells found in the granule_cell layer_(low fluorescence). (4): * $p < 0.05$, lateral ventricle ependymal cells contain more GSH than all other cell types examined. (B). The MCB conjugation activity (proportional to GST activity) at different brain regions estimated from the exponential fitting of the time course curves. Average values from 3 separate experiments are shown. (6): There was a trend but no significant difference in conjugation activity between meninges, astrocytes and neurons. (5): * $p < 0.05$ lateral ventricle ependymal cells had significantly higher GST activity than all other cell types except meninges. Data were given as mean \pm SEM and analyzed with repeated-measures one-way ANOVA.

3.4.6 Conclusion

By applying TPLSM to rat brain slices, we have found that GSH is enriched in meninges, lateral ependymal cells and subventricular cells, astrocytes, and immature neurons in dentate gyrus. Neocortical neurons in slices from mature animals can be labelled by MCB but at a much lower level of fluorescence suggesting that glial, meningeal, and ependymal cell sources may play a dominant role in buffering brain oxidative stress.

3.5 MCB labels a subpopulation of meningeal and neocortical cells *in vivo*.

It is conceivable that GSH metabolism in slices may be different from that *in vivo* for a variety of reasons including: the lack of slice blood supply and exposure to GSH precursors as well as the possibility of trauma in making brain slices. With two-photon *in vivo* microscopy we were able to image GSH distribution in the intact brain directly. Exposure of the cortical surface of anaesthetized mice to MCB resulted in staining of a subpopulation of neocortical cells with a plateau level of fluorescence reached in 30 min (Figure 3-23 G). In these experiments, small cranial windows (2x2 mm) were made on C57Bl/6 mice and 100 μ M MCB was applied directly to the somatosensory cortex surface and MCB-containing agarose was layered over the brain surface to continuously

supply MCB for on-going labelling. MCB-labelled cells were imaged down to 250 μm below the brain surface. At the brain surface, MCB labelled many cells, apparently meningeal cells (Figure 3-23 A). Side view projections demonstrate that in the neocortex, all the MCB-labelled cells showed astroglial morphology (Figure 3-23 E). These cells have multiple processes originating from the cell body, often forming end-feet attached to unstained blood vessels (Figure 3-23 C, arrow). In *in vivo* experiments we did not include MK571 and the preparation was at 37 $^{\circ}\text{C}$ so we expect the plateau level of fluorescence reached to reflect the steady state balance between GSH synthesis and efflux. Recently, Nimmerjahn and colleagues have demonstrated that sulforhodamine 101 (SR 101) can be a relatively specific marker of astroglia in the neocortex *in vivo* (Nimmerjahn et al., 2004). In these experiments SR 101 was co-localized with astrocyte markers in neocortex, but failed to stain neurons, microglia, or oligodendrocytes. By co-labeling with MCB and SR 101 *in vivo* and collecting the signal from the green and red channels respectively, we found that these two probes labelled the same population of astrocyte-like cells in the cortical parenchyma (Figure 3-23D). The meningeal cells labelled by MCB can also be labelled by SR 101 (Figure 3-23B). These results are consistent with our data from cortical slices where MCB robustly labels the meninges and astrocytes. A three-dimensional projection from the side view of the *in vivo* data stack showed that both in Layer I (approximately 0 \sim -100 μm) and Layer II (approximately -100 \sim -200 μm), MCB-labelled cells are astrocytes (Figure 3-23 E, F). No neurons in Layer II (SR 101 negative cells) were labelled by this approach using the mature mice we studied (>2 months of age). However, we have found that neurons in brain slices from young rats can be labelled by MCB, although with a very low fluorescence level (\sim 20% of astrocyte

levels). The reason why neurons *in vivo* are not labelled cannot be due to a lack of MCB tissue penetration, since astrocytes at the same depth level as neurons can be labelled. Perhaps in brain slices less attenuation of fluorescence signals takes place allowing the observation of Layer II neurons, which exhibit approximately 20% of the GSH found in astrocytes. It is also possible that the slices from young rats (P15~P21) contain more immature neurons that have relatively higher GSH. Consistent with this, using the Tietze assay (Tietze, 1969) we have seen higher GSH levels in tissue homogenates from young and embryonic rats when compared to adults (Shih et al., in preparation).

Figure 3-23

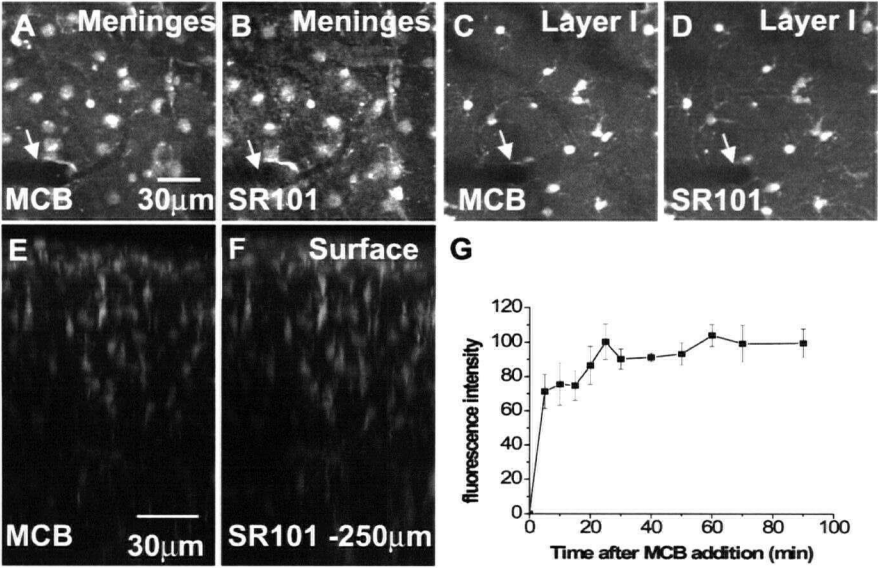


Figure 3-23. *In vivo* two-photon fluorescence image of the somatosensory cortex of a live anesthetized mouse after application of MCB and SR 101. (A). Image recorded at the brain surface after MCB labelling. A population of meningeal cells are labelled by MCB. Blood vessels appear as dark gaps (arrow). (B). SR 101 labelling of the same region in panel A. MCB and SR 101 labelled the same group of cells. (C). Optical section of MCB fluorescence recorded about 50 μm below the pial surface showing that a subpopulation of cells had taken up the dye deeper within the parenchyma. These cells had astroglial morphological features and some formed end-feet surrounding unstained blood vessels (arrow). (D). Optical section of fluorescence for the astrocyte marker SR 101 (applied to the brain surface simultaneously with MCB) at the same region as panel C. (E). Side view (X-Z image) of the MCB labelled meninges and astrocytes in neocortex (maximal intensity projections) from surface of the brain to a depth of approximately - 250 μm , reconstructed from planar scans acquired every 1 μm after MCB addition. (F). Side view of SR 101 labelled cells in meninges and neocortex. All images were taken with 40x objective. (G). Time course curve of MCB *in vivo* labelling showing that the fluorescence intensity reaches a plateau level within 30 min. Average values from 3 different experiments are shown.

3.6 Meningeal cells have a more active GSH system than astrocytes in neocortex

The meninges have received little attention in antioxidant defense and have mainly been highlighted for their physical role at the CSF-blood barrier (Nilsson et al., 1992; Smith and Shine, 1992; Tanno et al., 1993). Our findings provide a new insight into the possible role of the meninges in protecting the brain against oxidative stress. In order to look further into the GSH metabolism system in meninges and astrocytes, we prepared meninges and cortical cells cultures from new-born rats and used MCB to label the cultures. As described above, we have developed an assay to measure several parameters of GSH metabolism in glial cells, such as GSH content, GST activity, rate of GSH biosynthesis, etc, using plate reader (Sun et al., 2005). This assay is also applicable to measure parameters of GSH metabolism in meninges and cortical cells cultures.

3.6.1 Meninges contain higher level GSH and GST activity than cortical cells

In meninges and cortical cell cultures, the MCB labelling time course curve also fit well with a single exponential equation (Equation 1):

$$F = F_0 + F_{\max} (1 - \exp(-(t-t_0)/\tau))$$

F is the fluorescence intensity normalized to protein amount. F_{\max} is the maximum level of fluorescence intensity per mg protein, and τ is the time constant of the reaction. From Figure 3-24A, the curve from meninges showed a much faster increase and reached a

higher plateau than cortical cell cultures. The highest fluorescence level of meninges and cortical cultures are 1.541 ± 0.193 , 1.084 ± 0.153 (fluorescence intensity/ μg protein), respectively ($p=0.016$). The initial slopes of them are 0.652 ± 0.082 , 0.182 ± 0.132 (fluorescence intensity per μg protein/min) ($p=0.0022$). Therefore, we confirmed that meninges have higher GSH level and higher GSH activity than cortical cells.

3.6.2 Meninges cells are more efficient in taking up GSH precursors and synthesizing GSH

After the MCB labeling of endogenous GSH has reached a plateau level, we added $100 \mu\text{M}$ cystine, the rate-limiting precursor for GSH synthesis, or a cocktail of precursors, glutamate, glycine and cystine ($100 \mu\text{M}$ for each component), to the cultured cells. In both cultures, we found a significant linear increase in fluorescence intensity, with meningeal cultures showing a much larger slope, indicating meningeal cells are much more efficient than cortical cells in taking up precursors and synthesizing GSH (Figure 3-24 B). The slopes of increase after cystine addition are 0.096 ± 0.018 and 0.0088 ± 0.0018 (fluorescence intensity per μg protein/min) for meninges and cortical cells, respectively ($p=0.011$). The slopes after cocktail addition are 0.071 ± 0.0054 and 0.011 ± 0.0017 ($p=0.0016$), averaged from 4 experiments. HBSS was used as a control. Neither of them showed significant increase after HBSS addition, with the slope of 0.0032 ± 0.0007 and 0.0010 ± 0.0002 (fluorescence intensity per μg protein/min), respectively. When exogenous GSH ($100 \mu\text{M}$) was added, the fluorescence also showed a

linear increase, with a slope of 0.066 ± 0.0069 and 0.024 ± 0.0071 (fluorescence intensity per μg protein/min), respectively for meninges and cortical culture. The slope of meninges after GSH addition is significantly smaller than cystine ($p=0.048$), indicating that meninges are more efficient at taking up the precursors for GSH synthesis and then synthesizing GSH rather than taking up GSH directly (see Table 3-2).

Table 3-2. Comparison of kinetic parameters of GSH metabolism between meninges and cortical cell cultures.

	Meninges culture	Cortical culture
Fmax (fluor unit per mg protein) *	1.541 ± 0.193	1.084 ± 0.153
Initial slope (fluor unit per mg protein/min) **	0.652 ± 0.082	0.182 ± 0.132
Slope (Cys) (fluor unit per mg protein/min) *	0.096 ± 0.018	0.0088 ± 0.0018
Slope (Ckt) (fluor unit per mg protein/min) **	0.071 ± 0.0054	0.011 ± 0.0017
Slope (GSH) (fluor unit per mg protein/min) **	0.066 ± 0.0069	0.024 ± 0.0071
Slope (HBSS) (fluor unit per mg protein/min)	0.0032 ± 0.0007	0.0010 ± 0.0002

Figure 3-24

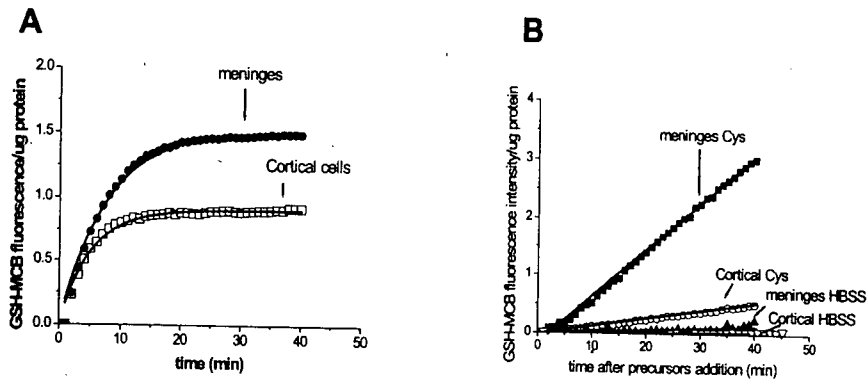


Figure 3-24. GSH metabolism is more active in meninges than in cortical cells. (A) Time course curve of MCB labelling of meningeal and cortical cells in culture at room temperature, showing that meningeal cells contain higher level of GSH and are more active in GST activity. **(B).** After the GSH-MCB fluorescence got to plateau level, we added Cys, GSH rate-limiting precursor, or HBSS, as a control to the culture, and found meningeal cells are more efficient in taking up precursors and synthesizing GSH.

3.6.3 Immunostaining of cortical cell cultures

In order to confirm the types of cells in the cortical cell cultures, we did immunostaining after MCB labeling. In order to fix MCB signal, we added 0.2% glutaldehyde to 4% PFA, and stained the cultures with astrocytes marker, s100 β . All the cells labeled by MCB are also labeled by s100 β (Figure 3-25 A-C). While counterimmunostaining with neuron marker, MapII, showed no staining at all in the cortical cultures (Figure 3-25 D-E). Therefore the GSH-containing cells in the cortical cultures are all astrocytes.

Figure 3-25

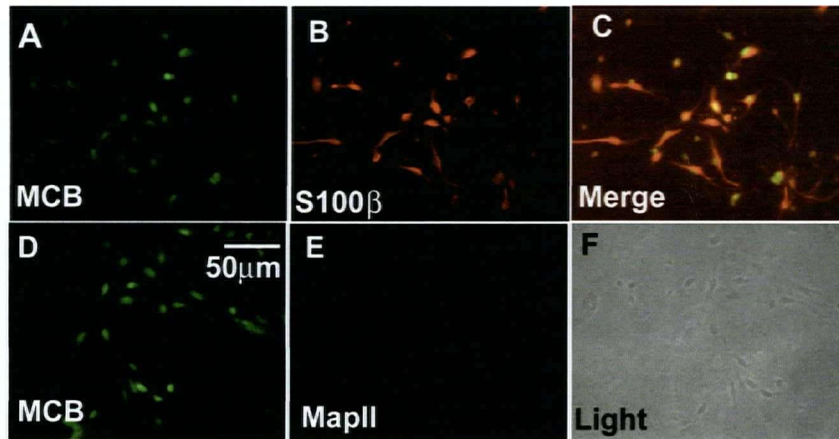


Figure 3-25. MCB labelled cells in cortical cells culture are S100β positive. MCB labelled cells in cortical cells cultures (A) are also labelled by S100 β (B). (C). The two signals are colocalized. (D, E). MapII cannot label any cells in the cortical cells cultures that are labelled by MCB. (F) is a picture of the cultured cells with light microscopy.

Chapter 4 Discussion

4.1 MCB labelling with two-photon microscopy resolves cellular GSH in situ.

Accumulating evidence indicates that alteration of GSH content and oxidative stress play substantial roles in neurological disorders such as stroke, Parkinson's, Alzheimer's, and Huntington's disease (Bains and Shaw, 1997; Schulz et al., 2000; Keelan et al., 2001; Perry et al., 2001; Shih et al., 2005b; Shih et al., 2005a). In view of the pivotal role of GSH in protecting cells (Cooper and Kristal, 1997; Herzenberg et al., 1997; Shih et al., 2003), there has been a considerable interest in the development of methods to quantify GSH content using biochemical assays (Tietze, 1969; Newton et al., 1981; Anderson, 1985). However, biochemical assays using cell lysates or tissue homogenates are unsuitable for examining GSH levels in intact single cells. The ability to measure GSH at the cellular level using two-photon imaging overcomes limitations inherent with conventional biochemical techniques and reveals a marked cellular heterogeneity in labelling patterns that would be lost in a biochemical assay for GSH.

However, it is important to note that light scattering by tissues limits the depth of two-photon microscopy to about 500 μm (Oheim et al., 2001; Helmchen and Denk, 2005). When measuring GSH concentration in slices we standardized for the effect of depth by measuring the fluorescence intensity of all regions at the same depth level,

about 50 μm . At this level, the damage caused by vibratome sectioning is negligible and the image depth will have similar effects on different brain regions.

Another potential caveat is that the MCB-GSH labelling technique is a means of measuring the total GSH content of a cell of interest (by converting all GSH to a fluorescent MCB conjugate) and will not provide a real-time sensor of GSH level. If one wants to measure GSH content at different time points within the same preparation they would need to allow for efflux of GSH-MCB and then reload with MCB. If reloading is done in the presence of GSH precursors the rate of GSH synthesis can also be measured (Sun et al., 2005).

A further caveat is that MCB labelling depletes the intracellular reservoir of reduced GSH as the MCB-GSH reaction proceeds to completion. Thus, long-term imaging may lead to increased oxidative stress and promote cellular apoptosis. Actually some groups have used MCB to cause GSH depletion. For example, Vesce et al. (2005) have reported that by exposing neurons cultures with MCB for 1h, mitochondria within neurons failed to hyperpolarize upon addition of oligomycin to inhibit their ATP synthesis. MCB progressively decreased cell respiration, but with no effect on mitochondrial proton leak or maximal respiratory capacity. However, in our experiments, we did not observed MCB-labelled cells show response under oxidative stress caused by GSH depletion. The possible reason is that with slices and cultures, we only exposed our slices to MCB for about half an hour, which is much shorter than the incubating time in Vesce et al (2005). When we performed MCB labelling *in vivo*, the labelling time is usually longer than 1h. But our *in vivo* labelling only showed MCB labelling of meninges and cortical astrocytes, which are much more efficient in defending against oxidative stress than neurons.

Therefore the MCB labelled cells *in vivo* seemed healthy during the total imaging procedure.

Although these limitations exist and are acknowledged to aid future researchers, we feel that two-photon imaging of MCB labelling in brain slices is major improvement over previously employed biochemical or imaging assays for GSH.

4.2 Cellular GSH distribution in brain slices.

4.2.1 GSH is highly expressed in cells at CSF interface

In this study we measure the GSH concentration in single cells in intact tissues directly with two-photon microscopy. Of all regions studied, lateral ventricle ependymal cells contain the highest level of GSH. Also of note, the meninges contain considerably higher GSH than neocortical astrocytes. Sato et al. have reported (Sato et al., 2002) that xCT (a high affinity cystine uptake system that is likely the rate limiting step in providing the precursor cysteine for GSH synthesis), is highly expressed both in meninges and in ependymal cells. Both of these regions are in direct contact with CSF making them ideally positioned to take up cystine for GSH synthesis and release to protect the brain against oxidative stress. The meninges have received little attention in antioxidant defense and have mainly been highlighted for their physical role at the CSF-blood barrier (Nilsson et al., 1992; Smith and Shine, 1992; Tanno et al., 1993). Our findings provide a new insight into the possible role of the meninges in protecting the brain against oxidative stress. In another article under preparation, we found that cultured meningeal

cells possess an active GSH antioxidant system and are even more efficient in protecting neurons against oxidative glutamate toxicity than astrocytes (Shih et al., in preparation; Sun et al, 2005a). However, in the intact brain, it is likely that all the GSH-enriched cell-types we have identified (meninges, ependyma, and astrocytes) contribute to redox buffering in the brain.

4.2.2 GSH in neurons

It has been well established that heterogeneity in GSH levels exists between neurons and astrocytes in brain parenchyma (Dringen, 2000). However, the relationship between GSH concentration in neurons versus astrocytes has not been consistent between all studies (Beiswanger et al., 1995; Rice and Russo-Menna, 1998; Tauskela et al., 2000). Perhaps these differences in part may be related to the developmental state or culture conditions of the preparations used. In our study, we found that in P15-P20d rat slices astrocytes contain 5 times more GSH than neurons in cortex. We also examined brain slices from young (P1-2) rats and found cells of presumably neuronal origin to have high GSH content (Figure 4-1). In these young slices, most cells are labelled by MCB. They can be separated to two groups. The high fluorescence group has GSH concentration of 1.70 ± 0.03 mM, the low group has GSH of 0.74 ± 0.04 mM (***) $p < 0.001$). Both of these groups contain significantly higher GSH than cortical neurons in mature (P15-20) rat slices (neurons: 0.21 ± 0.02 mM. *** $p < 0.001$ significantly lower than the two groups in young slices). We have hoped to identify the types of these cells in young slices. However, in these young animals it was difficult to costain MCB labelled neurons with

antibody markers since the neurons were not fully differentiated and the morphology of the slices was altered much by fixation.

Figure 4-1

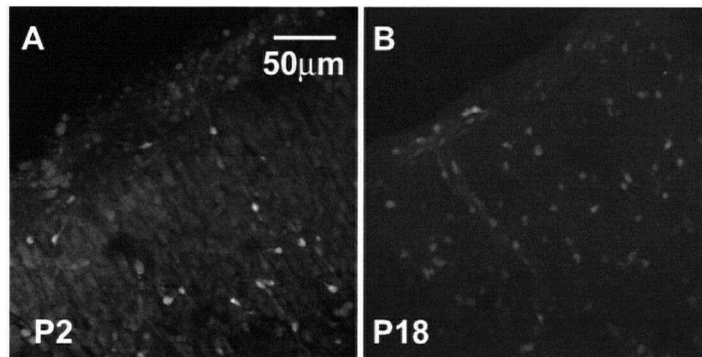


Figure 4-1. Comparison of MCB labelling in young and mature rat slices. (A). MCB labels almost all cells in P1-2 rat slices, with a subpopulation of cells show high fluorescence ($[GSH]=1.70 \pm 0.03$ mM, others show lower fluorescence ($[GSH]=0.74 \pm 0.04$ mM). (B). MCB labelling in mature (P18) rat slices. Only meningeal cells and cortical astrocytes are labelled robustly by MCB.

Developing neurons in mature brain also contained higher GSH-MCB levels. In the mature brain there are two major regions where neurogenesis is known to occur postnatally: the subventricular zone and the subgranular zone of the dentate gyrus (Li and Pleasure, 2005). Our results indicate that both neurogenic regions contain relatively high levels of GSH. In dentate gyrus, young neurons in the medial portion of granular cell layer contain GSH at a level much lower than the dividing precursor cells (subgranular zone), while the mature neurons in the lateral portion of granular cell layer contain only background levels of GSH. This suggests that when neurons are proliferating they are in great need of antioxidant buffer and thus contain high GSH. During the process of maturation, neurons lose most of their GSH content and henceforth seem to depend on astrocytes to provide them with this antioxidant buffer. This is consistent with the findings of Beiswanger et al (1995) who visualized GSH distribution in the mouse nervous system by mercury orange histochemistry and found that all neuronal and glial progenitor cells contain GSH, while most neurons lose the bulk of their GSH content by P5 and become surrounded by a GSH-rich neuropil. Other groups also reported that neurons lose their GSH content as they grow in co-culture with astrocytes (Sagara et al., 1993; Keelan et al., 2001). This low level of GSH content in mature neurons may explain their unique vulnerability to oxidative stress (Murphy et al., 1990; Ratan et al., 1994; Bolanos et al., 1995; Dringen et al., 1999; Schubert and Piasecki, 2001). In addition to the cell types described here it will be interesting to apply the MCB labelling approach to study GSH in oligodendrocytes that have a unique developmentally-dependent vulnerability to oxidative stress (Oka et al., 1993; Back et al., 1998).

4.2.3 Summary of types of cells labelled by MCB in slices

We have used immunostaining to verify the types of cells labelled by MCB. MCB-GSH signal can be fixed with 0.2% glutaraldehyde in 4% PFA. With immunostaining of meninges and cortical cell cultures, we fixed the culture with 0.2% glutaraldehyde in 4% PFA, and MCB-GSH signal was well preserved (Figure 3-25). However, glutaraldehyde will make slices impossible to be stained with antibodies (data not shown). In order to perform immunostaining, we can only fix slices with 4% PFA, which will cause completely lost of MCB-GSH signal. To find the previously imaged region after immunostaining, we used laminin, a marker for base membrane of blood vessels, or PI, a dead cell marker, as landmarks. Since MCB will label perivascular astrocytes, making blood vessel visible when imaging acute slices. After immunostaining, laminin will also label the same blood vessels, which can be used as landmarks. For PI, we usually colabeled the acute slices with MCB and PI together. PI will label dead cells in acute slices, which is usually on the surface of slices. After fixation, PI signal was preserved within these cells that had died during vibratome sectioning, which can also be used as landmarks. However, the fixation always caused some distortion of cell position, therefore we usually only examined colocalization over a relatively small area, based on cell morphology and the relative position of cells.

MCB can robustly label cells at the CSF interface, such as meninges and lateral ventricle ependymal cells. In cortex, MCB labelled cells can be separated to two groups. The high fluorescence group are S100 β positive, and NeuN negative, and are mostly found in Layer I, indicating they are astrocytes. The low fluorescence group are usually

found in Layer II, showing neuronal morphology and having their apical dendrites orienting towards the meninges. Immunostained with NeuN confirmed that they are neurons. In subventricular zone (SVZ) under the ependymal cells, lots of cells are also strongly labelled by MCB. Many of them are DCX positive, indicating they are neuron precursors, and need high GSH reservoir for their high metabolic activity. In dentate gyrus, the highest fluorescence cells are found in subgranular zone (SGZ), many of which are also DCX positive. In medial portion of granular cell layer, cells showed low MCB and NeuN signal, indicating they are young neurons. In lateral portion of granular cell layer, cells were labelled by NeuN strongly, indicating they are mature neurons. However, they have lost almost all of their GSH content (Table 4-1).

Table 4-1. Types of cells labelled by MCB

	Cortex		SVZ	SGZ
	High fluorescence group	Low fluorescence group		
S100 β	+	-	+	+
NeuN	-	+	-	-
DCX	-	-	+	+

4 . 3 Manipulation of GSH metabolism

We have developed an assay to monitor the metabolism of GSH in cultures, using a fluorescence plate reader and monitoring the kinetics of the GST catalyzed reaction between GSH and the substrate MCB. We were able to measure various kinetics parameters of GSH metabolism, such as the rates of GSH synthesis, conjugation and efflux under basal conditions and after tBHQ induction of Nrf2 driven antioxidant response element-mediated gene expression. Our assay can also be applied to meninges and cortical cells cultures, which showed that meninges are more active in GSH metabolism. They contain high level of GSH, higher activity of GST, and are more efficient in taking up GSH precursors and synthesizing GSH.

We have hoped to measure different kinetic parameters of GSH metabolism in rat brain slices, besides GSH content and GST activity. We added GSH 100 μ M, or Cystine 100 μ M, to the perfusion system and used two-photon microscopy to record the fluorescence change over time. However, we did not find significant increase in fluorescence intensity as we have hoped. A possible reason is that cells in slices cannot take up these substrates as efficiently as in cultures.

We also tried to examine whether we can increase intracellular GSH level by applying GSH precursor, cystine to animals. We injected Cystine (1mM) from tail vein to mice and measured GSH concentration in tissue homogenate with GSH assay. However, in all brain regions that we have examined, including cortex, striatum, hippocampus, and cerebellum, there is no significant difference between animals injected with Cystine and

control (data not shown). We only found significant increase in liver homogenate and blood (Liver: Cys group: 156.1 ± 17.9 mM, control group: 70.9 ± 10.3 mM, $p < 0.01$; Blood cells: Cys group: 417.9 ± 25.4 mM, control group: 53.2 ± 7.6 mM, $p < 0.01$). We supposed that cells in brain might already have enough GSH, therefore they won't take up GSH precursors. In order to test this, we first depleted GSH content with diethyl maleate (DEM) (Szaszi et al., 2005), which caused almost complete depletion of intracellular GSH, but did not affect GST activity (Figure 4-2). After GSH depletion, we injected Cystine through tail vein. However, we still cannot find significant difference between control group and Cystine group (data not shown). A possible reason is that it is difficult for cystine to cross blood-brain barrier (data not shown). We also used two-photon microscopy to image fluorescence level after tail vein injection of GSH or Cystine, and we did not find significant increase either (data not shown).

Figure 4-2

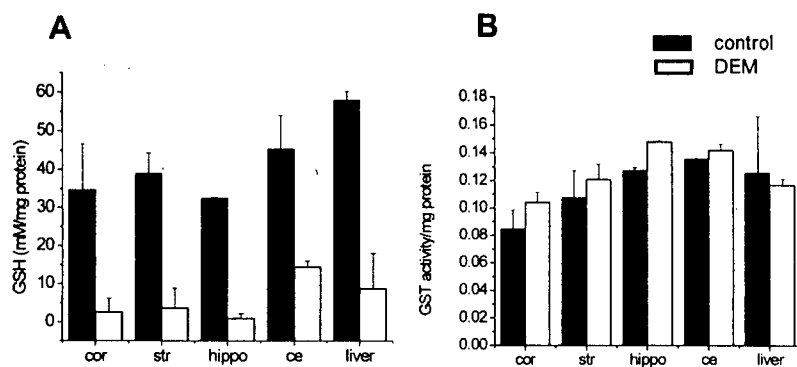


Figure 4-2. DEM depletion of intracellular GSH content. (A). GSH content in tissue homogenate from different brain regions and liver. DEM caused a significant decrease in GSH concentration in all regions ($p < 0.05$, for all groups). (B). GST activity in different regions. DEM did not affect GST activity. Data were averaged from 3 animals.

4.4 Measurement of GSH within the cortex of live animals.

In addition to examining MCB-GSH labelling in brain slices, we adapted the technique to an *in vivo* preparation. Brief exposure of the intact brain to MCB followed by two-photon imaging was proved to be a robust method for labelling GSH-containing cells in the somatosensory cortex *in vivo*. The specificity of MCB labeling of astrocytes in neocortex was verified by co-labelling with SR 101, a neocortex astrocyte marker (Nimmerjahn et al., 2004). This approach offers the opportunity to measure GSH content in live animals, which is closer to biological reality than measures performed in brain slices or cultures. The GSH antioxidant system can be activated when the brain is under oxidative stress, such as during the reperfusion period after an ischemic insult when GSH demand may be relatively higher (Rehncrona et al., 1980; Lyrer et al., 1991). It will also be affected by many neurological disorders, such as Parkinson's disease (Schapira et al., 1990), and Alzheimer's disease (Abramov et al., 2003). Recent data also indicates a role for GSH and its precursors in maintaining the viability of brain tumors (Chung et al., 2005). However, in most cases, data linking the GSH system to these disorders was derived from tissue homogenates, which cannot detect cellular heterogeneity. In addition there are some contrary reports on how the GSH levels change during these neurological diseases (Uemura et al., 1991; Mizui et al., 1992; Gotoh et al., 1994; Guegan et al., 1998). Our approach can be applied to animal models of these diseases and mouse mutants with abnormal handling of oxidative stress (Aoyama et al., 2005; Siddiq et al., 2005) to measure GSH levels in different brain regions directly. Recent studies from our lab have used electrophilic inducers of the redox-sensitive transcription factor Nrf2 to

4.4 Measurement of GSH within the cortex of live animals.

In addition to examining MCB-GSH labelling in brain slices, we adapted the technique to an *in vivo* preparation. Brief exposure of the intact brain to MCB followed by two-photon imaging was proved to be a robust method for labelling GSH-containing cells in the somatosensory cortex *in vivo*. The specificity of MCB labeling of astrocytes in neocortex was verified by co-labelling with SR 101, a neocortex astrocyte marker (Nimmerjahn et al., 2004). This approach offers the opportunity to measure GSH content in live animals, which is closer to biological reality than measures performed in brain slices or cultures. The GSH antioxidant system can be activated when the brain is under oxidative stress, such as during the reperfusion period after an ischemic insult when GSH demand may be relatively higher (Rehncrona et al., 1980; Lyrer et al., 1991). It will also be affected by many neurological disorders, such as Parkinson's disease (Schapira et al., 1990), and Alzheimer's disease (Abramov et al., 2003). Recent data also indicates a role for GSH and its precursors in maintaining the viability of brain tumors (Chung et al., 2005). However, in most cases, data linking the GSH system to these disorders was derived from tissue homogenates, which cannot detect cellular heterogeneity. In addition there are some contrary reports on how the GSH levels change during these neurological diseases (Uemura et al., 1991; Mizui et al., 1992; Gotoh et al., 1994; Guegan et al., 1998). Our approach can be applied to animal models of these diseases and mouse mutants with abnormal handling of oxidative stress (Aoyama et al., 2005; Siddiq et al., 2005) to measure GSH levels in different brain regions directly. Recent studies from our lab have used electrophilic inducers of the redox-sensitive transcription factor Nrf2 to

induce multiple antioxidant systems as a therapeutic strategy for neurodegeneration and stroke (Shih et al., 2005b; Shih et al., 2005a). Interestingly, evaluation of brain tissue homogenates showed dynamic increases in GSH content after the administration of Nrf2 inducers. Animals receiving inducers exhibited reduced lesion size and improved recovery compared to controls. In future studies, the technique we have described here could be used to image and quantify the cellular sites of GSH induction by Nrf2 inducers, as well as other drugs that influence the GSH system (Kamencic et al., 2001).

4.5 Meninges may be an ideal position for protecting brain against oxidative load

Little attention has been paid to the meninges covering the brain parenchyma except for the physical role at the CSF-blood barrier (Nilsson et al., 1992; Smith and Shine, 1992; Tanno et al., 1993). In the current study, we have found that meninges contain significantly higher GSH content than astrocytes. With plate reader assay, we found that meninges are more active in GSH metabolism than cortical cells. They contain higher activity of GST, and are more efficient in taking up GSH precursors and synthesizing GSH. This suggests that meninges may play an important role in antioxidant defence. Consistent with this, Shih AY, a PhD student in our lab, used RT-PCR and western blot to show that meninges express higher level of xCT than cortex, striatum and liver. xCT is a subunit of x_c^- , an exchange agency specific for anionic forms of cystine and glutamate (Bannai, 1986). The x_c^- antiporter is composed of two subunits, xCT and 4F2hc. Whereas xCT confers cystine specificity, 4F2hc is present as a structural subunit

in a variety of amino acid transporters (Sato et al, 1999). With this high xCT level, meninges can take up ^{35}S -cystine 20-fold greater than cortical cells (Shih AY et al., paper in preparation). Shih AY further tested whether meninges are more efficient in protecting neurons against oxidative stress than astrocytes with a well-established NMDA receptor-independent oxidative glutamate toxicity paradigm in which neurons die from GSH depletion (Murphy et al., 1989, 1990). He cocultured neurons with glia, meninges or fibroblast cells, which will protect neurons against the oxidative stress caused by addition of 3 mM glutamate. By comparing the percentage of viable neurons in each group, he found that meninges are the most efficient in neuroprotection. The percentage of NSE⁺ (a neuron-selective marker) cells in meninges-neuron coculture is significantly higher than in other coculture (Shih et al., paper in preparation).

Meninges are filled with CSF, whose antioxidant potential seems to be important for keeping brain healthy. The highly expressed x_c system seems to have two functions. First, clearance of cystine via x_c system and release of cysteine from the cells via neutral amino acid transporters may contribute to maintain the reduced state in the CSF against oxidative stress. Second, the uptake of cystine from x_c⁻ provides meninges with plenty of precursors for GSH synthesis, which makes meninges efficient in protecting brain against oxidative stress. From all the above, we supposed meninges may be an ideal position for protecting brain against oxidative stress.

4.6 Conclusion

I have described a new technique to measure glutathione, the major cellular antioxidant, in the intact brain using two-photon scanning laser microscopy. By applying and imaging the glutathione specific dye, monochlorobimane, in rat brain slices and the neocortices of live anesthetized mice, I was able to resolve glutathione levels within individual cells. This is a considerable improvement on conventional biochemical assays for glutathione since brain homogenates and cell lysates only provide information about the average glutathione level in the sample. Using this technique, I revealed the heterogeneity of glutathione distribution throughout the brain and identify ependymal and meningeal cells (CSF-brain barrier), and astrocytes as the major glutathione reservoirs within the brain. Surprisingly, I also find that developing neurons found within two neurogenic regions (subventricular zone and subgranular zone of the dentate gyrus) are particularly rich in glutathione, suggesting that adequate redox buffering is important for the metabolic demands of neuronal proliferation.

I have described a new technique to measure glutathione, the major cellular antioxidant, in the intact brain using two-photon scanning laser microscopy. By applying and imaging the glutathione specific dye, monochlorobimane, in rat brain slices and the neocortices of live anesthetized mice, I was able to resolve glutathione levels within individual cells. This is a considerable improvement on conventional biochemical assays for glutathione since brain homogenates and cell lysates only provide information about the average glutathione level in the sample. Using this technique, I revealed the heterogeneity of glutathione distribution throughout the brain and identify ependymal and meningeal cells (CSF-brain barrier), and astrocytes as the major glutathione reservoirs within the brain. Surprisingly, I also find that developing neurons found within two neurogenic regions (subventricular zone and subgranular zone of the dentate gyrus) are particularly rich in glutathione, suggesting that adequate redox buffering is important for the metabolic demands of neuronal proliferation.

Reference

- Abramov AY, Canevari L, Duchen MR (2003) Changes in intracellular calcium and glutathione in astrocytes as the primary mechanism of amyloid neurotoxicity. *J Neurosci* 23:5088-5095.
- Akerboom T, Sies H (1990) Glutathione transport and its significance in oxidative stress. In: Vina, J, *Glutathione: Metabolism and Physiological Functions*. CRC Press, Boca Raton, FL, USA, pp.45-55.
- Alam J, Stewart D, Touchard C, Boinapally S, Choi A.M, Cook J.L (1999) Nrf2, a Cap 'n' Collar transcription factor, regulates induction of the heme oxygenase-1 gene. *J.Biol. Chem* 274:26071-26078.
- Amara A, Coussemaq M, Geffard M (1994) Antibodies to reduced glutathione. *Brain Res.* 659: 237-242.
- Ameriso SF, Sahai S (1997) Mechanisms of ischaemia in situ vascular occlusive disease. In: *Primer on cerebrovascular diseases* (Welsh, K.M.A. Caplan, L.R. Reis, D.J. Siesjo, B.K. and Weir, B., eds), pp.279-285. Academic Press, San Diego.
- Anderson ME (1985) Determination of glutathione and glutathione disulfide in biological samples. *Methods Enzymol* 143:548-555.
- Anderson ME, Underwood M, Bridges RJ and Meister A (1989) Glutathione metabolism at the blood-cerebrospinal fluid barrier. *FASEB J* 3: 2527-2531.

- Anderson M.F (1998) Glutathione: an overview of biosynthesis and modulation. *Chem Biol Interact* 111-112: 1-14.
- Anderson MF, Sims NR (2002) The effects of focal ischemia and reperfusion on the glutathione content of mitochondria from rat brain subregions. *J Neurochem* 81: 541-549.
- Anderson M.F, Blomstrand F, Blomstrand C, Eriksson P.S, Nilsson M (2003) Astrocytes and Stroke: Network for Survival? *Neurochemical Research* 28:293-305.
- Anderson MF, Nilsson M, Sims NR (2004a) Glutathione monoethylester prevents mitochondria glutathione depletion during focal cerebral ischemia. *Neurochem International*. 44:153-158.
- Anderson MF, Nilsson M, Eriksson PS, Sims NR (2004b) Glutathione monoethylester provides neuroprotection in a rat model of stroke. *Neurosci Letters*. 354:163-165.
- Aoyama K, Suh SW, Hamby AM, Liu J, Chan WY, Chen Y, Swanson RA (2005) Neuronal glutathione deficiency and age-dependent neurodegeneration in the EAAC1 deficient mouse. *Nat Neurosci*.
- Back SA, Gan X, Li Y, Rosenberg PA, Volpe JJ (1998) Maturation-dependent vulnerability of oligodendrocytes to oxidative stress-induced death caused by glutathione depletion. *J Neurosci* 18:6241-6253.
- Bains JS, Shaw CA (1997) Neurodegenerative disorders in humans: the role of glutathione in oxidative stress-mediated neuronal death. *Brain Res Brain Res Rev* 25:335-358.
- Bannai S (1986) Exchange of cystine and glutamate across plasma membrane of human fibroblasts. *J. Biol Chem* 261: 2256-2263.

- Barhoumi R, Bailey RH, Burghardt RC (1995) Kinetic analysis of glutathione in anchored cells with monochlorobimane. *Cytometry* 19: 226-234.
- Beiswanger C.M., Diegmann M.H., Novak R.F., Philbert M.A., Graessle T.L., Reuhl K.R., Lowndes H.E (1995) Developmental changes in the cellular distribution of glutathione and glutathione-S-transferases in the murine nervous system. *Neurotoxicology* 16: 425-440.
- Bharath S, Hsu M, Kaur D, Rajagopalan S, and Anderson JK (2002) Glutathione, iron and Parkinson's disease. *Biochem. Pharmacol.* 64: 1037-1048.
- Bolanos JP, Heales SJ, Land JM, Clark JB (1995) Effect of peroxynitrite on the mitochondrial respiratory chain: differential susceptibility of neurones and astrocytes in primary culture. *J Neurochem* 64:1965-1972.
- Bolanos JP, Heales SJ, Peuchen S, Barker JE, Land JM, and Clark JB. (1996) Nitric oxide-mediated mitochondrial damage: a potential neuroprotective role for glutathione. *Free Radic. Biol. Med.* 21: 995-1001.
- Borst P, Evers R, Kool M, and Wijnholds J (1999) The multidrug resistance protein family. *Biochim. Biophys. Acta* 1461:347-357.
- Borst P and Oude Elferink R (2002) Mammalian ABC transporters in health and disease. *Annu. Rev. Biochem.* 71:537-592.
- Brigelius-Flohe R (1999) Tissue-specific functions of individual glutathione peroxidases. *Free Radic. Biol. Med.* 27: 951-965.
- Brown JP, Couillard-Despres S, Cooper-Kuhn CM, Winkler J, Aigner L, Kuhn HG (2003) Transient expression of doublecortin during adult neurogenesis. *J. Comp. Neurology.* 467:1-10.

- Cao XH, and Phillis JW (1994) α -Phenyl-tert-butyl-nitrone reduces cortical infarct and edema in rats subjected to focal ischemia. *Brain Res.* 644: 267-272.
- Chance B, Sies H, Boveris A. (1979) Hydroperoxide metabolism in mammalian organs. *Physiol. Rev.* 59: 527-605.
- Chatterjee S, Noack H, Possel H, Keilhoff G, Wolf G (1999) Glutathione levels in primary glial cultures: monochlorobimane provides evidence of cell type-specific distribution. *Glia.* 27 (2): 152-161.
- Chen Y, Vartiainen NE, Ying W, Chan PH, Koistinaho J, and Swanson RA (2001) Astrocytes protect neurons from nitric oxide toxicity by a glutathione-dependent mechanism. *J. Neurochem.* 77: 1601-1610.
- Chung WJ, Lyons SA, Nelson GM, Hamza H, Gladson CL, Gillespie GY, Sontheimer H (2005) Inhibition of cystine uptake disrupts the growth of primary brain tumors. *J Neurosci* 25:7101-7110.
- Clancy RM, Levartovsky D, Leszczynska-Piziak J, Yegudin J, Abramson, SB (1994) Nitric oxide reacts with intracellular glutathione and activates the hexose monophosphate shunt in human neutrophils: evidence for S-nitrosoglutathione as a bioactive intermediate. *Proc. Natl. Acad. Sci. USA* 91: 3680-3684.
- Clarke DD, and Sokoloff L (1999) Circulation and energy metabolism of the brain. In: *Basic Neurochemistry: Molecular, Cellular, and Medical Aspects*, G.J. Sigel, B.W.Agranoff, R.W.Albers, S.K. Fisher, and M.D. Uhler, eds. (Philadelphia, USA: Lippincott-Raven). pp. 637-669.

- Commandeur JNM, Stijntjes GJ, Vermeulen NPE (1995) Enzymes and transport systems involved in the formation and disposition of glutathione S-conjugates. *Pharmacol. Rev.* 47: 271-230.
- Cook JA, Iype SN, Mitchell JB (1991) Differential specificity of monochlorobimane for isozymes of human and rodent glutathione-S-transferases. *Cancer Res* 31: 1606-1612.
- Cooper AJL, Kristal BS (1997) Multiple roles of glutathione in the central nervous system. *Biol Chem* 378: 793-802.
- Copeland RA (2000) *Enzymes: A practical introduction to structure, mechanism, and data analysis*. Second edition. Wiley-VCH, pp 109-113.
- Cotgreave IA, Gerdes RG (1998) Recent trends in glutathione biochemistry-glutathione protein interactions: a molecular link between oxidative stress and cell proliferation? *Biochem. Biophys. Res. Commun.* 242: 1-9.
- Cruz-Aguado R, Francis-Turner L, Diaz CM and Antunez I (2002a) Quinolinic acid lesion induces changes in rat striatal glutathione metabolism. *Neurochem Int.* 37:53-60.
- Cruz-Aguado R, Turner LF, Diaz CM and Pinero J (2002b) Nerve growth factor and striatal glutathione metabolism in a rat model of Huntington's disease. *Restor. Neurol. Neurosci.* 17: 217-221.
- Decleves Z, Regina A, Laplanche JL, Roux F, Boval B, Launay JM, and Scherrmann JM (2000) Functional expression of P-glycoprotein and multidrug resistance-associated protein (Mrp1) in primary cultures of rat astrocytes. *J. Neurosci. Res.* 60: 594-601.

- Deloulme JC, Raponi E, Gentil BJ, Bertacchi N, Marks A, Labourdette G, Baudier J (2004) Nuclear expression of S100B in oligodendrocyte progenitor cells correlates with differentiation toward the oligodendroglial lineage and modulates oligodendrocytes maturation. *Mol Cell Neurosci* 27:453-465.
- Devesa A, O'Connor J.E, Garcia C, Puertes I.R, Vina J.R (1993) Glutathione metabolism in primary astrocyte cultures: flow cytometric evidence of heterogeneous distribution of GSH content. *Brain Res* 618: 181-189.
- Dexter DT, Sian J, Rose S, Hindmarsh JG, Mann VM, Cooper JM, Wells FR, and Marsden CD (1994) Indices of oxidative stress and mitochondrial function in individuals with incidental Lewy body disease. *Ann. Neurol.* 35: 38-44.
- Do KQ, Trabesinger AH, Kirsten-Kruger M, Lauer CJ, Dydak U, Hell D, Holsboer F, Boesiger P and Cuenod M (2000) Schizophrenia: glutathione deficit in cerebrospinal fluid and prefrontal cortex in vivo. *Eur. J. Neurosci.* 12: 3721-3728.
- Doetsch F, Alvarez-Buylla A (1996) Network of tangential pathways for neuronal migration in adult mammalian brain. *PNAS.* 93: 14895-14900.
- Dringen R, Kranich O and Hamprecht B (1997) The gamma-glutamyl transpeptidase inhibitor acivicin preserves glutathione released by astroglial cells in culture. *Neurochem. Res.* 22:727-733.
- Dringen R and Hamprecht B (1998) Glutathione restoration as indicator for cellular metabolism of astroglial cells. *Dev Neurosci.* 20:401-407.
- Dringen R, Kussmaul L, Gutterer JM, Hirrlinger J, Hamprecht B (1999) The glutathione system of peroxide detoxification is less efficient in neurons than in astroglial cells. *J Neurochem* 72:2523-2530.

- Dringen R, Gutterer JM, and Hirrlinger J (2000) Glutathione metabolism in brain metabolic interaction between astrocytes and neurons in the defense against reactive oxygen species. *Eur. J. Biochem.* 267:4912-4916.
- Dringen R (2000) Metabolism and functions of glutathione in brain. *Prog in Neurobiol* 62:649-671.
- Dringen R, Gutter JM, Gros C, and Hirrlinger J (2001) Aminopeptidase N mediates the utilization of the GSH precursor CysGly by cultured neurons. *J. Neurosci. Res.* 66: 1003-1008.
- Dringen R and Hirrlinger J (2003) Glutathione pathways in the brain. *Biol Chem.* 384:505-516.
- Duck FA (1990) Physical Properties of Tissue. Academic Press, London.
- Eftekharpour E, Holmgren A, Juurlink B.H (2000) Thioredoxin reductase and glutathione synthesis is [sic] upregulated by t-butylhydroquinone in cortical astrocytes but not in cortical neurons. *Glia* 31:241-248.
- Fernandez-Checa JC, Takikawa H, Horie T, Ookhtens M and Kaplowitz N (1992) Canalicular transport of reduced glutathione in normal and mutant Eisai hyperbilirubinemic rats. *J. Biol. Chem.* 267: 1667-1673.
- Finkel T and Holbrook NJ (2000) Oxidants, oxidative stress and the biology of ageing. *Nature* 409: 239-247.
- Francis F, Koulakoff A, Boucher D, Chafey P, Schaar B, Vinet M, Friocourt G, McDonnell N, Reiner O, Kahn A, McConnell SK, Berwald-Netter Y, Denoulet P, Chelly J (1999) Doublecortin is a developmentally regulated, microtubule-

associated protein expressed in migrating and differentiating neurons. *Neuron*. 23:247-256.

- Gate L, Paul L, Nguyen BA, Tapeiro H (1999) Oxidative stress induced pathologies: the role of antioxidants. *Biomed. Pharmacother.* 53: 169-180.
- Gherzi-Egera JF, Leninger-Muller B, Suleman G, Siest G, and Minn A (1994) Localization of drug-metabolizing enzyme activities to bloodbrain interfaces and circumventricular organs. *J. Neurochem.* 62: 1089-1096.
- Ghibelli L, Fanelli C, Rotilio G, Lafavia E, Coppola S, Colussi C, Civitareale P, Ciriolo MR (1998) Rescue of cells from apoptosis by inhibition of active GSH extrusion. *FASEB J.* 12: 479-486.
- Gotoh O, Yamamoto M, Tamura A, Sano K (1994) Effect of YM737, a new glutathione analogue, on ischemic brain edema. *Acta Neurochir Suppl (Wien)* 60:318-320.
- Gu M, Owen AD, Toffa SE, Cooper JM, Dexter DT, Jenner P, Marsden CD, and Schapira AH (1998) Mitochondria function, GSH and iron in neurodegeneration and Lewy body diseases. *J. Neurol. Sci.* 158: 24-29.
- Guegan C, Ceballos-Picot I, Nicole A, Kato H, Onteniente B, Sola B (1998) Recruitment of several neuroprotective pathways after permanent focal ischemia in mice. *Exp Neurol* 154:371-380.
- Hall AG (1999) The role of glutathione in the regulation of apoptosis. *Eur. J. Clin. Invest.* 29:238-245.
- Han J, Cheng FC, Yang Z, and Dryhurst G (1999) Inhibitors of mitochondrial respiration, iron and hydroxyl radical evoke release and extracellular hydrolysis of glutathione

- in rat striatum and substantia nigra: potential implications to Parkinson's disease. *J. Neurochem.* 73: 1683-1695.
- Hedley D.W, Chow S (1994) Evaluation of methods for measuring cellular glutathione content using flow cytometry. *Cytometry* 15:349-358.
- Helmchen F, Denk W (2005) Deep tissue two-photon microscopy. *Nat Methods* 2:932-940.
- Henderson JT, Javaheri M, Kopko S, Roder JC (1996) Reduction of lower motor neuron degeneration in wobbler mice by N-acetyl-L-cysteine. *J. Neurosci.* 16: 7574-7582.
- Hermesen WLJM, McMahon PJ, Anderson JW (1997) Determination of glutathione in plant extracts as the 1-chloro-2, 4-dinitrobenzene conjugate in the presence of glutathione-S-transferase. *Plant Physiol. Biochem.* 39: 491-496.
- Hertz L, Dringen R, Schousboe A, and Robinson SR (1999) Astrocytes: glutamate producers for neurons. *J. Neurosci. Res.* 57: 417-428.
- Herzenberg LA, De Rosa SC, Dubs JG, Roederer M, Anderson MT, Ela SW, Deresinski SC (1997) Glutathione deficiency is associated with impaired survival in HIV disease. *Proc Natl Acad Sci U S A* 94:1967-1972.
- Hirrlinger J, König J, Keppler D, Linddenau J, Schulz JB and Dringen R (2001) The multidrug resistance protein MRP1 mediates the release of glutathione disulfide from rat astrocytes during oxidative stress. *J. Neurochem.* 76: 627-636.
- Hirrlinger J, König J and Dringen R. (2002a) Expression of mRNAs of multidrug resistance proteins (Mrps) in cultured rat astrocytes, oligodendrocytes, microglial cells and neurons. *J. Neurochem.* 82: 716-719.

- Hirrlinger J, Schulz JB, and Dringen R (2002b) Effects of dopamine on the glutathione metabolism of cultured astroglial cells: implications for Parkinson's disease. *J. Neurochem.* 82: 458-467.
- Hirrlinger J, Schulz J.B, and Dringern R (2002c) Glutathione release from cultured brain cells: multidrug resistance protein 1 mediates the release of GSH from rat astroglial cells. *J. Neurosci. Res.* 69:318-326.
- Hjelle OP, Chaudhry FA, Ottersen OP (1994) Antisera to glutathione: characterization and immunocytochemical applications to the rat cerebellum. *Eur J Neurosci.* 6: 793-804.
- Ishii T, Itoh K, Takahashi S, Sato H, Yanagawa T, Katoh Y, Bannai S, Yamamoto M (2000) Transcription factor Nrf2 coordinately regulates a group of oxidative stress-induced genes in macrophages. *J. Biol Chem.* 275:16023-16029.
- Ishikawa K, Kabeya K, Shinoda M, Katakai K, Mori M, and Tatemoto K. (1995) Meninges play a neurotrophic role in the regeneration of vasopressin nerves after hypophysectomy. *Brain Res.* 677: 20-28.
- Ishikawa T and Sies H (1998) Glutathione as an antioxidant: toxicological aspects. In: *Glutathione: Chemical, Biochemical, and Medical Aspects*, B. Dolphin, O. Avramovic and R. Poulson, eds. (New York, USA: John Wiley), pp. 85-109.
- Itoh K, Ishii T, Wakabayashi N, Yamamoto M (1999) Regulatory mechanisms of cellular response to oxidative stress. *Free Radic Res.* 31:319-324.
- Iwata-Ichikawa E, Kondo Y, Miyazaki I, Asanuma M, Ogawa N (1999) Glial cells protect neurons against oxidative stress via transcriptional up-regulation of the glutathione synthesis. *J. Neurochem:* 72, 2334-2344.

- Jacewicz M, Tanabe J, and Pulsinelli WA (1992) The CBF threshold and dynamics for focal cerebral infarction in spontaneously hypertensive rats. *J. Cereb. Blood Flow Metab.* 12:359-370.
- Jain A, Madsen DC, Auld PA, Frayer WW, Schwartz MK, Meister A, Martensson J (1995) L-2-oxothiazolidine-4-carboxylate, a cysteine precursor, stimulates growth and normalized tissue glutathione concentration in rats fed a sulphur amino acid-deficient diet. *J. Nutr.* 125: 851-856.
- Janaky R, Ogita K, Pasqualotto BA, Bains JS, Oja SS, Yoneda Y, and Shaw CA (1999) Glutathione and signal transduction in the mammalian CNS. *J. Neurochem.* 73: 889-902.
- Janaky R, Shaw CA, Varga V, Hermann A, Dohovics R, Saransaari P, and Oja SS. (2002a) Specific glutathione binding sites in pig cerebral cortical synaptic membrane. *Neuroscience.* 95: 617-624.
- Janaky R, Varga V, Hermann A, Saransaari P and Oja SS (2002b) Mechanisms of L-cysteine neurotoxicity. *Neurochem. Res.* 25:1397-1405.
- Jenner P and Olanow CW (1998) Understanding cell death in Parkinson's disease. *Ann. Neurol.* 44: S72-S84.
- Johnson D.A, Andrews G.K, Xu W, Johnson J.A (2002) Activation of the antioxidant response element in primary cortical neuronal cultures derived from transgenic reporter mice. *J. Neurochem* 81:1233-1241.
- Johnson JA, El Barbary A, Kornguth SE, Brugge JF, Siegel FL (1993) Glutathione S-transferase isoenzymes in rat brain neurons and glia. *J. Neurosci* 13: 2013-2023.

- Kamencic H, Griebel RW, Lyon AW, Paterson PG, Juurlink BH (2001) Promoting glutathione synthesis after spinal cord trauma decreases secondary damage and promotes retention of function. *Faseb J* 15:243-250.
- Kaplowitz N, Fernandez-Checa JC, Kannan R, Garcia-Ruiz, Ookhtens M, Yi JR (1996) GSH transporters: molecular characterization and role in GSH homeostasis. *Biol Chem. Hoppe-Seyler* 377: 267-273.
- Keelan J, Allen NJ, Antcliffe D, Pal S, Duchon MR (2001) Quantitative imaging of glutathione in hippocampal neurons and glia in culture using monochlorobimane. *J Neurosci Res* 66:873-884.
- Kempermann G, Gast D, Kronenberg G, Yamaguchi M, Gage FH (2003) Early determination and long-term persistence of adult-generated new neurons in the hippocampus of mice. *Development* 130:391-399.
- Kempermann G, Jessberger S, Steiner B, Kronenberg G (2004) Milestones of neuronal development in the adult hippocampus. *Trends Neurosci* 27:447-452.
- Kinouchi H, Epstein CJ, Mizui T, Carlson E, Chen SF and Chan PH (1991) Attenuation of focal cerebral ischemic injury in transgenic mice overexpressing CuZn superoxide dismutase. *Proc. Natl. Acad. Sci. USA* 88: 11158-11162.
- Kleinfeld D, Mitra PP, Helmchen F, Denk W (1998) Fluctuations and stimulus-induced changes in blood flow observed in individual capillaries in layers 2 through 4 of rat neocortex. *Proc Natl Acad Sci USA* 95: 15741-15746.
- Kleinfeld D, Denk W (2000) *Imaging neurons: a laboratory manual*. Cold Spring Harbor, NY: Cold Spring Harbor Laboratory.

- Konig J, Nies AT, Cui Y, Leier I and Keppler D (1999) Conjugate export pumps of the multidrug resistance protein (MRP) family: localization, substrate specificity, and MRP2-mediated drug resistance. *Biochem. Biophys. Acta* 1461: 377-394.
- Kraft AD, Johnson DA, Johnson JA (2004) Nuclear factor E2-dependent antioxidant response element activation by tert-butylhydroquinone and sulforaphane occurring preferentially in astrocytes conditions neurons against oxidative insult. *J. Neurosci.* 24(5):1101-1112.
- Kranich O, Hamprecht B, and Dringen R (1996) Different preferences in the utilization of amino acid for glutathione synthesis in cultured neurons and astroglial cells derived from rat brain. *Neurosci Lett.* 219:211-214.
- Kranich O, Dringen R, Sandberg M, and Hamprecht B (1998) Utilization of cysteine and cysteine precursors for the synthesis of glutathione in astroglial cultures: preference for cystine. *Glia* 22:11-18.
- Kusmaul L, Hamprecht B, and Dringen R. (1999) The detoxification of cumene hydroperoxide by the glutathione system of cultured astroglial cells hinges on hexose availability for the regeneration of NADPH. *J. Neurochem.* 73: 1246-1253.
- Kyoshima K, Matsuda M, and Handa J (1992) Growth of the graft and astrocytic reaction following transplantation of fetal brain to adult rat's brain. Part II: Cell suspension transplantation into the subarachnoid space. *Nippon Geka Hokan.* 61: 27-34.

- Lada MW, and Kennedy RT (1997) In vivo monitoring of glutathione and cysteine in rat caudate nucleus using microdialysis on line with capillary zone electrophoresis-laser induced fluorescence detection. *J. Neurosci. Methods* 72: 153-159.
- Lee J.M, Moehlenkamp J.D, Hanson J.M, Johnson J.A (2001) Nrf2-dependent activation of the antioxidant response element by tert-butylhydroquinone is independent of oxidative stress in IMR-32 human neuroblastoma cells. *Biochem Biophys Res Commun* 280:286-292.
- Leier I, Jedlitschky G, Buchholz Um Cole SP, Deeley RG, and Keppler D (1996) ARP-dependent glutathione disulphide transport mediated by the MRP gene encoded conjugate export pump. *Biochem. J.* 314: 433-437.
- Leslie E.M, Deeley R.G, and Cole S.P (2001) Toxicological relevance of the multidrug resistance protein 1, MRP1 (ABCC1) and related transporters. *Toxicology* 167: 3-23.
- Li G, Pleasure SJ (2005) Morphogenesis of the dentate gyrus: what we are learning from mouse mutants. *Dev Neurosci* 27:93-99.
- Liu TH, Beckman JS, Freeman BA, Hogan EL, and Hsu CY (1989) Polyethylene glycol-conjugated superoxide dismutase and catalase reduce ischemic brain injury. *Am. J. Physiol.* 256: H589-H593.
- Loe DW, Deeley RG and Cole SP (2000) Verapamil stimulates glutathione transport by the 190kDa multidrug resistance protein 1(MRP1). *J. Pharmacol. Exp. Ther.* 293: 530-538.

- Lowndes HE, Beiswanger CM, Philbert MA, Reuhl KR (1994) Substrates for neural metabolism of xenobiotics in adult and developing brain. *Neurotoxicology*. 15: 61-73.
- Lyrer P, Landolt H, Kabiersch A, Langemann H, Kaeser H (1991) Levels of low molecular weight scavengers in the rat brain during focal ischemia. *Brain Res* 567:317-320.
- Matthias K, Kirchhoff F, Seifert G, Huttmann K, Matyash M, Kettenmann H, Steinhauser C (2003) Segregated expression of AMPA-type glutamate receptors and glutamate transporters defines distinct astrocyte populations in the mouse hippocampus. *J. Neurosci*. 23: 1358-1365.
- Maybodi L, Pow DV, Kharazia VN, Weinberg RJ (1999) Immunocytochemical demonstration of reduced glutathione in neurons of rat forebrain. *Brain Res*. 817:199-205.
- McKinnon SG (1998) Anatomy of the cerebral veins, dural sinuses, sella, meninges, and CSF spaces. *Neuroimaging Clin N Am* 8:101-117.
- Meister A (1994) Glutathione-ascorbic acid antioxidant system in animals. *J. Biol Chem*. 269: 9397-9400.
- Meister A, Anderson ME (1983) Glutathione. *Annu. Rev. Biochem*. 52: 711-760
- Meister A, Tate SS, Griffith OW (1981) γ -Glutamyl transpeptidase. *Meth. Enzymol*. 77: 237-253.
- Memezawa H, Minamisawa H, Smith ML, and Siesjo BK (1992a) Ischemic penumbra in a model of reversible middle cerebral artery occlusion in the rat. *Exp. Brain. Res*. 89:67-78.

- Memezawa H, Smith MLm and Siesjo BK (1992b) Penumbra tissues salvaged by reperfusion following middle cerebral artery occlusion in rats. *Stroke* 23:552-559.
- Meyer AJ and Fricker MD (2000) Direct measurement of glutathione in epidermal cells of intact Arabidopsis roots by two-photon laser scanning microscopy. *J. Microscopy*. 198: 174-181.
- Meyer AJ, May MJ, Fricker M (2001) Quantitative in vivo measurement of glutathione in Arabidopsis cells. *Plant J.* 27:67-78.
- Misra I, Griffith Ow (1998) Expression and purification of human γ -glutamylcysteine synthetase. *Prot Expr Purific.* 13: 268-276.
- Mizui T, Kinouchi H, Chan PH (1992) Depletion of brain glutathione by buthionine sulfoximine enhances cerebral ischemic injury in rats. *Am J Physiol* 262:H313-317.
- Moss SJ, and Smart TG (2001) Constructing inhibitory synapses. *Naure Rev. Neurosci.* 2: 240-250.
- Mueller SG, Trabesinger AH, Boesiger P and Wieser HG (2001) Brain glutathione levels in patients with epilepsy measured by in vivo H-MRS. *Neurology* 57: 1422-1427.
- Mullen RJ, Buck CR, Smith AM (1992) NeuN, a neuronal specific nuclear protein in vertebrates. *Development.* 116:201-211.
- Murphy TH, Miyamoto M, Sastre A, Schnaar RL, Coyle JT (1989) Glutamate toxicity in a neuronal cell line involves inhibition of cystine transport leading to oxidative stress. *Neuron.* 2: 1547-1558.

- Murphy TH, Schnaar RL, Coyle JT (1990) Immature cortical neurons are uniquely sensitive to glutamate toxicity by inhibition of cystine uptake. *FASEB J* 4:1624-1633.
- Murphy T.H, Yu J, Ng R, Johnson D.A, Shen H, Honey C.R, Johnson J.A (2001) Preferential expression of antioxidant response element mediated gene expression in astrocytes. *J. Neurochem* 76:1670-1678.
- Nedergaard M, Takano T, and Hansen AJ (2002) Beyond the role of glutamate as a neurotransmitter. *Nature Rev. Neurosci.* 3: 748-755.
- Newton GL, Dorian R, Fahey RC (1981) Analysis of biological thiols: derivatization with monobromobimane and separation by reverse-phase high-performance liquid chromatography. *Anal Biochem* 114:383-387.
- Newton GL, Fahey, RC (1995) Determination of biothiol by bromobimane labelling and high-performance liquid chromatography. *Meth. Enzym.* 251: 148-166.
- Nilsson C, Lindvall-Axelsson M, Owman C (1992) Neuroendocrine regulatory mechanisms in the choroid plexus-cerebrospinal fluid system. *Brain Res Brain Res Rev* 17:109-138.
- Nimmerjahn A, Kirchhoff F, Kerr JN, Helmchen F (2004) Sulforhodamine 101 as a specific marker of astroglia in the neocortex in vivo. *Nat Methods* 1:31-37.
- O'Coonor, Devesa A, Garcia C, Puertes IR, Pellin A, and Vina JR (1995) Biosynthesis and maintenance of GSH in primary astrocytes cultures: role of L-cystine and ascorbate. *Brain Res.* 680: 157-163.

- Ogita K, Enomoto R, Nakahara F, Ishitsubo N, and Yoneda Y (1995) A possible role of glutathione as an endogenous agonist at the NMDA recognition domain in rat brain. *J. Neurochem.* 64: 1088-1096.
- Ohe Y, Ishikawa K, Itoh Z, Tatemoto K (1996) Cultured leptomeningeal cells secrete cerebrospinal fluid proteins. *J. Neurochem.* 67: 964-971.
- Oheim M, Beaurepaire E, Chaigneau E, Mertz J, Charpak S (2001) Two-photon microscopy in brain tissue: parameters influencing the imaging depth. *J Neurosci Methods* 111:29-37.
- Oka A, Belliveau MJ, Rosenberg PA, Volpe JJ (1993) Vulnerability of oligodendroglia to glutamate: pharmacology, mechanisms, and prevention. *J Neurosci* 13:1441-1453.
- Olney JW, Zorumski C, Price MT, Labruyere J (1990) L-cysteine, a bicarbonate-sensitive endogenous excitotoxin. *Science* 248: 596-599.
- Paulusma CC, van Geer MA, Evers R, Heijn M, Ottenhoff R, Borst P and Oude Elferink RP (1999) Canalicular multispecific organic anion transporter/multidrug resistance protein 2 mediates low-affinity transport of reduced glutathione. *Biochem. J.* 338: 392-401.
- Pearce RK, Owen A, Daniel S, Jenner P and Marsden CD (1997) Alterations in the distribution of glutathione in the substantia nigra in Parkinson's disease. *J. Neural Transm.* 104: 661-677.
- Perry G, Avila J, Espey MG, Wink DA, Atwood CS, Smith MA (2001) Biochemistry of neurodegeneration. *Science* 291:595-597.
- Peuchen S, Duchon MR, and Clark JB (1996) Modulation of the glutathione redox state in adult astrocytes. *Biochem. Soc. Trans.* 24: 449S.

- Philbert MA, Beiswanger CM, Manson MM, Green JA, Novak RF, Primiano T, Reuhl KR, Lowndes HE (1995) Glutathione S-transferases and gamma-glutamyl transpeptidases in the rat nervous systems: a basis for differential susceptibility to neurotoxicants. *Neurotoxicology* 16: 349-362.
- Pileblad E, Magnusson T (1992) Increase in rat brain glutathione following intracerebroventricular administration of gamma-glutamylcysteine. *Biochem. Pharmacol.* 44: 895-903.
- Poot M, Teubert H, Rabinovitch PS, Kavanagh TJ (1995) De novo synthesis of glutathione is required for both entry into and progression through the cell cycle. *J. Cell. Physiol.* 163:555-560.
- Poot M, Hudson FN, Grossmann A, Rabinovitch PS, Kavanagh TJ (1996) Probenicid inhibition of fluorescence extrusion after MCB-staining of rat-1 fibroblasts. *Cytometry* 23: 78-81.
- Ratan RR, Murphy TH, Baraban JM (1994) Oxidative stress induces apoptosis in embryonic cortical neurons. *J Neurochem* 62:376-379.
- Rehncrona S, Folbergrova J, Smith DS, Siesjo BK (1980) Influence of complete and pronounced incomplete cerebral ischemia and subsequent recirculation on cortical concentrations of oxidized and reduced glutathione in the rat. *J Neurochem* 34:477-486.
- Rice ME, Russo-Menna I (1998) Differential compartmentalization of brain ascorbate and glutathione between neurons and glia. *Neuroscience* 82:1213-1223.
- Risling M, Sorbye K and Culheim S. (1992) Aberrant regeneration of motor axons into the pia mater after ventral root neuroma formation. *Brain Res.* 570: 27-34.

- Saez GT, Bannister WH, Bannister JV (1990) Free radicals and thiol compounds-the role of glutathione against free radical toxicity. In: Vina, J. (Ed), *Glutathione: Metabolism and Physiological Functions*. CRC Press, Boca Raton, FL, USA, pp237-254.
- Sagara JI, Miura K, Bannai S (1993) Maintenance of neuronal glutathione by glial cells. *J Neurochem* 61:1672-1676.
- Sagara J, Makino N, and Bannai S (1996) Glutathione efflux from cultured astrocytes. *J Neurochem*. 66: 1876-1881.
- Salinas AE, Wong MG (1999) Glutathione S-transferases-a review. *Curr. Med. Chem.* 6: 279-309.
- Sato H, Tamba M, Ishii T and Bannai S (1999). Cloning and expression of a plasma membrane cystine/glutamate exchange transporter composed of two distinct proteins. *J. Biol Chem.* 274 (17): 11455-11458.
- Sato H, Tamba M, Okuno S, Sato K, Keino-Masu K, Masu M, Bannai S (2002) Distribution of cystine/glutamate exchange transporter, system x_c⁻, in the mouse brain. *J. Neurosci.* 22(18): 8028-8033.
- Schapira AH, Cooper JM, Dexter D, Clark JB, Jenner P, Marsden CD (1990) Mitochondrial complex I deficiency in Parkinson's disease. *J Neurochem* 54:823-827.
- Schubert D, Piasecki D (2001) Oxidative glutamate toxicity can be a component of the excitotoxicity cascade. *J Neurosci* 21:7455-7462.
- Schulz J.B, Lindenau J, Seyfried J, Dichgans J (2000) Glutathione, oxidative stress and neurodegeneration. *Eur. J. Biochem* 267:4907-4911.

- Shih AY, Johnson DA, Wong G, Kraft AD, Jiang L, Erb H, Johnson JA, Murphy TH. (2003) Coordinate regulation of glutathione biosynthesis and release by Nrf2-expressing glia potently protects neurons from oxidative stress. *J. Neurosci.* 23(8): 3394-3406.
- Shih AY, Li P, Murphy TH (2005a) A small-molecule-inducible Nrf2-mediated antioxidant response provides effective prophylaxis against cerebral ischemia *in vivo*. *J Neurosci* 25:10321-10335.
- Shih AY, Imbeault S, Barakauskas V, Erb H, Jiang L, Li P, Murphy TH. (2005b) Induction of the Nrf2-driven antioxidant response confers neuroprotection during mitochondrial stress *in vivo*. *J Biol Chem.* 280(24): 22925-36.
- Sian J, Dexter DT, Lees AJ, Daniel S, Agid Y, Javoy-Agid F, Jenner P, and Marsden CD (1994) Alterations in glutathione levels in Parkinson's disease and other neurodegenerative disorders affecting basal ganglia. *Ann. Neurol.* 36: 348-355.
- Siddiq A, Ayoub IA, Chavez JC, Aminova L, Shah S, Lamanna JC, Patton SM, Connor JR, Cherny RA, Volitakis I, Bush A, Langsetmo I, Seeley T, Gunzler V, Ratan RR (2005) HIF prolyl 4-hydroxylase inhibition: A target for neuroprotection in the central nervous system. *J Biol Chem.*
- Sies H, Akerboom TP (1984) Glutathione disulfide (GSSG) efflux from cells and tissues. *Methods Enzymol.* 105: 445-451.
- Singh SP, Wishnok JS, Keshive M, Deen WM, Tannenbaum SR (1996) The chemistry of the S-nitrosoglutathione/glutathione system. *Proc. Natl. Acad. Sci. USA* 93: 14428-14433.

- Sisodiya SM, Lin WR, Harding BN, Squier MV, and Thom M (2002) Drug resistance in epilepsy: expression of drug resistance proteins in common causes of refractory epilepsy. *Brain* 125: 22-31.
- Slivka A, Mytilineou C, Cohen G (1987) Histochemical evaluation of glutathione in brain. *Brain Res.* 409: 275-284.
- Smith GM, Shine HD (1992) Immunofluorescent labeling of tight junctions in the rat brain and spinal cord. *Int J Dev Neurosci* 10:387-392.
- Sofic E, Lange KW, Jellinger K, and Riederer P (1992) Reduced and oxidized glutathione in the substantia nigra of patients with Parkinson's disease. *Neurosci. Lett* 142: 128-130.
- St John PA, Kell WM, Mazzetta JS, Lange GD, Barker JL (1986) Analysis and isolation of embryonic mammalian neurons by fluorescence-activated cell sorting. *J. Neurosci.* 6: 1492-1512.
- Steward VC, Stone R, Gegg ME, Sharpe MA, Hurst RD, Clark JB, Heales SJ (2002) Preservation of extracellular glutathione by an astrocyte derived factor with properties comparable to extracellular superoxide dismutase. *J. Neurochem.* 83: 984-991.
- Stone R, Stewart VC, Hurst RD, Clark JB, Heales SJ (1999) Astrocytes nitric oxide causes neuronal mitochondrial damage, but antioxidant release limits neuronal cell death. *Ann NY Acad Sci.* 893: 400-403.
- Sucher NJ, Lipton SA (1991) Redox modulatory site of the NMDA receptor-channel complex: regulation by oxidized glutathione. *J. Neurosci Res.* 30: 582-591.

- Sun X, Johannssen H, Imbeault S, Murphy T (2004) In vivo and in vitro 2-photon imaging of glutathione indicates that meningeal and ependymal cells are the major antioxidant buffer in mammalian brain. Poster for Society for Neuroscience Annual Meeting.
- Sun X, Erb H, Murphy TH (2005a) Coordinate regulation of glutathione metabolism in astrocytes by Nrf2. *Biochem. Biophys. Res. Com.* 326: 371-377.
- Sun X, Shih A, Erb H, Li P, Murphy T.H (2005b) Meninges can protect brain against oxidative stress by GSH dependent mechanism. Poster for Society for Neuroscience Annual Meeting.
- Szaszi K, Jones JJ, Nathens AB, Lo A-Y, Marsden PA, Kapus A, Rotstein OD (2005) Glutathione depletion inhibits lipopolysaccharide-induced intercellular adhesion molecule 1 synthesis. *Free Radical Biology & Medicine* 38:1333-1343.
- Tanno H, Nockels RP, Pitts LH, and Noble LJ (1993) Immunolocalization of heat shock protein after fluid percussive brain injury and relationship to breakdown of the blood-brain barrier. *J. Cereb. Blood Flow Metab.* 13: 116-124.
- Tate SS (1985) Microvillus membrane peptidases that catalyze hydrolysis of cysteinylglycine and its derivatives. *Meth. Enzymol.* 113:471-484.
- Tauskela JS, Hewitt K, Kang L, Comas T, Gendron T, Hakim A, Hogan M, Durkin J, Morley P(2000) Evaluation of glutathione sensitive fluorescent dyes in cortical culture. *Glia.* 30:329-341.
- Thomas M, Nicklee T, Hedley D.W (1995) Differential effects of depleting agents on cytoplasmic and nuclear non-protein sulphhydryls: a fluorescence image cytometry study. *Br J Cancer* 72:45-50.

- Tietze F (1969) Enzymic method for quantitative determination of nanogram amounts of total and oxidized glutathione: applications to mammalian blood and other tissues. *Anal Biochem* 27: 502-522.
- Toffa S, Kunikowska GM, Zeng BY, Jenner P and Marsden CD (1997) Glutathione depletion in rat brain does not cause nigrostriatal pathway degeneration. *J. Neural. Transm.* 104: 67-75.
- Ublacker GA, Johnson JA, Siegel FL, Mulcahy RT (1991) Influence of glutathione-S-transferases on cellular glutathione determination by flow cytometry using monochlorobimane. *Cancer Res* 51: 1783-1788.
- Ueda S, Tanabe T, Ihara N and Sano Y (1989) Immunohistochemical study of fetal raphy samples transplanted into the leptomeningeal tissues of 5,6-dihydroxytryptamine-treated adult rats. *Cell Tissue Res.* 256: 457-463.
- Uemura Y, Miller JM, Matson WR, Beal MF (1991) Neurochemical analysis of focal ischemia in rats. *Stroke* 22:1548-1553.
- Van den Dobbelen DJ, Nobel CSI, Schlegel J, Cotgreave IA, Orrenius S, Slater AF (1996) Rapid and specific efflux of reduced glutathione during apoptosis induced by anti-Fas/APO-1 antibody. *J. Biol Chem.* 271: 15420-15427.
- Van der Ven AJ, Mier P, Peters WH, Dolstra H, van Erp PE, Koopmans PP, van der Meer JW (1994) Monochlorobimane does not selectively label glutathione in peripheral blood mononuclear cells. *Anal Biochem* 217: 41-47.
- Varga V, Janaky R, Saransaari P and Oja SS (1994) Endogenous γ -L-glutamyl and L-aspartyl peptides and excitatory aminoacidergic neurotransmission in the brain. *Neuropeptides* 27: 19-26.

- Varga V, Jenei Z, Janaky R, Saransaari P and Oja SS (1997) Glutathione is an endogenous ligand of rat brain NMDA and AMPA receptors. *Neurochem Res.* 22: 1165-1171.
- Vesce S, Jekabsons MB, Johnson-Cadwell LI, Nicholls DG (2005) Acute glutathione depletion restricts mitochondrial ATP export in cerebellar granule neurons. *J Biol Chem* 280 (46): 38720-38728.
- Vila M, Jackson-Lewis V, Guegan C, Wu DC, Teismann P, Choi DK, Tieu K and Przedborski S (2001) The role of glial cells in Parkinson's disease. *Curr Opin. Neurol.* 14: 483-489.
- Walz W, Lang MK (1998) Immunocytochemical evidence for a distinct GFAP-negative subpopulation of astrocytes in the adult rat hippocampus. *Neurosci Lett* 257:127-130.
- Winterbourn CC, Metodiewa D (1994) The reaction of superoxide with reduced glutathione. *Arch Biochem Biophys.* 314: 284-290.
- Wolf R, Wolf D, Ruocco V (1998) Vitamine E: the radical protector. *J. Eur. Acad. Dermatol. Venerol.* 10: 103-117.
- Yamamoto M, Sakamoto N, Iwai A, Yatsugi S, Hidaka K, Noguchi K, Yuasa T (1993) Protective actions of YM737, a new glutathione analog, against cerebral ischemia in rats. *Res. Commun. Chem. Pathol. Pharmacol.* 81: 221-232.
- Yang CS, Chou ST, Lin NN, Liu L, Tsai PJ, Kuo JS, and Lai JS (1994) Determination of extracellular glutathione in rat brain by microdialysis and high-performance liquid chromatography with fluorescence detection. *J. Chromatogr. B. Biomed. Appl.* 661: 231-235.

Yu ZF, Bruce-Keller AJ, Goodman Y and Mattson MP (1998) Unic acid protects neurons against excitotoxic and metabolic insults in cell culture, and against focal ischemic brain injury in vivo. *J. Neurosci Res.* 53: 613-625.

Yudkoff M, Pleasure D, Cregar L, Lin ZP, Nissim I, Stern J, and Nissim I (1990) Glutathione turnover in cultured astrocytes: studies with glutamate. *J. Neurochem.* 55: 137-145.

Zeevalk GD, Bernard LP, Albers DS, Mirochnitchenko O, Nicklas WJ, and Sonsalla PK (1997) Energy stress-induced dopamine loss in glutathione peroxidase-overexpressing transgenic mice and in glutathione-depleted mesencephalic cultures. *J. Neurochem.* 68: 426-429.

Zeevalk GD, Bernard LP, Sinha C, Ehrhart J and Nicklas WJ, (1998) Excitotoxicity and oxidative stress during inhibition of energy metabolism. *Dev. Neurosci.* 20: 444-453.

Zhang S, Boyd J, Delaney K, Murphy TH (2005) Rapid Reversible Changes in Dendritic Spine Structure *In Vivo* Gated by the Degree of Ischemia. *J. Neurosci.* 25(22): 5333-5338.

Zigmond MJ, et al (1999) *Fundamental Neuroscience.* San Diego: Academic Press.